PHILIPP KENKEL

SUSTAINABLE ALTERNATIVES FOR THE PETROCHEMICAL INDUSTRY

DEVELOPMENT OF AN OPEN-SOURCE OPTIMIZATION TOOL FOR MULTI-CRITERIA DECISION-MAKING IN THE EARLY DESIGN PHASE

Philipp Kenkel

Sustainable alternatives for the petrochemical industry: Development of an open-source optimization tool for multi-criteria decision-making in the early design phase

SUSTAINABLE ALTERNATIVES FOR THE PETROCHEMICAL INDUSTRY

DEVELOPMENT OF AN OPEN-SOURCE OPTIMIZATION TOOL FOR MULTI-CRITERIA DECISION-MAKING IN THE EARLY DESIGN PHASE

Vom Fachbereich Produktionstechnik

der

UNIVERSITÄT BREMEN

zur Erlangung des Grades

Doktor der Ingenieurswissenschaften (Dr.-Ing.)

genehmigte

Dissertation

von

M.Sc. Philipp Kenkel

Gutachter

Prof. dr. ir. Edwin Zondervan, Universität Twente

Prof. Dr.-Ing. Mirko Skiborowski, Technische Universität Hamburg

Tag der mündlichen Prüfung: 12.12.2022

ABSTRACT

Petroleum and petrochemical products accompany us every day. From transportation fuels like gasoline, diesel or jet fuel to plastics based on polyethylene or polypropylene, a wide range of petrochemicals are required in the modern-day life. Nonetheless, the production and consumption of such oil-based products contributes substantially to the emission of greenhouse gases and hence to the climate change which is one of the biggest challenges of the current time. To tackle this challenge the defossilization of the (petro)chemical industry is critical. A plethora of renewable alternatives, some well-known others still emerging, are already available to date. However, the decision for one of these competing process options and its subsequent sustainable design is a complex task which has to consider numerous criteria including technical-, economic- and environmental metrics as well as case specific boundary conditions. The discipline of process systems engineering provides a general toolset to support the complex decision-making in the early design phase. Its focus is on computer aided mathematical modeling, simulation, control and optimization of process systems. Nonetheless, most available applications of this toolset in the domain of process synthesis are either very case specific or closed-source leading to incomprehensibilities, non-reproducible work and finally to unnecessary redundancy.

To tackle this challenge, this thesis introduces the fully open-source framework OUTDOOR (**O**pen s**U**pers**T**ructure mo**D**eling and **O**ptimizati**O**n f**R**amework) which is developed in Python using the Pyomo modeling language and combines the approach of superstructure optimization for process synthesis with object-oriented programming and modeling. Herein, a superstructure depicts a large number of possible flowsheets to produce certain products from given raw materials by myriad processing steps. By optimizing the superstructure for suitable objective functions, optimal process designs are created and mass- and energy balances as well as costs and greenhouse gas emissions are calculated.

In this thesis first, an overview on the object-oriented programming framework is provided, which gives insight on the object-based modeling as well as preparation of data structures required for the mathematical model. Afterwards the detailed optimization model is explained. This model is based on mixed-integer linear programming and depicts the mathematical representation of the superstructure. Subsequently a set of methodologies are presented especially developed to improve the capabilities of superstructure optimization in sustainable process design. These methodologies include an approach for multi-criteria optimization as well as a screening algorithm to deal with uncertainties in data input.

Furthermore, to demonstrate OUTDOORs capabilities and contribute to the complex design questions of alternatives for the petrochemical industry, the software is applied to two case studies. The first case study is used to investigate the integrated production of methanol based on renewable electricity and biogas. The process design is optimized for different objectives such as minimal production costs, greenhouse gas emissions and fresh water demand as well as combined multi-criteria metrics. The results proof that renewable methanol is approximately four times more expensive than conventional methanol. Nonetheless, electricity-based methanol can contribute greatly to defossilizing the petrochemical industry saving up to 2.9 $t_{CO_2-eq.}/t_{MeOH}$ compared to its fossil counterpart, while a combination with direct air capture reduces the fresh water demand to zero.

The second case study deals with the renewable production of jet fuel which is difficult to substitute by other renewables, especially for long intercontinental flights. By-products are typical transportation fuels like diesel, gasoline or liquefied petroleum gas. The investigated production routes include electricity-based production via a Fischer-Tropsch or methanol-route as well as an microalgae-based biorefinery. Owing to OUTDOORs versatile mathematical model, a deep integration of electricity- and bio-based production is realized and operating windows for both general concepts evaluated for different base parameters like processing costs, algae cultivation costs or electricity prices. The results show that a combination of electricity- and bio-based production can have a positive influence on the economics of the process. Nonetheless, such an integrated refinery still is approximately five times more expensive than oil-based production, due to high algae production costs and electricity prices. Further results show that bio-based production comes with a high impact on fresh water demand, thus indicating that an electricity-based production is a good trade-off if multiple environmental criteria are considered simultaneously.

Zusammenfassung

Erdöl und petrochemische Produkte spielen eine wichtige Rolle in unserem alltäglichen Leben. Von Kraftstoffen wie Benzin, Diesel oder Kerosin bis hin zu Kunststoffen auf der Basis von Polyethylen oder Polypropylen werden zahllose Produkte im modernen Alltag benötigt. Allerdings ist die Produktion und Verwendung dieser Erdöl-basierten Produkte für einen beträchtlichen Anteil der gesamten Treibhausgasen verantwortlich. Somit ist sie letztendlich auch zu beträchtlichen Anteilen am Klimawandel, einem der größten Herausforderungen der Gegenwart, beteiligt. Daher ist die Defossilisierung der petrochemischen Industrie eine Hauptaufgabe des Klimaschutzes. Glücklicherweise stehen schon heute eine Vielzahl verschiedener regenerativer Alternativen bereit von denen manche zwar noch in der Entwicklung sind, andere allerdings schon kommerziell Verfügbar. Nichtsdestotrotz ist die Wahl einer geeigneten Technologie sowie deren optimale Auslegung ein komplexer Prozess der von technischen, ökonomischen und ökologischen Parametern abhängt und immer situationsabhängig ist. Zur Unterstützung dieser Endscheidungsprozesse stellt die Disziplin der Systemverfahrenstechnik eine Reihe an Methoden und Werkzeugen bereit. Die Systemverfahrenstechnik konzentriert sich hierbei auf die computer-gestützte Modellierung, Simulation als auch Steuerung und Optimierung verfahrenstechnischer Prozesse und Anlagen. Leider sind viele verfügbare Anwendungen, insbesondere im Bereich des Prozessdesigns entweder sehr situationsspezifisch oder nicht frei verfügbar. Dadurch sind vorhandene Modelle und Lösungen schwierig nachzuvollziehen oder gar nachzubilden, was wiederum zu unnötiger Redundanz in der wissenschaftlichen Arbeit bezüglich dieser Themen führt.

Um der Redundanzproblematik zu begegnen wurde im Rahmen dieser Arbeit das open-source Werkzeug OUTDOOR (**O**pen s**U**pers**T**ructure mo**D**eling and **O**ptimizati**O**n f**R**amework) entwickelt. Diese Software vereint den Ansatz der Superstructure-Optimierung zur Prozessdesigngestaltung mit Konzepten der objekt-orientieren Programmierung und Modellierung und basiert auf der Programmiersprache Python sowie der Modelltoolbox Pyomo. Das Konzept der Superstructure beschreibt hierbei die Darstellung einer Vielzahl an möglichen Prozesskonzepten und -flussdiagrammen um verschiedene Produkte aus gegeben Rohstoffen zu produzieren. Mithilfe der mathematischen Optimierung kann darauf aufbauend das optimale Prozessdesign sowie Designparameter wie Massen- und Energiebilanzen sowie Kosten oder Treibhausgasemissionen für verschiedene Zielfunktionen bestimmt werden.

Für einen detaillierten Einblick in die entwickelte Software wird zunächst der generelle Rahmen beschrieben. Dieser Umfasst unter anderem die objekt-

orientierte Softwarearchitektur als auch das Konzept der objekt-orientierten Modellierung sowie deren Übersetzung in eine geeignete Datenstruktur für gegebene mathematische Modelle. Darauf aufbauend wird das inkludierte Optimierungsmodell dargestellt. Dieses basiert auf gemischt-ganzzahliger linearer Programmierung und stellt eine mathematische Repräsentation der gegebenen Superstructure dar. Anschließend werden im Rahmen der Arbeit entwickelte Methoden genauer erläutert. Die erste behandelt die multi-kriterielle Prozessdesignoptimierung, die zweite einen Suchalgorithmus der als Antwort auf Unsicherheiten der gegebenen Eingangsparameter entwickelt wurde.

Mithilfe zweier Fallstudien wird zum einen die Funktionalität von OUTDOOR nachgewiesen, und zum anderen Lösungsvorschläge für Teilprobleme im Design petrochemischer Alternativprozesse bereitgestellt.

Die erste Fallstudie umfasst die Produktion von Methanol auf Basis einer Kombination von erneuerbarer elektrischer Energie und Biogas. Verschiedene Zielfunktionen der Designoptimierung wie minimale Produktionskosten, Treibhausgasemissionen oder der Verbrauch von Frischwasser kommen zum Einsatz. Desweiteren findet eine Optimierung unter multiplen Kriterien statt. Die Ergebnisse deuten auf viermal höhere Kosten hin, wenn Methanol regenerativ hergestellt wird. Allerdings zeigen sie auch, dass diese Art der Methanolproduktion bis zu 2.9 $t_{CO_2-eq.}/t_{MeOH}$ sparen kann, und somit einen deutlichen Beitrag zur Treibhausgasminderung beisteuern könnte. Zusätzlich zeigt die Studie, dass eine strombasierte Methanolproduktion mit CO_2 Gewinnung durch Luftabscheidung zu einem wasserneutralen Prozess führen können.

Aufgrund der mittelfristigen Alternativlosigkeit, insbesondere für Interkontinentalflüge, untersucht die zweite Fallstudie die Produktion von Kerosin. Weitere dargestellt Nebenprodukte sind Benzin, Diesel oder Flüssiggas. Inkludierte Prozesspfade sind strombasierte Fischer-Tropsch und Methanol-Routen als auch eine auf Mikroalgen-basierte Bioraffinerie. Mithilfe von OUTDOORs vielseitigen mathematischen Modells wird eine automatische tiefgreifende Integration der beiden Konzepte (strom- vs. bio-basiert) vorgenommen und untersucht. Verschiedene grundlegende Parameter wie Prozesskosten, Algenkosten oder Strompreise werden variiert und die jeweiligen ökonomischen Betriebsfenster sowie Integrationspotentiale aufgezeigt. Die Ergebnisse deuten darauf hin, dass eine Kombination von strom- und biobasierten Technologien ökonomische Vorteile bieten kann. Trotz der ökonomischen Vorteile sind die regenativen Kraftstoffe, aufgrund hoher Algen- und Strompreise, mit einem fünfmal höheren Preis im Vergleich zu Öl-basierten Gegenspielern nicht konkurrenzfähig. Zusätzlich benötigt das Wachstum von Biomasse signifikante Mengen Frischwasser, weshalb ein rein strombasierter Prozess im Sinne eine multi-kriteriellen Analyse als optimaler Trade-off gesehen werden kann.

ACKNOWLEDGEMENTS

Diese Arbeit und die letzten knapp 3.5 Jahre wären niemals zustande gekommen ohne die Hilfe und die Einflüsse einer Vielzahl an Menschen.

Zunächst einmal möchte ich mich bei Prof. Edwin Zondervan bedanken, der mich mit seiner stets positiven Art und Weise hervorragend durch meine Zeit als Doktorand begleitet hat. Er hat mir stets die Freiheiten gelassen die ich brauchte um mich selbst zu entfalten und zu verwirklichen. Selbst nach seinem Wechsel in die Niederlande hat er sich durchgängig um eine gute und persönliche Betreuung gekümmert. Besonders dankbar bin ich für das persönliche und zwischenmenschliche Verhältnis, dass wir zueinander aufbauen konnten.

Vielen Dank möchte ich auch an Herrn Prof. Skiborowski sagen, der sich dazu bereit erklärt hat als Zweitgutachter meiner Arbeit zu fungieren.

Desweiteren möchte ich mich beim KEROSyN100 Team und insbesondere bei Timo Wassermann bedanken. Durch seinen vertrauensvollen und kompetenten Führungsstil fühlte ich mich stets wertgeschätzt. Desweiteren wäre meine Dissertation sicher nicht, dass was sie nun ist ohne die zahlreichen Diskussionen und Hinweise seinerseits.

Weiterer Dank gilt meiner Arbeitsgruppe der Resiliente Energiesysteme für die gute Atmosphäre, die unzähligen Kaffeerunden und Gespräche beim Mittagessen, ob sie nun fachlicher Art waren oder nicht. Zusätzlich möchte ich mich bei meinen beiden studentischen Mitarbeitern Celina und Joshua bedanken, die mir tatkräftig unter die Arme gegriffen haben und ohne die OUTDOOR nicht das geworden wäre was es heute ist.

Meiner Familie und dir Jorina gilt besonderem Danke. Danke, dass ich mich auf eure Unterstützung und euren Zuspruch verlassen konnte. Zu guter Letzt möchte ich mich bei meinen Eltern Olaf und Ulrike bedanken. Danke dafür, dass ihr mir mit eurer Unterstützung und Erziehung die Möglichkeit bereitet habt bis zu diesem Punkt in meinen Leben zu kommen.

TABLE OF CONTENTS

1 INTRODUCTION

This chapter sets the scope and objectives of this thesis. First Germany's greenhouse gas emissions and targets as well as the problem of petrochemical industries and their defossilization are discussed. Next, the current state of petrochemicals production is presented. Subsequently an overview of already existing alternatives is compiled and an overview on mathematical tools for aid of sustainable process design is provided which leads to the research question of this thesis.

Parts of this chapter have been published in:

- Kenkel, P., Wassermann, T., Rose, C., & Zondervan, E. (2021). OUTDOOR–An open-source superstructure construction and optimization tool. In Computer Aided Chemical Engineering (Vol. 50, pp. 413-418). Elsevier.

- Parts of this chapter are in the process of publication in:

- Kenkel, P., Schnuelle, C., Wassermann, T., & Zondervan, E. (2022) Integrating Multi-Objective Superstructure Optimizationand Multi-Criteria Assesment: A novel methodology for sustainable process design. Physical Science Reviews.

1.1 BACKGROUND AND MOTIVATION

Due to the urgent threat of climate change induced by anthropogenic greenhouse gas (GHG) emissions, Germany and other countries have set out ambitious targets for GHG reductions of 80-95 % in 2050 compared to 1990 [1]. In some sectors like energy production a reduction of ca. 50 % (cf. Figure 1.1) has already been achieved. However, other sectors like transport and industry are much harder to defossilize and display much less reduction [2]. If the current trends and velocity continue, Germany will miss their reduction goals by ca. 100 % (ref. Figure 1.1) [1].

From the hard-to-defossilize sectors the petroleum industry produces a tremendous amount of greenhouse gas emissions. Most of these emissions are emitted indirectly in the mobility sector by usage of fossil transportation fuels (31% of Germanys total emissions) [1], [3]. However, about 12% of Germany's total GHG emissions are caused by processing in the petroleum industry which includes operation of crude oil refineries, heating in chemical industry parks as well as non-energy related emissions in production of base chemicals such as ammonia, olefins or methanol [3]. To meet the ambitious GHG reduction goals, not only the energy sector but all sectors must be defossilized in the upcoming years, posing a major challenge in identifying, designing and realizing renewable alternatives for the petroleum and petrochemical industry.
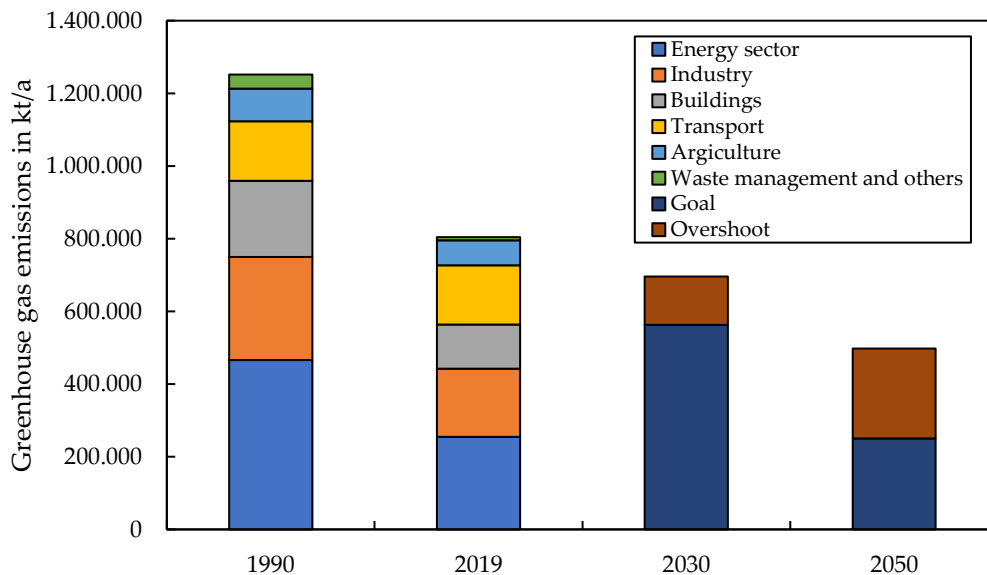
FIGURE 1.1: GERMANYS GREENHOUSE GAS EMISSIONS IN DIFFERENT YEARS BY SECTORS AS WELL AS DESIGNATED GOALS AND EXTRAPOLATION [2].

The petroleum and petrochemical industry are closely connected. The petroleum industry deals with the general conversion of crude oil to several products like gasoline, diesel or naphtha. The petrochemical industry concentrates on producing a wide range of intermediate- and final non-fuel products based on crude oil fractions but also natural gas as raw materials. Often both industries are

directly intertwined e.g. when oil refineries produce hydrocarbon fuels in combination with petrochemicals, while consuming hydrogen produced by steam methane reforming of natural gas. Owning to this deep connection the term petrochemical industry can also regarded as *"The production of different commodities, both fuel and non-fuel from petroleum and natural gas"*.

Final applications of such petrochemical products vary from mobility and heating (diesel, gasoline, kerosene, natural gas) and polymers (polyethylene, polypropylene etc.) to pharmaceuticals (aspirin, sterilization, etc.), food industries (fertilizer, fat hardening etc.) and the textile industry (polyester and textile fibers) [4], [5]. Most final non-fuel products are based on a hand full of primal compounds which are relatively simple hydrocarbons [4]. These hydrocarbons are: Light olefins (ethylene, propylene, butene), aromatics (benzene, xylene, toluene), methanol, methane and hydrogen (ref. Table 1.1) [4], [5].

TABLE 1.1: BASIC PETROCHEMICALS WITH INTERMEDIATES AND FINAL APPLICATIONS [4].

Base chemical	Intermediate chemicals	End use
Ethylene	Ethylene dichloride, ethyl chloride, ethylbenzene, vinyl acetate, polyglycol, ethylene glycol, vinyl chloride Aacetaldehyde	Polyethylene (PE), fibers, solvents, resins, synthetic rubber, polyesters, PVC, PET, Polystyrene
Propylene	Cumene, acetone, acrylonitrile, propylene oxide, glycerol, alkylbenzene, phenol	Polypropylene (PP), acrylics, rubbing alcohol, epoxy glue, carpets, Aspirin, Humectant
Butene	Butadiene, di- and tributylene, T-Butyl alcohol	Synthetic rubber, carpet fibers, paper coatings, plastic pipes
Benzene	Cumol, ethylbenzene, cyclohexane	Nylon, polystyrene, epoxy resins, phenolic resins, polyurethane
Toluene	Toluene diisocyanate	Polyurethane, gasoline blend, TNT
Xylene	Terephthalic acid, isophtalic acid, phthalic anhydride	PET
Methanol	Acetic acid, olefins, formaldehyde, methycrylates	Gasoline, resins, glue, acrylic glass

Figure 1.2 depicts a simplified line of production of base petrochemicals and fuels from crude oil and natural gas feedstock. Crude mineral oil is the raw material for most of these basic compounds as well as liquid fuels. It is refined in conventional oil refineries to produce fuels such as diesel and gasoline (51%), heating oil (15 %), naphtha (10 %) and kerosene (9 %) (ref. Figure 1.3) [6]. While the applications of fuels and heating oil is rather straight forward, naphtha is used as an intermediate in the petrochemical industry [7]. It is converted via steam cracking and purification to hydrogen (H_2), methane (CH_4), olefins and aromatics. Often hydrogen and methane are used internally for heat supply resulting in olefins and aromatics as final products [7].

Natural gas on the other hand is used as heating agent as well as main source for H_2 and synthesis gas (syngas) production via. steam- or autothermal reforming [4]. H_2 is mainly used for ammonia production and as reactant in oil refineries. Syngas, a mixture of H_2 and carbon monoxide (CO) is used in methanol synthesis.
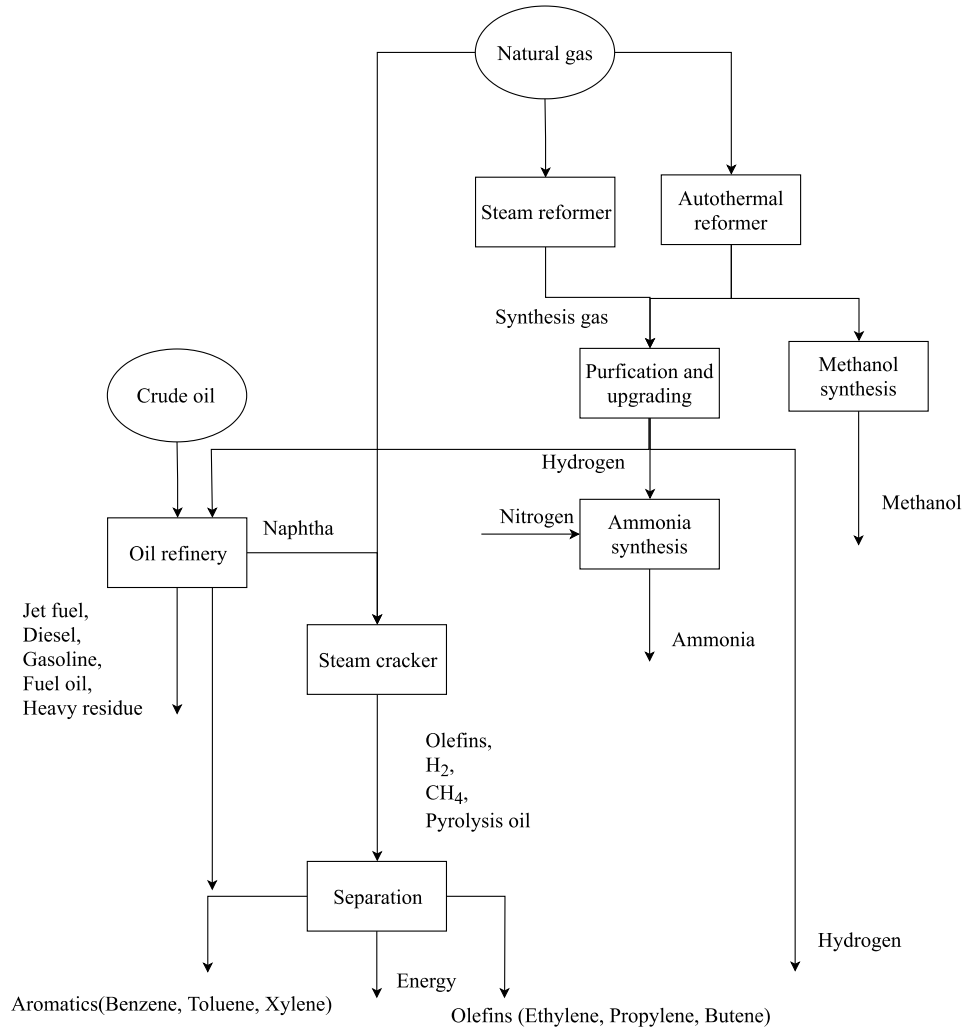
FIGURE 1.2: OVERVIEW ON CONVENTIONAL BASIC PETROCHEMICALS AND FUELS PRODUCTION ROUTES.
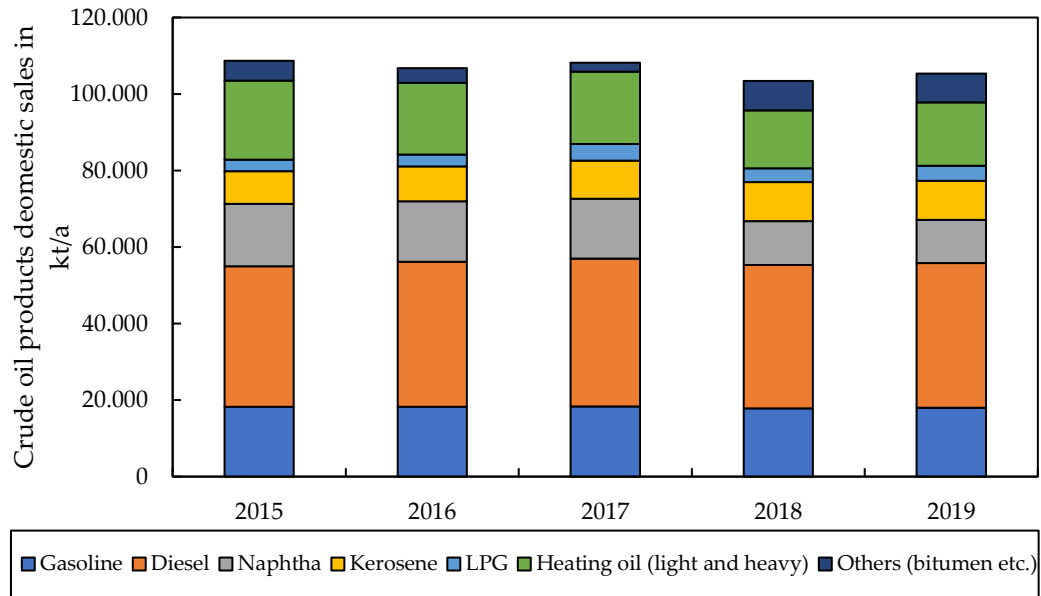
FIGURE 1.3: DOMESTIC SALES OF CRUDE OIL PRODUCTS IN GERMANY (OWN REPRESENTATION BASED ON [6]).

1.2 RENEWABLE CHEMICALS AND FUELS

To defossilize the petrochemical industry production processes like oil refining, steam cracking and natural gas steam reforming have to be substituted by alternative processes. Luckily numerous renewable processes and chemicals, that can replace their fossil counterparts, already exist to date (ref. Figure 1.4) [8], [9]. These processes can be distinguished as either electricity-based, also called Power-to-X (PtX), or as biomass-based, also called Biomass-to-X (BtX) processes.
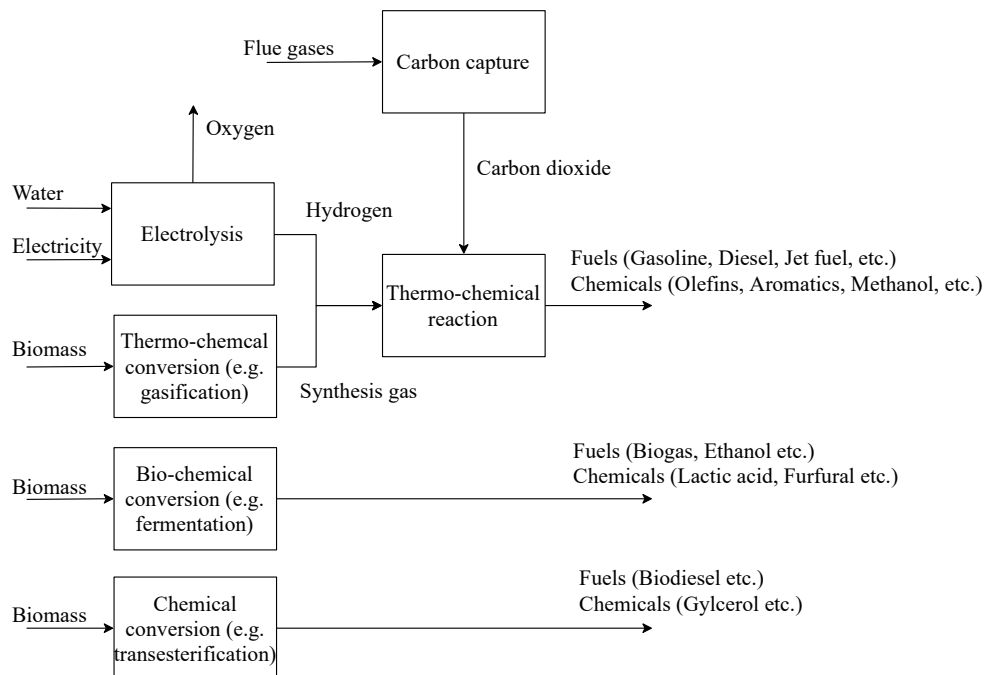
FIGURE 1.4: OVERVIEW OF RENEWABLE ALTERNATIVE PATHWAYS FOR PETROCHEMICALS PRODUCTION.

1.2.1 Power-to-X (PtX)

Figure 1.5 gives an overview on existing Power-to-X pathways. PtX processes utilize renewable electricity from wind, solar or other sources as their main energy carrier. This electricity is used to produce H_2 by water electrolysis (cf. Figure 1.5 left hand side) [8]. Carbon is supplied by so-called carbon capture and utilization processes, where CO_2 is captured from different flue gases or directly from air (Figure 1.5 right hand side). Using H_2 and CO_2 as raw material, different hydrocarbons can be produced by thermochemical synthesis.
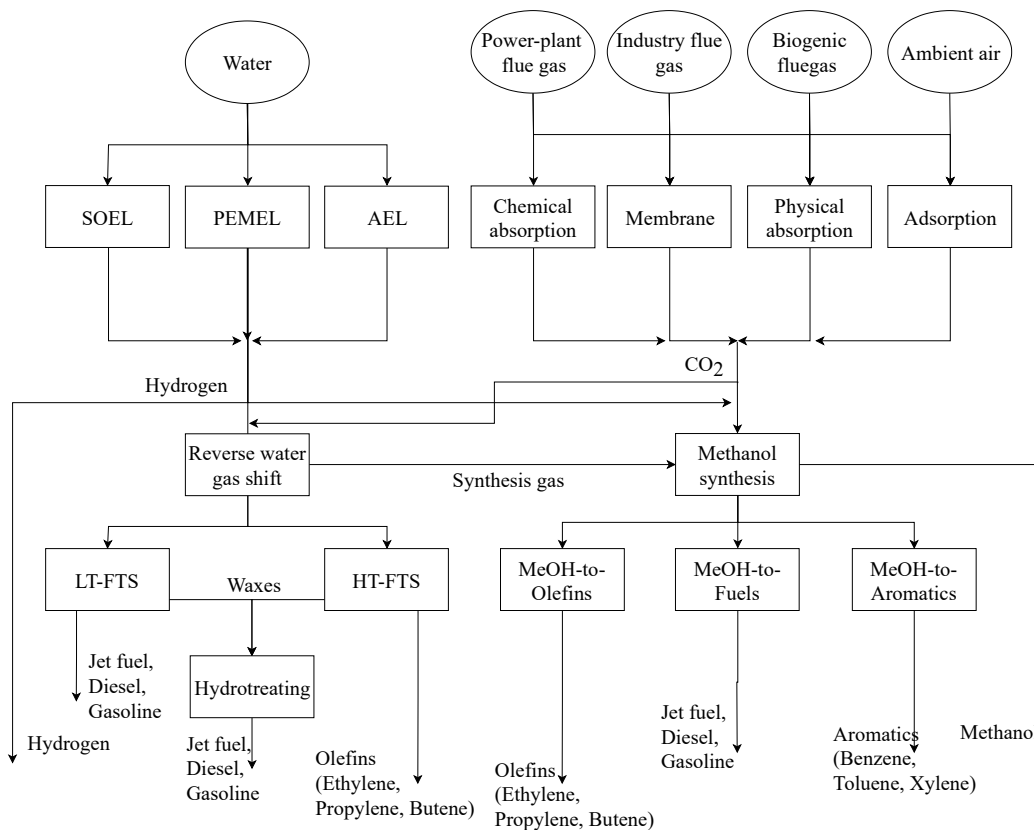
FIGURE 1.5: OVERVIEW OF POWER-TO-X PROCESS PATHWAYS.

Water electrolysis

In water electrolysis water is split into pure H_2 and oxygen (O_2) via an electrochemical process [8], [10]. Three main water electrolysis technologies are currently used and developed. These are alkaline electrolysis (AEL), polymer electrolyte membrane electrolysis (PEMEL) and solid oxide electrolysis (SOEL) [10], [11]. AEL and PEMEL operate at low to intermediate pressure (1-30 bar) and low temperature of approx. 70°C with high electricity demand. SOEL on the other hand operates at low pressure (1 bar) and high temperatures up to 1000°C. Here electricity demand is reduced due to energy input by high temperature steam. The AEL technology is mature, while PEMEL is currently tested in large scale and SOEL is still in development, only tested on small scale [10], [11].The pure H_2 could

be used to substitute natural gas steam reforming e.g. in ammonia production or oil refineries in the first step [12]. Next to industrial uses, H_2 can also be used as fuel in combination with fuel cells. This would be especially interesting for shipping, where direct usage of battery electric vehicles is no option due to high weights in batteries. The by-product from electrolysis, pure O_2, could be used in applications like waste water treatment or the steel industry.

Carbon capture and utilization

To produce hydrocarbons by thermochemical synthesis, next to H_2 also a carbon source has to be available. One potential candidate which is often discussed is CO_2 which can be acquired from different sources. Potential CO_2 sources are widely spread from power plants to the cement- or steel industry as well as bioprocesses like biogas or bioethanol production and even via direct air capture from ambient air [13], [14]. A broad spectrum of carbon capture processes has been developed already using concepts like chemical or physical absorption, adsorption or membrane processes. Some of these processes like amine scrubbing, pressure swing adsorption or physical absorption are already state-of-the art large scale processes [13], [14]. Other processes like direct air capture are developed and tested in mid- to large-scale at the moment. Nonetheless, hydrocarbon production will only be GHG neutral if the carbon source is also GHG neutral. Hence most industrial sources like coal or natural gas power plants cannot have a part in a future chemical industry, and sources like bio-based flue gases of direct air capture have to be pursued.

Thermochemical synthesis

From methanol and olefins to aromatics and liquid fuels, a wide range of chemicals can be produced using H_2 and CO_2 as raw materials utilizing different thermochemical synthesis reactions. Most prominent are Methanol-synthesis as well as Fischer-Tropsch synthesis.

Conventionally methanol synthesis uses synthesis gas (H_2/CO). Therefore, one way to use CO_2 as raw material is to convert H_2 and CO_2 to CO and H_2O prior by the reverse water-gas-shift reaction. However, direct hydrogenation of CO_2 using adapted catalysts and operating conditions have been investigated thoroughly [15]. Methanol itself is often proposed as a major platform chemical in a so-called methanol economy [15]. There have been several arguments brought up that support the methanol economy, e.g., the ease of handling the chemicals, the available large-scale infrastructures as well as wide range of further processing alternatives. Methanol can be used to produce all major petrochemicals including olefins, aromatics or even gasoline, diesel and kerosene [15]–[18].

Fischer-Tropsch synthesis (FTS) depicts the direct competition to methanol-synthesis. It also is available at large-scale, commonly utilizing coal or natural gas as raw material [19]. In FTS, first synthesis gas is produced, afterwards this gas is further converted to a broad mixture of hydrocarbons [19]. Depending on H_2/CO ratio, as well as operating temperature, pressure and catalyst choice the product spectrum varies. Low temperature FTS at 180 – 250°C mainly produces longer hydrocarbons such as diesel, kerosene or waxes [19]. High temperature FTS at 300 – 350°C produces shorter hydrocarbons like short chain olefins or gasoline [19]. Additional purification steps like separation, cracking and hydrotreating allows the production of basically every major hydrocarbon [19].

1.2.2 Biomass-to-X (BtX)

Next to an electricity-based production, different bio-based production routes exist [9]. In contrast to PtX processes, biomass depicts a complex and diverse raw material which has a varying composition of sugars, (hemi)cellulose, lipids, starch, minerals and lignin [20]. The different raw materials can be utilized for different product spectrums, which is why BtX is often discussed in the frame of biorefineries [21]. Similar to their oil-based counterpart, these facilities fractionate and process the distinct shares to required final products (Figure 1.6) [21]. The design of such a biorefinery is strongly dependent on the initial raw biomass as well as the desired products [21]. Depending on the type of biomass used and products produced, a distinction of first to third generation biofuels as well as platform chemicals can be made [9].
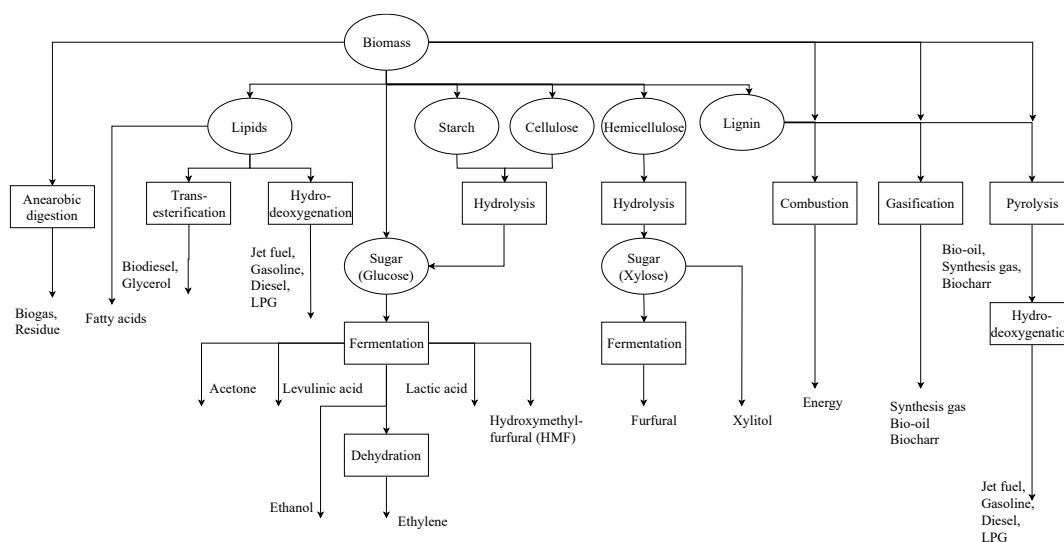
FIGURE 1.6: OVERVIEW ON BIOMASS-TO-X PROCESS PATHWAYS.

First-generation biofuels

Generally first-generation biofuels are bioethanol, biodiesel, bio-kerosene and biogas from edible crops like sugarcane, rapeseed or corn [9]. Bioethanol and biogas are produced utilizing the sugars (glucose) and starch by applying fermentation and anaerobic digestion with the help of microorganisms like yeasts or micro bacteria [9], [21]. Bioethanol is an already widely used gasoline blend, while biogas can substitute natural gas after purification [22], [23]. Biodiesel (fatty acid methyl ester = FAME) is produced by transesterification of lipids with methanol and functions as diesel blend [9], [21]. Bio-kerosene (hydroprocessed esters and fatty acids = HEFA) is based on hydrodeoxygenation of the raw bio-oil by using hydrogen [9]. This process removes the large oxygen content of the bio-oil, which makes it accessible as kerosene substitute [9]. All three processes are operated at industrial scale. Nonetheless, a general debate on food-or-fuel is held due to the direct competition to the food and feed sector.

Second generation biofuels

Second generation biofuels and biochemicals utilize lignocellulosic and waste biomass [9]. Hence, they are a direct reaction to the food-or-fuel competition of first-generation bioproducts. Lignocellulosic and waste biomasses are in general cheaper than normal food crops, however their composition requires a more complex pretreatment to gain final products [9]. Lignocellulosic materials consist of a mixture of cellulose (a polysaccharide based on glucose), hemi-cellulose (polysaccharides based on C5 and C6-sugars) and lignin (a biopolymer based on phenolic precursors) [20]. Two different ways for processing lignocellulosic materials arise: biochemical and thermochemical [9].

Thermochemical conversion uses heat in processes like gasification or pyrolysis. Using low temperatures (250 – 350°C) and absence of oxygen the whole biomass undergoes torrefication producing mainly biochar [9], [19]. Increased temperatures (550 – 750°C) with absence of oxygen (pyrolysis) produces mainly bio-oil [9], [19]. This bio-oil can be further upgraded to fuels using technologies like steam or catalytic cracking as well as hydrotreating. At very high temperatures and limited oxygen input (gasification) biomass is converted to syngas with biochar and bio-oil as by-products [9]. Syngas can be purified and used as raw material for methanol-synthesis or Fischer-Tropsch synthesis [9], [19].

Biochemical conversion varies for the different components of the lignocellulosic biomass. Therefore, the raw biomass has to be divided into its constituents first [9], [21]. This process can be very complex as well as energy- and cost intensive [9]. Afterwards the polysaccharides of the cellulose biomass can be broken into glucose by enzymes or acid hydrolysis [9], [21]. The resulting glucose can be used similarly as to first-generation biomass. The hemi-cellulose polysaccharides can be

broken to single-sugars using hydrolysis. However, the C5-sugars can only be converted to bioethanol using specialized microorganisms [9], [21]. Lignin is a very complex and hard to decompose biopolymer. Therefore, it is often used as energy carrier in co-generation [9], [21].

Third generation biofuels

Micro-algae are often considered as the third generation biomass [9]. Their main advantages are higher cultivation productivity, lower water demand, high oil contents and no application in food-supply [24]. There are thousands of different algae strains, all of them implicate different advantages and disadvantages. Some strains use sea water, while others can be utilized to clean municipal waste water by consuming nitrogen and phosphorus [20]. Additionally, depending on the strain the shares of carbohydrates, lipids and proteins can vary drastically, which enables various fields of applications from ethanol, FAME and HEFA production to the production of value-added chemicals and compounds [20], [25]. Cultivation of algae is performed in reactor systems which can be designed as simple open-ponds or more complex photobioreactors using tubular, flat-panel of thin-layered cascade designs. The different reactor designs differ in terms of costs, efficiency or land use. However, all concepts combine, that the utilized land does not has to fulfill classical requirements for crop cultivation [9], [20]. Main disadvantage of algae cultivation are high costs, which is why only special applications like food supplements production are implemented right now [9], [20].

Platform chemicals

One way to produce platform chemicals from biomass is to use gasification to reduce the complex structures to their main components, H_2 and CO. The synthesis gas can afterwards be used to produce olefins, aromatics etc. by either FTS or methanol-synthesis with included upgrading technologies.

However, since biomass already consists of complex structures it can be preferable to not completely reduce the complexity, but to synthesize so-called platform chemicals. These platform chemicals, in general C2 – C6 hydrocarbons, depict intermediates which are conventionally produced from base petrochemicals. Some of these chemicals include furfural, succinic acid, lactic acid or 3-hydroxycaleric acid. These platform chemicals are derived by biotechnology using sugar, starch as well as (hemi)cellulosic biomass components. Their applications range from textile to polymer production. Lactic acid for example is used to produce polylactide (PLA) which is already produced at industrial scale and exhibits similar properties to polyethylene terephthalate (PET). For a detailed overview Jang et al. present the wide variety of existing platform chemicals and their production pathways [26].

1.3 SUSTAINABILITY

PtX and BtX processes present various alternatives to save GHG emissions on the way of producing base chemicals that are needed for a large number of end products. Nonetheless, future technologies should not only be CO_2-neutral but overall sustainable. Sustainability can be derived from the definition of sustainable development which describes *"development that meets the need of the present without compromising the ability of future generations to meet their own needs."* [27]. Sustainable development is often discussed under the three dimensions environment, economics and social justice [28]. The environmental dimension addresses ecological consequences like global warming by GHG emissions, but also resource depletion, eutrophication from nutrients, acidification or ozone depletion [20]. The economic pillar covers costs of processes and products and its main statement is, that products also have to be affordable [20]. The social side of sustainability addresses problem categories like working conditions (work hours, child labor, health and safety etc.) but also aspects like community engagement, cultural heritage, corruption and fair competition [20].

Different sustainability assessment methods have been proposed over the time, ranging from sets of indicators, to material and energy flow analysis, environmental accounting methods or life cycle analysis methods [28]. Ren et al. give a detailed overview over the different concepts [28]. In general, they conclude that life cycle analysis methods are especially fitting for sustainability analysis [28]. These assessment methodologies can be used to investigate products and product systems over their complete life cycle, meaning from the acquisition of raw materials, over the production of goods and their use-phase to their end-of-life and disposal or recycling [20], [29]. The most prominent analysis is the life cycle analysis (LCA) which depicts the environmental pillar of life cycle methods. It is standardized in the ISO 14040/44 and studies impact categories like climate change, land and water use, ecotoxic effects or biodiversity [29]. The economic pillar is represented by the life cycle costing (LCC) method which uses the same standards and calculates arising costs from production, usage and disposal [20]. The last dimension, the social dimension, is treated in the social life cycle assessment (sLCA). This method is not as standardized as the other two, due to the main challenges in quantifying social impacts [20]. Often the combination of all three methods is called a life cycle sustainability analysis (LCSA) [20], [28]. Such an analysis demands serious knowledge on different aspects of a product or process. Additionally, it produces numerous results which have to be interpreted and set into context. Nonetheless, it also gives a much deeper insight on given processes which is important to design real sustainable process alternatives for the future.

1.4 PROCESS SYSTEMS ENGINEERING

In situations where numerous process alternatives are available and many criteria have to be considered, conceptual and final process design configuration poses a major challenge. The domain of petrochemical alternatives presents exactly such a case. Various processes exist and sustainability includes a vast number of criteria, meanwhile the call for optimal, sustainable solutions is increasing. During the design process, several aspects have to be considered, ranging from boundary conditions and feasibility to process costs and environmental burdens.

The discipline of process systems engineering (PSE) provides a set of tools to aid with the arising decision-problems. PSE is a sub-discipline of chemical engineering and was defined by on a conference on Kyoto in 1982 [30] and further described by Sargent in 1983 [30], [31]. Grossmann and Westerberg define process systems engineering as the discipline "[…] *concerned with the improvement of decision-making processes for the creation and operation of the chemical supply chain. It deals with the discovery, design, manufacture, and distribution of chemical products in the context of many conflicting goals."* [32], where the chemical supply chain spans from designing usable molecules to producing industrial commodities and developing optimal supply chains and logistics [32].

The main focus of PSE is process modeling, simulation, optimization and control with the aid of mathematical models, computer algorithms and software tools [30]. Typical available tools are process simulators like Aspen Plus or DWSim and modeling and optimization software like GAMS or Pyomo in combination with mathematical solvers like Gurobi or Baron [30].

Based on modeling and simulation, assessment and optimization in regards of techno-economics, life cycle assessment (LCA) or sustainability analysis are applied in PSE to gain deeper insights on developed process metrics [30]. One particularly type of optimization problem is the superstructure optimization which depicts a method for conceptual process design where a plethora of possible design options is given [33], [34].

1.4.1 Superstructure optimization

Superstructure optimization is a tool for systematic process synthesis introduced by Umeda et al. in 1972 [35]. The concept utilizes mathematical models and optimization algorithms to identify optimal process design for different product systems [33]. Herein a superstructure represents a large number of possible flowsheets. In these flowsheets different unit-operations interact with each other in order to perform the general task of providing desired products from a given set of raw materials [36]. Every unit-operation inside this superstructure can be described by the same set of generic equations representing different processing

tasks such as mixing, reaction, separation or utility consumption [37] [38]. The complete superstructure is translated into a mathematical optimization model, which can be solved using fitting optimization solvers in order to identify optimal process designs [36], [39].

Superstructure optimization for process design

The methodology of superstructure optimization was developed for conceptual process design in general, hence it was utilized for various applications in the past. Initially, its use was restricted to subsystems, and later complete flowsheet design optimization was adopted [40], [41]. Relevant work was performed in early years by Yee and Grossmann as well as Ciric and Floudas in the area of heat exchanger network (HEN) optimization [42], [43].

Recent work concentrates especially on designing biorefineries, BtX systems and integrating detailed thermodynamic models into superstructure approaches. Zondervan et al. proposed a superstructure optimization for a wheat straw biorefinery , while Gong et al. utilized superstructure optimization to identify cost-optimal algae biorefineries producing biodiesel and other value-added products [24], [36]. Meanwhile Galanopoulos et al. integrated a wheat straw and algae refinery for identification of synergies leading to cost reduction up to 80 % [44]. Restrepo-Flórez et al. designed a biorefinery to produce advanced fuels with tailored properties from ethanol. They maximized the refinery profit and showed, that a change of fuel specification changes the general refinery outlet [45]. AlNouss et al. present an optimization of biomass gasification for the production of fuels, fertilizer and energy using detailed models in Aspen Plus. Krone et al. include accurate CAPE-OPEN thermodynamic models into their superstructure representation. They use the resulting MINLP to design a separation for a ternary mixture [46]. Meanwhile, Huster et al. design an organic Rankine cycle using artificial neural networks as thermodynamic surrogate models. They show that a thermo-economic optimization can reduce investment costs by 47 % [47].

In terms of chemicals production, Lee et al. define a MINLP using MATLAB and Aspen Plus which optimizes a methanol production by direct hydrogenation of CO_2. They conclude that a cost optimization can reduce processing cost to 416 $/$t_{MeOH}$ [48]. Maggi et al. investigate Power-to-Synthesis gas options using a MILP formulation and biogas and CO_2 from ambient air as carbon source. Their model is implemented in MATLAB and minimizes the power input, especially for H_2 production from electrolysis [49]. Onel et al., Baliban et al. and Niziolek et a. designed large superstructure formulations for the production of liquid fuels, olefins and aromatics from biomass, natural gas and coal [50]–[52].

Superstructure optimization frameworks

The developed models are often formulated differently and tend to be very large and complex, written as mixed integer (non)linear programming models. It has become common practice in science that every research group develops its own model and implements it for its specific case using commercial algebraic modeling software such as GAMS or AIMMS [33], [34], [36], [38], [39], [52]–[54]. Nonetheless, a number of general frameworks exists that tackle the challenge of automating superstructure model formulation and optimization. Mencarelli et al. give a broad review on the different modeling approaches as well as existing and developed software solutions [33].

They point to ProCAFD as the most sophisticated tool featuring a graphical user interface and the ability to automatically generate process alternatives from sets of raw materials, products and reactions [55]. The software is developed and sold by PSEforSPEED. Other software mentioned is P-Graph Studio, MIPSYN, SYNOPSIS and Pyosyn, the latter two being newer synthesis frameworks [56]–[59]. P-Graph Studio also includes a graphical user interface but is not tailored for chemical engineering [57]. MIPSYN and SNYOPSIS use MINLP or general disjunctive programming (GDP) models, with an interface to the commercial GAMS modeling software [57]. Pyosyn describes a newer framework which is part of the IDEAS energy project [60]. It is written in Python using Pyomo as modeling language, hence it depicts an open-source alternative. However, it focuses on support for high level modeling and solution strategies instead of providing a specialized tool [60]. An additional new framework is COMANDO, which aims to provide general object-oriented energy systems modeling capabilities [61]. It includes features like MINLP modeling with interfaces to different solvers, while enabling a component-based construction of energy systems model. It however, is also not specialized for superstructure optimization.

Mencarelli et al. conclude their review with the need for a fully open-source framework specialized for superstructure modeling and optimization [33]. Such an open-source framework would enable the scientific and industry community to develop together and to benefit from each other [33].

1.4.2 Optimization under uncertainty

Superstructure optimization is a tool especially suitable in the early design phase, where multiple alternatives are available and optimal processes are to be determined. However, during this phase the amount of information on different options can be limited [62], [63]. Such limited information inevitably leads to uncertain parameters or uncertainty in general. To handle such uncertainties in optimization, a number of approaches have been proposed over the last decades.

These include simple approaches like sensitivity analysis and more elaborate methods like stochastic or fuzzy programing as well as sampling methods [64].

Two-stage stochastic programming is one prominent approach. It includes uncertainty as probability functions and partitions the given decision variable into two sets. While variables of the first set have to be fixed before the realization of the uncertainties, variables of the second set can be used as recourse afterwards. This can be used for example in the design and operation of a distillation column, where the number of trays has to be fixed first and operational variables like operation temperature can be adjusted later [62], [63].

Sampling-based methods like Monte-Carlo simulation use a representative amount of actual scenarios of the uncertain parameters and map the objective functions and decision variables dependency on the given uncertain parameters as distribution function [65].

All given methods find applications in superstructure optimization, however they come with the drawback that they increase the complexity of the optimization problem as well as the required calculation expenses. A more detailed review on available methods is presented by Sahinidis et al. [64].

1.4.3 Multi-criteria decision-analysis

A different pool of decision-support tools is consolidated under the term multi-criteria decision-analysis (MCDA) [66], [67]. Their main goal is to compare and rank different alternatives under a set of different criteria. These methods are divided into multi-attribute decision making (MADM) and multi-objective decision making (MODM) approaches [66], [67].

MADM compares a known discrete number of alternatives with respect to a set of criteria to gain knowledge on advantages and disadvantages of the given alternatives [66], [67]. These methods can be further sub-categorized into full aggregation methods (American school) or outranking methods (European school) [66], [67].

Full aggregation methods include simple approaches such as the weighted sum method (WSM), but also more complex techniques like the analytical hierarchy process (AHP) or the multi-attribute utility theory (MAUT). All of these methods include an evaluation of different alternatives with respect to a given set of criteria using numerical scores in combination with a subjective weighting of criteria importance. With the given performance values and weighting, a total score is calculated, which can be compared for all alternatives to perform a ranking. The approach assumes compensable scores, meaning a bad score can be compensated completely by a good score for a different criterion [66], [67].

Outranking methods include the Preference Ranking Organization Method for Enrichment Evaluations (PROMETHEE) or ÉLimination et Choix Traduisant la REalité (ELECTRE). These approaches also use concepts like weighting and performance evaluation. However, they do not assume the concept of compensable scores. This can lead to results where different alternatives have similar final scores but are incomparable due to different incomparable criteria [66], [67].

Next to MADM methods MODM is a concept which is often used where "fixed process alternatives" are not already known. Hence, it is a method utilized in process systems engineering and especially in superstructure optimization. Methods like goal programming or vector optimization are easily combined with optimization models to find optimal solutions from an unknown indefinite solution space. Goal programming defines an objective function which includes different goals into one mathematical equation. It can be extended by weighting of the different objective parts, or split into a series of optimization by using lexicographical goal programming. Vector optimization is often performed as pareto-optimization in terms of an ϵ-constraint programming. In this approach different solutions are derived, each presenting a point where one objective is at an optimal point and cannot be improved further without worsen the other criteria [66], [67]. Also using the goal-programming approach is the Technique for Order Preference by Similarity to Ideal Solution (TOPSIS). However, it is neither a full aggregation approach nor an outranking approach. While it is used for existing definite numbers of alternatives like MADM methods, it uses the definition of goals or aspiration levels to compare all alternatives to this ideal goal [66], [67].

It is clear, that both concepts, MADM and MODM have advantages and disadvantages. MADM concepts are often simple to apply and do not require large computational power. However, they are designed for the application to already known process alternatives and require the knowledge of process data to evaluate with regard to the defined criteria. Therefore, they are more or less appropriate for a small number of process alternatives. MODM concepts are harder to implement because they are based on mathematical programming and optimization. On the other hand, they can be used to search an indefinite number of possible process concepts and therefore are very well suited to investigate the integrated processes. However, one major drawback for concepts like ϵ-constraint programming is that they generate numerous trade-off solutions which are hard to represent and interpret for a rising number of criteria. Nevertheless, both approaches have been used in process design in the past. Erdinc et al. as well as Løken give detailed reviews on MCDA applications to (renewable) energy systems [68], [69]. ϵ-constraint optimization is used for bi-criteria process synthesis e.g. by Gong and You [24]. The combination of ϵ-constraint and superstructure optimization provides a powerful tool for the investigation of novel concepts like integrated PtX

and BtX processes. However, if more than two objectives are considered, the representation of trade-off solutions via pareto-fronts is not overly helpful in the decision process anymore. Here more aggregated approaches like MADM are helpful. For this reason, methods like MAUT or PROMETHEE are sometimes used in sustainability analysis to aggregate the large amount of results for a small number of alternatives. What is somewhat missing is a methodology which integrates the computational capabilities of superstructure optimization with the structured aggregation approach of MADM methods to investigate many process alternatives under many criteria as presented in sustainability analysis.

1.5 SCOPE AND OBJECTIVE OF THE THESIS

Summarizing the above it is evident, that urgent defossilization of the petrochemical industry is required to battle anthropogenic climate change. To achieve this, a set of renewable process alternatives are available. Nonetheless, renewable (CO_2 neutral) process design is not equal to sustainable process design which also includes additional environmental, economic and social aspects. To aid with the emerging complex decision-making processes of designing sustainable petrochemical alternatives the discipline of process systems engineering provides a set of tools.

In spite of this given toolset a number of serious challenges in the actual design optimization of petrochemical alternatives can be identified:

  i. To this date it is hardly possible to include and integrate large numbers of process alternatives in a systematic optimization approach, which is why a coupled Power-to-X and biorefinery approach has not be investigated yet.

  ii. Available studies on superstructure optimization are often restricted to single- or bi-criteria optimization concentrating on production costs and greenhouse gas emissions, which is why sustainability is underrepresented in process design.

 iii. Presented models and software solutions are either case specific or closed-source, inhibiting adaptability and scientific output, which is why high unnecessary redundancy is created.

The investigation of not only Power-to-X or biorefinery but an integrated approach (challenge 1), would require a systematic modeling approach which can handle a large number of process alternatives with sufficient modeling detail in acceptable calculation times. Such a framework requires on the one hand a well-suited model and on the other hand a simple user interface and overall generality. The selected modeling approach has to be detailed enough to allow representations of process integration, however it should be simple enough to reduce data requirement and

computational time. Additionally, the model should be designed in a generic way to enable modeling of different types of applications.

The limitation of superstructure optimization to single- or bi-criteria problems (challenge 2) arises from a set of reasons. Greenhouse gas emissions and the affiliated climate change is discussed as the major environmental threat of the current time. Climate change as well as overly costly renewable processes dominate the general discussion on the transition of the energy system, which is why the focus is often set on these areas. Additionally, pareto-optimization is well designed for visualization of bi-criteria optimization, but is less suitable for rising numbers of criteria. Combined with the fact that disciplines like life cycle assessment and multi-criteria decision-analysis are in fact a niche in process systems engineering, the combination of the different aspects is easily neglected.

The problem of case specific or closed-source tools (challenge 3) emerges on the one hand due to availability of different modeling languages and software packages, on the other hand due to personal interests as well as the complex nature of the given optimization problems. Closed-source modeling languages like GAMS or AIMMS are well-known and -developed and therefore also widely used. Open-source options like Pyomo require Python programing skills and more initial time invest. Overall, companies but also scientists have to invest a lot of time and work to develop models and software, which is why they also have a certain interest in keeping the established competence. On the other hand, the developed (often case-specific) models are complex and hence hard to comprehend and adapt which sometimes makes building new models from scratch more attractive.

Overall, to tackle the presented challenges the following is required:

    i.   A toolbox for open-source process design optimization which considers more criteria than production costs and CO_2 emissions, but keeps the modeling and decision-making process simple enough to include numerous process alternatives while enabling third-party usage and development.

    ii.   A detailed investigation on fully integrated PtX and BtX concepts for the production of base chemicals and hydrocarbon fuels, which emphasizes potential integration benefits and demonstrates the greenhouse gas reduction potential while considering sustainability concepts.

The goal of this thesis is to provide the necessary open-source toolbox to investigate fully integrated novel process concepts in terms of sustainability, while keeping the modeling and decision-making workload at a reasonable level. This toolbox will be used to investigate integration potentials of combined BtX and PtX processes for the production of hydrocarbon fuels and petrochemicals and to compare the sustainability performance of such novel processes to their conventional counter-parts.

1.6 OUTLINE

In **Chapter 2** an open-source superstructure modeling and optimization framework is introduced. This framework is developed in Python using the Pyomo modeling language and completely distributed via Github. Chapter 2 focusses on the general idea of the framework as well as its modular software architecture to give a broad insight on the program algorithm and included classes and methods. The framework itself includes a general, reusable and adaptable superstructure optimization model.

The mathematical details of this model are presented in **Chapter 3**. It is formulated as a mixed-integer linear programming (MILP) model and can be utilized for different applications from HEN optimization to (combined) PtX and BtX processes as well as conventional chemical processes. Its MILP formulation ensures fast solution times and allows integrated heat integration.

Chapter 4 presents a set of developed methodologies, which improve conceptual process design by including multi-criteria optimization concepts as well as two-way sensitivity analysis as part of an optimal design screening algorithm as reaction of data-uncertainty in novel technologies.

Chapter 5 presents a multi-criteria design optimization of renewable methanol production. A combined PtX and BtX concept is investigated under multiple criteria like production costs, GHG emissions and fresh water demand. Single-criterion optimal process designs as well as multi-criteria trade-offs are presented as results. Afterwards an integrated Power-to-X and biorefinery for the production of jet fuel is investigated in **Chapter 6**. Using the developed screening algorithm, operating windows of stand-alone algae-biorefinery, Fischer-Tropsch-to-Jet and Methanol-to-Jet as well as their coupling are explored.

Finally, a conclusion is provided and an outlook to further research in process systems engineering concerned with the upcoming challenges presented in **Chapter 7**.

2   OUTDOOR

The following chapter presents the developed **O**pen s**U**pers**T**ructure mo**D**eling and **O**ptimizati**O**n f**R**amework (OUTDOOR). OUTDOOR is an open-source software written in Python 3 utilizing the Python Optimization Modeling Objects package (Pyomo). OUTDOOR provides the tools to intuitively set up superstructure models, implement data for different types of unit-operations and perform process synthesis optimization for different objective functions. It includes several pre- and postprocessing algorithms to minimize user-input and thus enable non-professionals to set up case studies and generate and interpret results derived by state-of-the art optimization solvers. OUTDOOR is programmed for maximum convenience in user-handling but it is also written as a modular, open-source software which is accessible via GitHub, hence providing an important contribution to scientific collaboration. The chapter is structured as follows: First the general software architecture is presented, while simultaneously giving an overview on the algorithm sequence. Afterwards, a deeper insight on included program structure, object-oriented class definition and graphical representation is given.

Parts of this chapter have been published in:

- Kenkel, P., Wassermann, T., Rose, C., & Zondervan, E. (2021). OUTDOOR– An open-source superstructure construction and optimization tool. In Computer Aided Chemical Engineering (Vol. 50, pp. 413-418). Elsevier.

- Parts of this chapter are in the process of publication in:

- Kenkel, P., Schnuelle, C., Wassermann, T., & Zondervan, E. (2022) Integrating Multi-Objective Superstructure Optimizationand Multi-Criteria Assesment: A novel methodology for sustainable process design. Physical Science Reviews.

2.1 OUTLINE

OUTDOOR (**O**pen s**U**pers**T**ructure mo**D**eling and **O**ptimizati**O**n f**R**amework) is an open-source software, written in Python, which provides the necessary tools to easily build superstructure models and subsequently perform optimized flowsheet synthesis for different applications and objectives. Its other task is to provide of a modular modeling and optimization toolbox which permits simple modifications and further development by other scientists. OUTDOORs functionality can be structured in five major part:

i.   An open-source, Python-based, object-oriented superstructure construction framework based on interacting unit-operation classes inside a surrounding superstructure-system class (Further described in this chapter).

ii. An algebraic mixed-integer linear programming model written in Pyomo with three different pre-programmed objective functions, namely minimal net production costs (NPC), greenhouse gas emissions (NPE) and fresh water demand (NPFWD) (Further described in chapter 3).

iii. A Microsoft Excel-based interface and Python-based Excel-wrapper which allows an intuitive unit-operation-based data input- and saving method (Example template and source code available at: *https://github.com/PKenkel/OUTDOOR*).

iv. Advanced methodologies and tailor-made implementations for automated multi-criteria optimization, sensitivity analysis and two-way sensitivity analysis for decision-support in early design phases (Further described in chapter 4).

v.   A general modeling toolbox which connects the different functionalities, as well as provides additional classes and methods for pre- and postprocessing of data (Further described in the chapter).

The idea of OUTDOOR originates from the discrepancy of data structures and "conventional" optimization modeling. Superstructure modeling describes the interaction of different unit-operations in possible flowsheets and aims to synthesize the optimal flowsheet from the given options. In order to model the unit-operations and their interaction various data like specific utility demand or separation performance has be known. The intuitive way to collect this data could be called "object-oriented" or "unit-operation-based": All required information is gathered centered around every unit-operation e.g. by literature research or flowsheet simulation. Nonetheless, optimization models are traditionally not written and expressed in such an object-oriented way. Their formulation follows the concept of a structured program which centers around parameters and variables that are indexed over defined sets and put into context by constraints

written as equations. Hence, their format could be called "parameter-based" or "list-oriented". The major role of OUTDOOR is to overcome this discrepancy by providing smart translation functions. Figure 2.1 depicts a simplified example of this phenomena: Data, like the specific electricity demand (denoted *el*) or split factors (denoted *sp*) are collected for every unit-operation *u* (see left hand side of Figure 2.1). The data input of the model formulation nonetheless is given in structured lists for every parameter indexed over the defined sets of all unit-operations *U* (see right hand side of Figure 2.1). Utilizing OUTDOOR and its translation functions, data is collected and implemented in a unit-operations-based structure, while the underlaying optimization model is formulated using a traditional style.
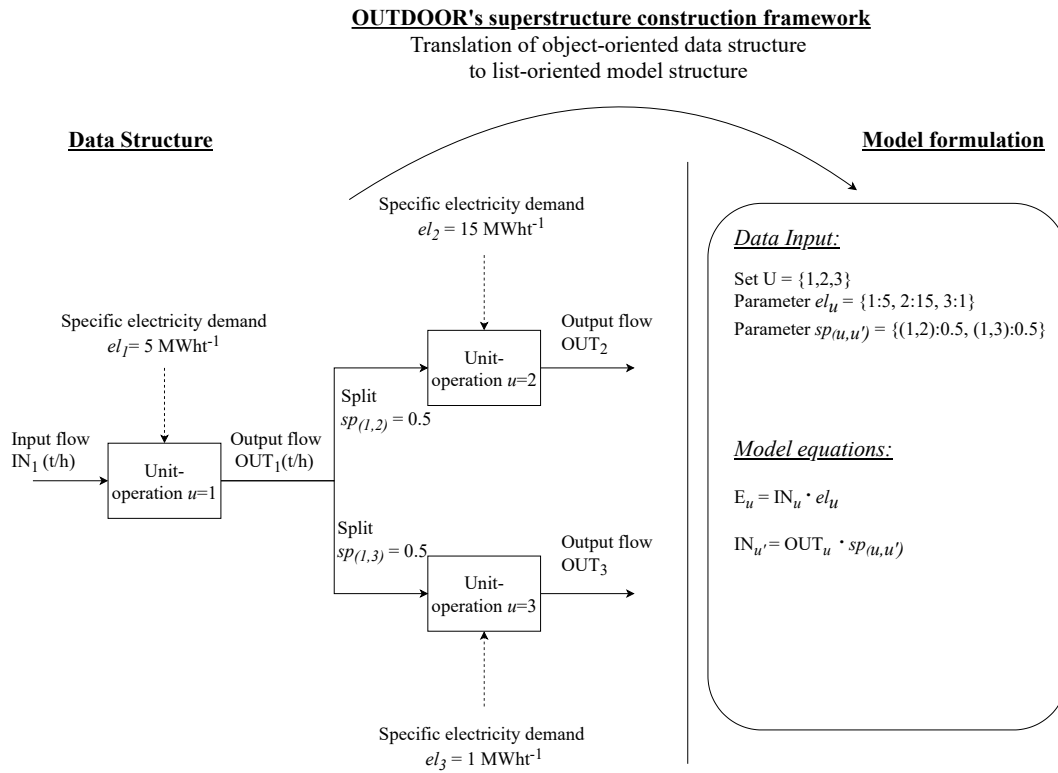
FIGURE 2.1: SIMPLE REPRESENTATION OF OUTDOOR'S ROLE IN TRANSFORMING OBJECT-ORIENTED DATA STRUCTURES TO LIST-ORIENTED MODEL FORMULATIONS.

2.2 SOFTWARE ARCHITECTURE

OUTDOOR is written as an object-oriented software, where objects of different classes interact with each other to perform the task of superstructure modeling / construction, optimization and data storage as well as post-processing and analysis of results. Figure 2.2 gives an overview of the included classes, their main tasks and interaction in the software architecture. If read from left to right, it can also be used as a simplified communication diagram to explain the algorithm sequence. First the user has to input his data. The data input can be divided in three general steps:

i.   Create Unit-operation class objects and their data like capital costs functions, or split factors.

ii.   Generate a surrounding superstructure system that includes boundary conditions like external utility prices, required components or the objective function.

iii. Add the generated unit-operations to the superstructure system to build the complete data basis.

Data input can either be done using the integrated Python application programming interface (API) inside an integrated development environment (IDE) or the more intuitive and cleaner Excel-wrapper interface. If manual IDE coding is used, objects are created and filled with data using the programmed class-methods inside a fitting Python script. However, if the Excel-interface is utilized, unit-operations can be added by simple adding new predefined template sheets and data is filled in directly in Excel. OUTDOOR afterwards provides a function to generate the Python classes and link them together to a filled Superstructure object by automatically calling the class-methods.

The combination of unit-operations and superstructure classes depict the superstructure construction framework. Their main task is to provide methods to input data in object-oriented style as well as the required methods to translate this data to the "list-oriented" data file which is model-readable.

Subsequent to creating the data basis, the user has to create an object of the SuperstructureProblem class. This class functions as a handler-class that connects the remaining classes and their methods in the right order. By calling its *solve_optimization()* method, using the created Superstructure as well as solver name and optimization mode as input, the user starts the rest of the automated algorithm. During this procedure the SuperstructureProblem first creates an object of the SuperstructureModel class, which includes the required mixed-integer linear programming model (MILP). This class inherits from Pyomos AbstractModel class and displays empty equations with the affiliated sets, parameters, variables and constraints. However, the actual data of the sets and parameters, that define the case study are not implemented yet. Afterwards the SuperstructureProblem collects the data file from the Superstructure by calling its translation methods. This data file is used to create a (filled) model instance of the SuperstructureModel which inherits from Pyomos ConcreteModel class and describes the desired case study.

The resulting model instance is afterwards processed by an appropriate Optimizer class. This Optimizer connects the Pyomo model to an external solver, which in turn optimizes the flowsheet for the selected objective function. OUTDOOR can connect the solving procedure to various commercial and open-source MILP

solvers like Gurobi, Cplex and CBC. To achieve this, it utilizes the implemented links provided by the Pyomo package. After the model is solved by the solver, it is handed back to the Optimizer. The Optimizer then stores the included data inside a ModelOuput class, which provides the necessary attributes and methods to store and save the data. If it is required to analyze the acquired results in terms of techno-economic or environmental metrics, a ModelAnalyzer class can be created by the user and loaded with a ModelOutput object.
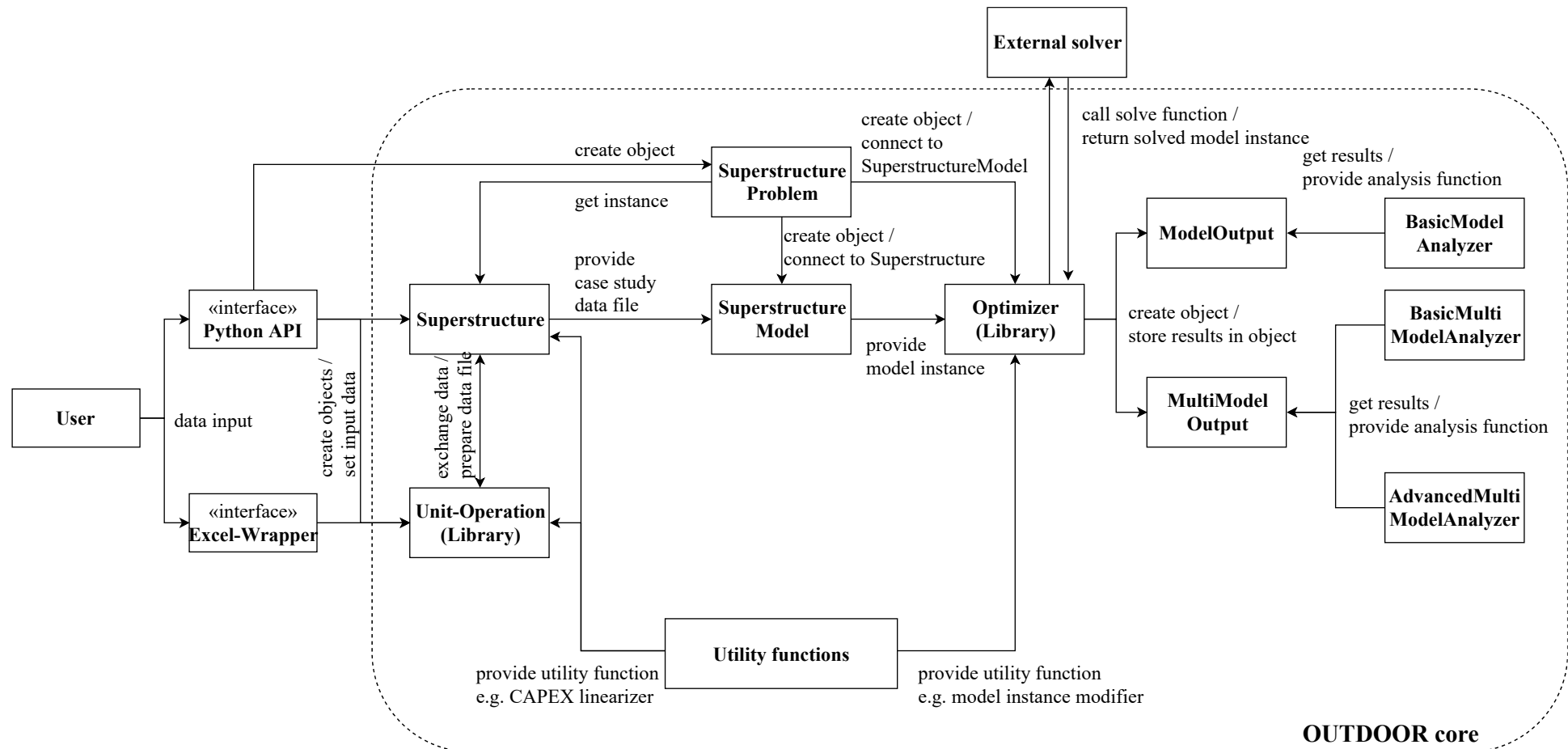
2.3 DETAILED CLASS DESCRIPTION

Every class has its distinctive role in the optimization framework. To perform the required tasks a number of parameters and functions (called attributes and methods for object-oriented programming) are included in the class definition. The following section will give a deeper insight on the individual roles of the different classes in the order of which they are called in the program.

2.3.1 Unit-operation classes

A superstructure is described by different unit-operations which interact with each other. To model different behaviors, OUTDOOR comes with several unit-operation classes which provide different tasks. The fundamental tasks in OUTDOOR include mixing, reaction, separation and distribution. Detailed descriptions and visualizations of these tasks are given in Table 2.1.

Based on the fundamental tasks a set of different unit-operation classes are defined in OUTDOOR which combine various tasks. These unit-operation classes are: Splitters (simple processes), reactors, turbines, furnaces, distributors, product pools and raw material sources. The detailed description and visualization of these unit-operations is depicted in Table 2.2.

Every unit-operation class includes the necessary attributes to provide the model with the data which is required to depict the type of process. To set the attributes with values, single-attribute setter methods as well as lumping-multi-attributes setter methods are implemented. One feature is the modularity of the class's definitions, which uses the object-oriented concept of inheritance, where specialized unit-operation classes like a furnace inherits from more general classes like a stoichiometric reactor, which in turn inherits again from the more general class simple process. The complete inheritance tree, with major respecting attributes is depicted in Figure 2.3.

TABLE 2.1: GENERAL PROCESSING TASKS IN OUTDOOR'S UNIT-OPERATION MODELS.
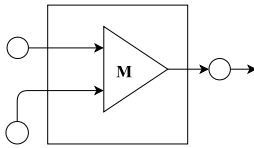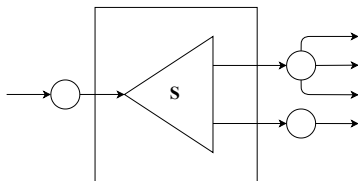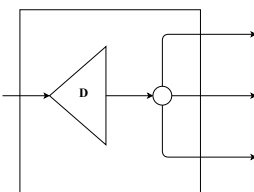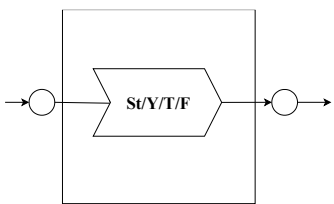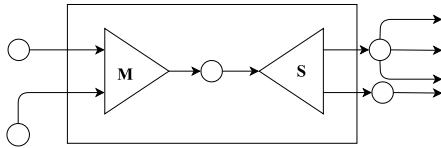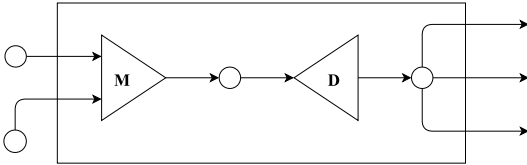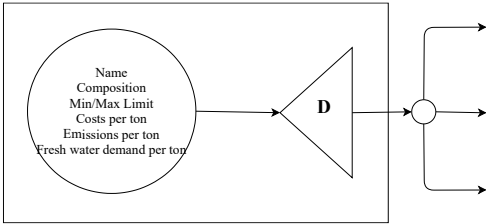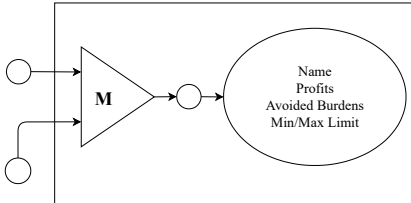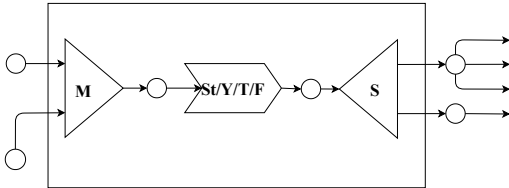
Task/ Visualization	Description
Mixing	Mixing takes different inlet streams with different states (visualized by small circles) and calculates the resulting oulet flow and state. A state is generally defined by the composition of the stream as well as the pressure an temperature. However, it should be noted, that the mixing operation neither includes thermodynamic calculations in terms of temperature or pressure. It simply calculates the outlet flow composition. Additionally, it does not include a logic to check if streams are mixable or should be mixed. Example: Simple Mixers.
Separation	Separation takes a single inlet flow with a given state and calculates different outlet states and outletflows by (predefined) splitfactors. Different "output-circles" visualize different states (e.g real separation like flash evaporation). The start-location of the flow streams on the circle describe^ the type of splitting. If more then one flow starts on the same location on the same circle this depicts an either/or decision (e.g 100 % of this state to choice a or b). If multiple flows start on the same circle but on different locations a co-decision is made (e.g. 50 % of this state to a and 50 % to b). Examples: Pre-calculated distillation columns or flash evaporators.
Distribution	Distribution takes a single inlet flow with a given state and distributes this stream to a set of given (predefined) target processes. The state of every outlet flow is equal to the inlet flow. The splitting ratio is not predefined as with the separation task but a variable solved by the system during optimization. Examples: Valves.
Reaction	Reaction calculates the outlet state / composition from given inlet flow based on stochiometric (St) or yield functions (Y). For stoichiometric reactions there are additional subclasses which are turbine mode (T) and furnace mode (F) which use stoichiometric functions together with given efficiencies and lower heating values of inlet components to calculate produced electricity or steam. Examples: Methanol reactor, electricity steam turbine, steam producing furnace.

TABLE 2.2: UNIT-OPERATIONS IMPLEMENTED IN OUTDOOR.

Unit-operation name / Visualization	Description
Simple process / Splitter (S) 	A simple process is a combination of the mixing and the separation task. Most of the time the main goal is to split incoming streams into predefined output streams. If there is only one input stream the mixing part is omitted without any loss of generality. However, if mixing is part of the simple process, it should be noted that no internal logic is implemented that checks for feasibility. Hence, it should be secured that the predefined split factors are valid for the arising mixture from the mixing.
Distributor unit (D) 	The distributor unit combines the mixing and the distributing task. Different inlet streams form an intermediate stream which is afterwards distributed to given target processes.
Raw material source 	Raw material sources are predefined flows with given costs, emissions and fresh water demand per ton as well as minimum and maximum availability. These sources are connected to target processes by the distributor task, so that one source can feed different processes. It should be noted, that while the concept is similar to a normal distributor unit, due to fixed composition the modeling is simplified.
Product pool 	The product pool is a mass flow sink which mixes incoming flows and calculates profits and avoided burdens. It is possible to predefine required minimum and maximum inlet flows for given products. It is important that the intermediate state after the mixing task meets the characteristics of the defined product.
Stoichiometric (St-R) /Yield reactor (Y-R), Turbine (TUR) and Furnace (FUR). 	The different reactor units display a combination of mixing, reaction and separation tasks. Different input streams are mixed to an intermediate flow which is converted by either stoichiometric or yield reaction and finally separated to different outlet flows by given split factors. If only one inlet (outlet/target) is defined the mixing (separation) task is omitted without loss of generality. If the reactors are defined as turbine or furnace, reaction is calculated by stoichiometric reaction while electricity or steam production are calculated from efficiencies and lower heating value of reaction compounds.
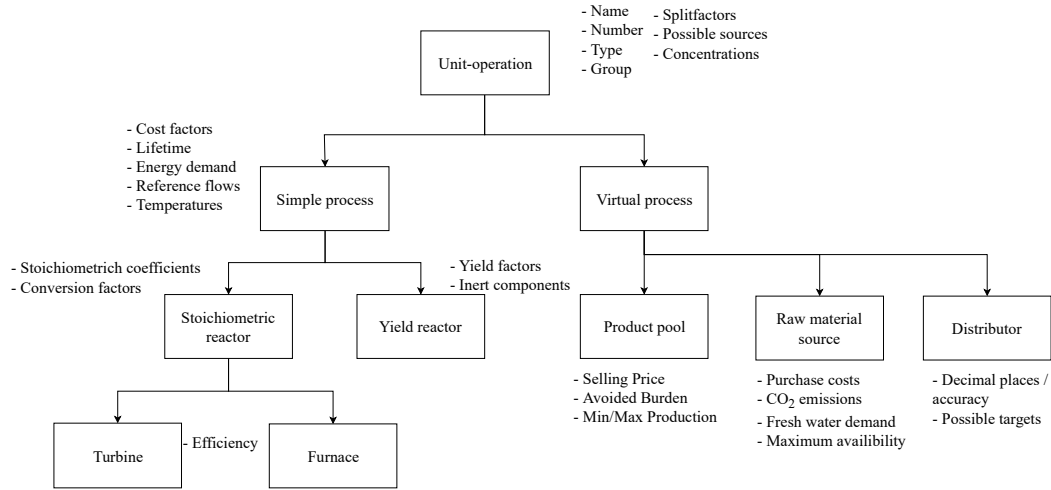
FIGURE 2.3: OUTDOOR'S UNIT-OPERATION CLASS INHERITANCE TREE.

2.3.2 Superstructure class

The Superstructure class is the main input class. It saves boundary condition data such as the electricity price, the considered species or data regarding sensitivity analysis or multi-criteria optimization. Additionally, it functions as a frame for the defined unit-operations and provides the functionality to collect the required data from those unit-operations to create an overall data file which is readable by the SuperstructureModel class. To achieve those tasks, the Superstructure class includes several attributes together with associated setter methods. Additionally, it contains a set of methods which are designed to create the final data file in a series of steps as depicted in Figure 2.4. During this sequence, first certain parameters have to prepared which are crucial for the heat balance and capital cost equations. Afterwards the boundary conditions data is loaded into a parameter list. Those parameters include non-indexed parameters such as the list of used species as well as indexed parameters such as the lower heating value of each species. When the boundary conditions data is loaded into the parameter list, remaining data from the different included unit-operations are added to the parameter list. Afterwards the parameter list is used to create a correctly formatted data file which is returned and can be used to initialize the SuperstructureModel.
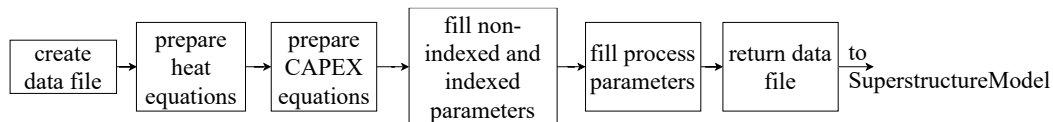
FIGURE 2.4: SEQUENCE OF CREATING THE MODEL DATA FILE FROM THE SUPERSTRUCTURE.

Certain aspects of the model, namely the heat balance and capital costs equations have to be prepared in more detail. This originates from the requirement of certain data which is dependent on both, the individual unit-operations as well as the boundary conditions. Therefore, those parameters cannot be set until both sets of classes are combined.

The process of the heat balance preparation is shown in Figure 2.5. First a temperature grid is specified to enable a temperature-based consideration of heat exchange. For that reason, the different unit-operations are scanned for heating and cooling demand and their associated inlet and outlet temperatures, which are added to temperature grid list. Included external heating and cooling utilities temperatures are directly added to the grid while they are defined. Afterwards the complete temperature grid is translated into a number of temperature intervals. Additionally, if a high temperature heat pump is to be included, its inlet and outlet temperatures are cross-referenced with the temperature grid and a capital recovery factor is calculate, both being used in the optimization model. Afterwards, the defined utility costs are distributed to all heat intervals in order to ensure, that no interval mistakenly receives external heat free of charge. In the end, the defined heating and cooling demands of the different unit-operations are partitioned for the different heat intervals based on the temperature grid as well as the defined inlet and outlet temperatures. The results of this procedure (temperature intervals, heat pump data, utility costs, temperature-depended heat shares (β-parameters)) are provided to the parameter list for later use in the optimization model.
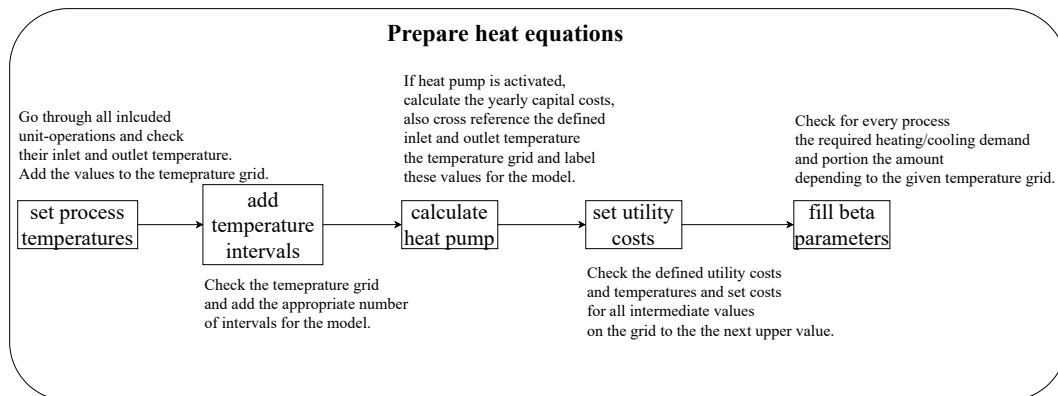
FIGURE 2.5: DETAILED VIEW INTO THE HEAT BALANCE PREPARATION METHOD.

The procedure of setting up the capital costs equations is depicted in Figure 2.6. In a first step non-linear capital cost functions of the unit-operations are linearized to keep the optimization model linear. This is done by using piece-wise linearization. Hence, the number of intervals is set up based on the input value. From that, the linear calculator (a utility function) is called, which calculates the linear pieces from economies of scale using defined reference costs, flows and scaling factors. Afterwards, every unit-operation saves its own linear cost pieces. Furthermore, the capital recovery factor for every unit operation is calculated based on its specific lifetime and the general interest rate. Two parameters that are important for cost calculation can be set independently for every unit-operation. These are the full load hours and the cost factor for operation and maintenance. However, if no specific value is set, a system wide default value is filled in. In the end yearly costs

of returning capital costs (e.g. catalysts in reactors or stacks in electrolyzers) are calculated based on either a yearly or hourly return rate. The calculated parameters are saved inside the unit-operation objects and loaded into the parameter list by the superstructure.
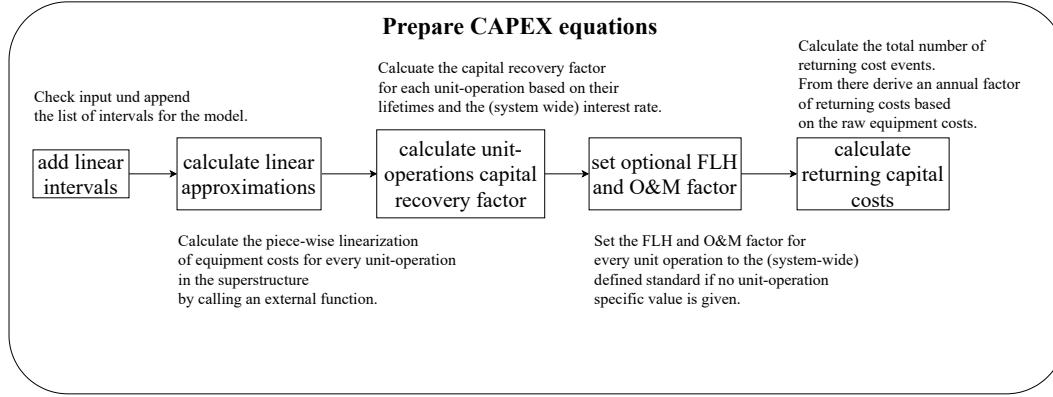
FIGURE 2.6: DETAILED VIEW INTO THE CAPITAL COST FUNCTIONS PREPARATION METHOD.

2.3.3 SuperstructureProblem class

The SuperstructureProblem class is the main handler of OUTDOOR. It manages the interaction of the other classes and ensures the right sequence of the algorithm. In order to do this, it has one public method. This method, the *solve_optimization()* method, takes the data input in form of a generated Superstructure object, as well as solver name, optimization type and solver option (if preferred). Internally it uses several private methods to setup the model instance and Optimizer object. Depending on the chosen optimization mode (single, sensitivity, multi-criteria, two-way sensitivity) it selects the appropriate Optimizer and prepares the affiliated data. For a sensitivity analysis this means in detail to set the appropriate model-parameters to mutable, as well as to calculate the sensitive parameter values from given start and end point as well as number of steps. After the Optimizer solved the problem and returns the (Multi)ModelOutput, the SuperstructureProblem forwards this output to the user.

2.3.4 SuperstructureModel class

The SuperstructureModel class inherits from Pyomos AbstractModel class. This class provides methods and attributes to write mathematical models in symbolic notation. Parameter values are unspecified at first and data values can be supplied at later time, which leads to an initialization of the model. This way the same model equations can be used to depict different cases by simply changing the data file. The SuperstructureModel class adds methods to the AbstractModel class for writing the required model equations. To achieve this, first sets are created and afterwards the different aspects of the models, namely mass balances, energy balances, cost function, greenhouse gas emissions (GHG) functions, fresh water

demand (FWD) functions, additional logic constraints and the objective function are formulated. Chapter 3 presents a detailed insight on the components and equations of OUTDOORs mathematical model.

2.3.5 Optimizer classes

There are currently four different Optimizer classes implemented in OUTDOOR. The main SingleOptimizer is the base class for three custom Optimizer. The SingleOptimizer simply takes a model instance, a solver name and, if desired, solver options like maximum time limit or allowed remaining optimality gap. The model instance has to inherit from Pyomos ConcreteModel class in order to be solvable by the Optimizer. To perform this task the SingleOptimizer creates an interface to the defined solver and simply hands over the model instance. After the model instance is solved by the external solver, the Optimizer creates the ModelOutput object and stores the model data and results into it.

The custom Optimizers include a SensitivityOptimizer, a MCDAOptimizer (MCDA=Multi-criteria decision-analysis) and a TwoWayOptimizer. All of these classes inherit from the SingleOptimizer class, therefore providing the same methods to solve optimization problems. However, their optimization procedure is adapted to their use case. The concept of those three custom Optimizers is similar, only differentiating in the operation details. All Optimizers first create an object of the SingleOptimizer, afterwards, they iteratively modify the model instance and solve a single-run using the SingleOptimizer. The returned ModelOutput object of the SingleOptimizer is stored in an overlaying MultiModelOutput object, which in the end is returned to the SuperstructureProblem and ultimately to the user. In terms of operation the Sensitivity- and TwoWayOptimizer iteratively change parameter values in the model instance, while the MCDAOptimizer changes the objective. More detail on the developed methodologies behind the MCDAOptimizer and TwoWayOptimizer is presented in chapter 4.

2.3.6 (Multi)ModelOutput class

The ModelOutput class is OUTDOOR's main output. Its purpose is to save the data from the memory intensive SuperstructureModel class and provide methods to save meta-data as well as the complete results either as .txt-file or as pickle-file which can be imported to Python for investigation at a later time. The meta-data of the model includes information on date and time of the performed calculation, the solver used and required time to solve the problem as well as the chosen objective function and the remaining optimality gap. The results data includes the models sets, parameters, variables and objective function.

The MultiModelOutput class is related to the ModelOutput class. The major difference is, that a MultiModelOutput includes a Python dictionary with multiple ModelOuput instances. By utilizing this approach, a sequence of ModelOutputs can be created in a multi-run (e.g. a sensitivity analysis) and lumped into one big object. Therefore, the MultiModelOutput includes the same information and options as the ModelOutput class using the same notation and method declarations. However, the meta-data is extended for the information on the optimization mode (e.g. sensitivity analysis, multi-criteria optimization) as well the according input data.

2.3.7 ModelAnalyzer classes

The (Multi)ModelOutput classes only store data and provide the necessary methods to save the output. However, OUTDOOR also includes three types of ModelAnalyzer classes which can perform different types of analyses using the (Multi)ModelOutput objects as inputs. The three analyzer classes are:

- BasicModelAnalyzer   → Used to analyze ModelOutput objects

- BasicMultiModelAnalyzer   → Used to analyze MultiModelOutput objects

- AdvancedMultiModelAnalyzer → Used to analyze advanced aspects of MultiModels

The BasicModelAnalyzer and BasicMultiModelAnalyzer provide the same functionalities, customized to their appropriate input file. These functionalities include:

- Display of main results (NPC, NPE, NPFWD, process alternative choices)

- Display of techno-economic analysis including:

    o Cost distribution

    o Capital cost distribution

    o Electricity demand distribution

    o Main results of energy balances and heat integration

- Display of environmental analysis including:

    o Greenhouse gas emissions distribution

    o Fresh water demand distribution

- Save different analyses as .txt-files or as bar-charts

- Automated flowsheet generation with given mass balances using distinguished shapes for different unit-operation classes

The AdvancedMultiModelAnalyzer adds special-feature analysis tools for MultiModelOutput objects. The special analysis features are tailor-made for the different optimization-modes and include:

- Automated generation and printing of sensitivity graphs → SensitivityOptimizer

- Automated generation and printing of MCDA scores → MCDAOptimizer

- Automated generation and printing of two-way sensitivity graphs → TwoWayOptimizer

2.3.8 Software modularization

OUTDOORs software architecture is designed using a modular approach for two main reasons. The first one is to enable other scientist and users to extent or customize different functionalities. This allows users to write their own Excel-reader and connecting it to the Python API, or to write additional unit-operation classes for more detailed process types e.g. using thermodynamic models. The second reason is to provide a more general modeling toolbox. This makes it possible to exchange different aspects of OUTDOOR with external parsers. For example, it would be possible to replace the SuperstructureProblem-based object management by other structures, only utilizing the remaining classes. Additionally, it is possible to supply the data file for the SuperstructureModel using other external programs and structures instead of the implemented Superstructure and Unit-Operation classes. The SingleOptimizer class solves MILP models not differentiating on the model type. Therefore, it would be possible to use only the Optimizer and provide other Pyomo models depicting e.g. supply-chain or dispatch optimization. In combination with the SingleOptimizer, also the ModelOutput class does not differentiate of the loaded model instance. This means, that this generic data container can also be connected to different model-types using the connection to the SingleOptimizer class.

3 THE MATHEMATICAL MODEL BEHIND OUTDOOR

This chapter presents the mathematical model underlaying in OUTDOOR. The model is written as a mixed-integer linear programming (MILP) model which is based on mass- and energy balances but it also includes balances for capital- and operational costs, direct and indirect greenhouse gas emissions as well as fresh water demand. Additionally, it includes a heat integration method as well as advanced mass-distribution models, both especially developed for OUTDOOR and tailored for the requirements of superstructure optimization. The chapter is structured as follows: First the objective functions are presented, afterwards the complete model is described, starting with the mass, - and energy balances, followed by costs, - and emission equations and finishing with additional logic constraints.

Parts of this chapter have been published in:

- Kenkel, P., Wassermann, T., Rose, C., & Zondervan, E. (2021). A generic superstructure modeling and optimization framework on the example of bi-criteria Power-to-Methanol process design. Computers & Chemical Engineering, 150, 107327.

3.1 OUTLINE

The mathematical model defined in the SuperstructureModel class is designed for a generic usability in superstructure optimization. One important aspect is that the model is formulated in such way that it can be applied to a wide range of applications (e.g. bioprocesses, chemical processes, heat exchanger networks etc.). Its basic function is single-criterion process design optimization considering heat, - and mass integration potentials. It should be noted, that equations are often valid for different sets and sub-sets of unit-operations, as they were already introduced in chapter 2.3.1. Therefore, a detailed look into the index-sets has to be taken. In the following, first the implemented objective functions are presented. Afterwards, a detailed insight on required model equations is given.

3.2 OBJECTIVE FUNCTIONS

Three (potential) objective functions are predefined in the modeling framework, which are depicted in Eqs. (3.1) to (3.3).

$$min\, NPC = (CAPEX + OPEX - PROFITS)/cap^{PROD} \tag{3.1}$$

$$min\, NPE \\ = (GWP^{EMITTED} + GWP^{UT,TOT} - GWP^{CAPTURE} - GPW^{CREDITS})/cap^{PROD} \tag{3.2}$$

$$min\, NPFWD = (FWD^{RM} + FWD^{UT,TOT} - FWD^{CREDITS})/cap^{PROD} \tag{3.3}$$

The first represents an economic metric. The total net production costs (*NPC*) are calculated based on the total annualized capital costs (*CAPEX*), total annual operational costs (*OPEX*), credits in form of sold by-products (*PROFITS*) and the annually produced main product (cap^{PROD}).

The total net production (greenhouse gas) emissions (*NPE*), i.e. a dedicated environmental impact, represents the second objective function. The induced emissions are derived from directly emitted greenhouse gases ($GWP^{EMITTED}$) as well as indirectly induced emissions from utilities such as electricity or heat ($GWP^{UT,TOT}$). The procedure is limited to cradle-to-gate system boundaries and inspired by the life cycle assessment approach. Additionally, to the direct and indirect emissions, indirect emissions of raw material acquisition are considered. This is done by including a term ($GWP^{CAPTURE}$) which is positive for captured CO_2 and negative for raw materials whose production induce GHG emissions. Finally, the total emissions are reduced by credits achieved by the avoided burden approach known from the life-cycle assessment methodology and set into context of yearly produced main product (cap^{PROD}) [29]. The last objective function displays the net production demand of fresh water (*NPFWD*). It is calculated from the direct consumption of fresh water and indirect consumption for the production

of other raw materials (FWD^{RM}) as well as indirectly consumed water from utilities supply ($FWD^{UT,TOT}$) and avoided burdens from by-products ($FWD^{CREDITS}$).

3.3 MASS BALANCES

The superstructure is built by the definition and interaction of the different unit-operations (unit-operations indexed as $u \in U$). The foundation of these unit-operations are their mass balances, which are formulated in a generic way according to Figure 3.1. Based on the mass balances, energy demands, costs as well as equipment sizes, emissions and fresh water are calculated for the different unit-operations. In the following, the general mass balance concept is elaborated.
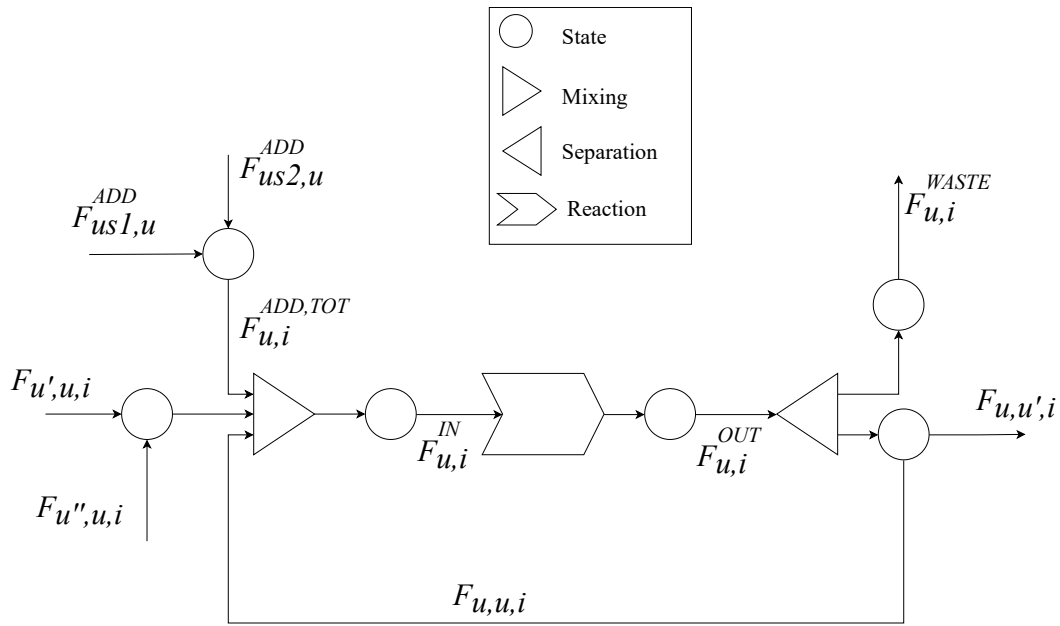
FIGURE 3.1: MASS BALANCE CONCEPT FOR A GENERIC UNIT-OPERATION $u \in U$ (E.G. A STOICHIOMETRIC/ YIELD REACTOR OR STREAM SPLITTER).

The input of a specific unit-operation u is defined by all feed streams $F_{u',u,i}$ from other unit-operations u', combined with a total added flow from different raw material sources $F_{u,i}^{ADD,TOT}$ (cf. Eq. (3.4)). The added flow $F_{u,i}^{ADD,TOT}$ is defined as the sum of added flows $F_{(u_s,u)}^{ADD}$ from raw material source u_s to unit-operation u, multiplied with their respective component composition $\varphi_{u_s,i}$ (Eq. (3.5)). To ensure, that only chosen processes consume raw materials Eq. (3.6) introduces a binary variable Y_u for every unit-operation, which turns one if the process is chosen and zero if the process is not chosen. Sometimes, raw materials are limited. Therefore, to account for mass flow limitations, the total amount of consumed raw material per hour is calculated using Eq. (3.7) and an upper limit ul_{u_s} is introduced with Eq. (3.8). flh_u and flh_{u_s} depict full load hours of different unit-operations, which could vary depending on the depicted process.

In some unit-operations, certain component concentrations con_u have to be met. This is ensured by Eq. (3.9). Depending on the process, several components of either the inlet or the outlet flow of the process are used as basis for a required concentration. Using Pyomo as modeling language it is possible to benefit from Pythons conditional programming abilities. Thus, the required choice is implemented by if-statement programming. Four parameters, $\kappa_u^{2,LHS}$, $\kappa_u^{2,RHS}$, $\kappa_{u,i}^{1,LHS}$ and $\kappa_{u,i}^{1,RHS}$ are implemented for every unit-operation. $\kappa_u^{2,LHS}$ and $\kappa_u^{2,RHS}$ are either zero or one if the output flow or the input flow has to be considered or three if no flow at all is important (visualized by the curved brackets in Eq. (3.9)). If a concentration value is included, $\kappa_{u,i}^{1,LHS}$ and $\kappa_{u,i}^{1,RHS}$ are 1 for every component i if it has to be considered for the concentration calculation. While building the model, OUTDOOR will inspect the given $\kappa_u^{2,LHS}$ and $\kappa_u^{2,RHS}$ for every unit-operation and write the matching type of equation to the model file.

$$F_{u,i}^{IN} = \sum_{u' \in U} F_{u',u,i} + F_{u,i}^{ADD,TOT} \qquad u \in U, i \in I \qquad (3.4)$$

$$F_{u,i}^{ADD,TOT} = \sum_{(u_s,u) \in U_{Sp}} F_{(u_s,u)}^{ADD} \cdot \varphi_{u_s,i} \qquad u \in U, u_s \in U_s, i \in I \qquad (3.5)$$

$$F_{(u_s,u)}^{ADD} \le \alpha_u \cdot Y_u \qquad \begin{matrix} u \in U, u_s \in U_s, \\[4pt] (u,u_s) \in US \end{matrix} \qquad (3.6)$$

$$F_{u_s}^{SOURCE} = \sum_{(u_s,u) \in U_{Sp}} F_{(u_s,u)}^{ADD} \cdot \frac{flh_u}{flh_{u_s}} \qquad u \in U, u_s \in U_s \qquad (3.7)$$

$$F_{u_s}^{SOURCE} \le ul_{u_s} \qquad u_s \in U_s \qquad (3.8)$$

$$\sum_{i \in I} \begin{cases} F_{u,i}^{OUT} \\ F_{u,i}^{IN} \end{cases} \cdot \kappa_{u,i}^{1,LHS} = con_u \cdot \sum_{i \in I} \begin{cases} F_{u,i}^{OUT} \\ F_{u,i}^{IN} \end{cases} \cdot \kappa_{u,i}^{1,RHS} \qquad u \in U \qquad (3.9)$$

Based on the inlet flows and the class of unit-operation, the outlet flow $F_{u,i}^{OUT}$ is calculated. This is done for stoichiometric classes like stoichiometric reactors, furnaces and steam turbines, but also for normal stream splitters using Eq. (3.10). $\gamma_{i,r,u}$ are stoichiometric factors of component i, in reaction r and unit u, $\theta_{m,r,u}$ are conversion factors of reactant m, in reaction r and unit u and $F_{u,m}^{IN}$ is the inlet flow of reactant m. If the process is not a reactor but a simple splitter unit, stoichiometric factors and conversion factors will be zero. Therefore, the outlet flow is equal to the inlet flow.

$$F_{u,i}^{OUT} = F_{u,i}^{IN} + \sum_{r \in R, \ m \in M} \gamma_{i,r,u} \cdot \theta_{m,r,u} \cdot F_{u,m}^{IN} \qquad u \in U_{STOIC}, i \in I \qquad (3.10)$$

If the process unit is modeled as a yield reactor, the outlet flow of components i are calculated differently for inert components and reactive components.

Reactive components output flows are calculated with Eq. (3.11) where $\zeta_{u,i}$ are yield coefficients of component i in unit u. The output flow of a non-reactive component is made up by its inlet flow plus the sum of built i from other components (ref. Eq. (3.12)).

$$F_{(u,i)}^{OUT} = \zeta_{u,i} \cdot \sum_{i \ \forall \ (u,i) \notin UI_{INERT}} F_{u,i}^{IN} \qquad \begin{aligned} &u \in U_{YIELD} \\ &(u,i) \notin UI_{INERT}, \\ &i \in I \end{aligned} \qquad (3.11)$$

$$F_{(u,i)}^{OUT} = F_{(u,i)}^{IN} + \zeta_{u,i} \cdot \sum_{i \ \forall \ (u,i) \notin UI_{INERT}} F_{u,i}^{IN} \qquad \begin{aligned} &u \in U^{YIELD} \\ &(u,i) \in UI_{INERT}, \\ &i \in I \end{aligned} \qquad (3.12)$$

To complete the mass balance, flows that are linked between two process units $F_{u,u',i}$ are defined and combined with the binary decision variables $Y_{u'}$. These turn one if a unit-operation u' is activated and zero if u' is not chosen.

To avoid non-linearities these equations are written as Big-M constraints as shown in Eqs. (3.13) – (3.15). $\mu_{u,u',i}$ depicts a predefined split factor of component i going from unit u to unit u'.

$$F_{u,u',i} \leq \alpha_u \cdot Y_{u'} \qquad u, u' \in U, i \in I \qquad (3.13)$$

$$F_{u,u',i} \leq \mu_{u,u',i} \cdot F_{u,i}^{OUT} + \alpha_u \cdot (1 - Y_{u'}) \qquad u, u' \in U, i \in I \qquad (3.14)$$

$$F_{u,u',i} \geq \mu_{u,u',i} \cdot F_{u,i}^{OUT} - \alpha_u \cdot (1 - Y_{u'}) \qquad u, u' \in U, i \in I \qquad (3.15)$$

All mass flows which are not directed from one to another process leave the system boundaries and hence are considered as waste flows $F_{u,i}^{WASTE}$. They are summed up to a total waste flow $F_i^{WASTE,TOT}$ using Eq. (3.16) and (3.17).

$$F_{u,i}^{WASTE} = F_{u,i}^{OUT} - \sum_{u' \in U} F_{u,u',i} \qquad u \in U, i \in I \qquad (3.16)$$

$$F_i^{WASTE,TOT} = \sum_{u \in U} F_{u,i}^{WASTE} \qquad i \in I \qquad (3.17)$$

The desired capacity of the plant is set by Eq. (3.18) where the annual capacity flow into the main product pool is divided by the full load hours per year.

$$\sum_{i \in I} F_{u,i}^{IN} = \frac{cap^{PROD}}{flh_u} \qquad \begin{aligned} u & \\ & = \{u \in U_{PP}|u \\ & = Main\ Pool\} \end{aligned} \qquad (3.18)$$

3.3.1 Distributor units

Connecting flows from unit-operations that are labelled as distributors are calculated differently as to normal unit-operations. The inlet $F_{u,i}^{IN}$ and outlet flow $F_{u,i}^{OUT}$ are derived similar to simple splitting units according to Eqs. (3.4) and (3.10). However, for distributor units, no predefined split factors are given. These unit-operations tasks are to simply mix incoming flows and split the product to predefined target processes with constant compositing while enabling variable split factors. In order to provide this functionality one continuous and one binary variable $F_{(u,u'),(u,k),i}^{DIST}$ and $Y_{(u,u'),(u,k)}^{DIST}$ as well as the indexed split parameter $d_{(u,k)}^{DIST}$ are introduced (ref. Figure 3.2). First the variable $F_{(u,u'),(u,k),i}^{DIST}$ is calculated for every distributor-target set $(u, u') \subseteq U_{DIST}$ every component i and every distributor split factor set $(u, k) \subseteq UK$ as shown in Eqs. (3.19) - (3.21).

$$F_{(u,u'),(u,k),i}^{DIST} \leq d_{(u,k)}^{DIST} \cdot F_{u,i}^{OUT} + \alpha_u \cdot \left(1 - Y_{(u,u'),(u,k)}^{DIST}\right) \qquad \begin{aligned} (u, u', u, k) \\ \in UK_D, i \in I \end{aligned} \qquad (3.19)$$

$$F_{(u,u'),(u,k),i}^{DIST} \geq d_{(u,k)}^{DIST} \cdot F_{u,i}^{OUT} - \alpha_u \cdot \left(1 - Y_{(u,u'),(u,k)}^{DIST}\right) \qquad \begin{aligned} (u, u', u, k) \\ \in UK_D, i \in I \end{aligned} \qquad (3.20)$$

$$F_{(u,u'),(u,k),i}^{DIST} \leq \alpha_u \cdot Y_{(u,u'),(k',k)}^{DIST} \qquad \begin{aligned} (u, u', u, k) \\ \in UK_D, i \in I \end{aligned} \qquad (3.21)$$

This is done by multiplying the outlet stream $F_{u,i}^{OUT}$ with the indexed split parameter $d_{(u,k)}^{DIST}$ and the binary variable $Y_{(u,u'),(u,k)}^{DIST}$ which is one if distributor u sends the k'th amount of the outlet stream to target u'. $d_{(u,k)}^{DIST}$ includes values that are inspired by the binary number system and whose sum can built every number from 0 to 1. The accuracy of the distributor units in terms of splitting depends on their parameter $d_{(u,k)}^{DIST}$ and the length of the k index. A length of K=5 leads to a parameter $d_{(u,k)}^{DIST} = [0, 0.1 , 0.2, 0.4, 0.8]$ depicting splits in 10% steps. A length of K = 9 leads to a parameter $d_{(u,k)}^{DIST} = [0, 0.1 , 0.2, 0.4, 0.8, 0.01, 0.02, 0.04, 0.08]$ allowing 1% splits and so on. Based on the flow $F_{(u,u'),(u,k),i}^{DIST}$ the real connecting flow $F_{(u,u'),i}$ is calculated as the sum of all used $F_{(u,u'),(u,k),i}^{DIST}$ as given in Eqs. (3.22) and (3.23). To

ensure mass balance, the sum of the flows $F_{(u,u'),i}$ to all considered targets has to be equal to the total outlet flow (ref. Eq. (3.24)).

$$F_{u,u',i} = F_{(u,u'),(u,k=1),i}^{DIST} + F_{(u,u'),(u,k=2),i}^{DIST} + \dots$$

Index k	Split fraction
1	0
2	0.1
3	0.2
4	0.4
5	0.8
....	....
n	m

$$F_{(u,u'),(u,k=2),i}^{DIST} = F_{u,i}^{OUT} \cdot d_{u,k}^{DIST} \cdot Y_{(u,u'),(u,k=2),i}^{DIST}$$

$$F_{(u,u''),(u,k=5),i}^{DIST} = F_{u,i}^{OUT} \cdot d_{u,k}^{DIST} \cdot Y_{(u,u''),(u,k=5),i}^{DIST}$$

$$F_{u,u'',i} = F_{(u,u''),(u,k=1),i}^{DIST} + F_{(u,u''),(u,k=2),i}^{DIST} + \dots$$
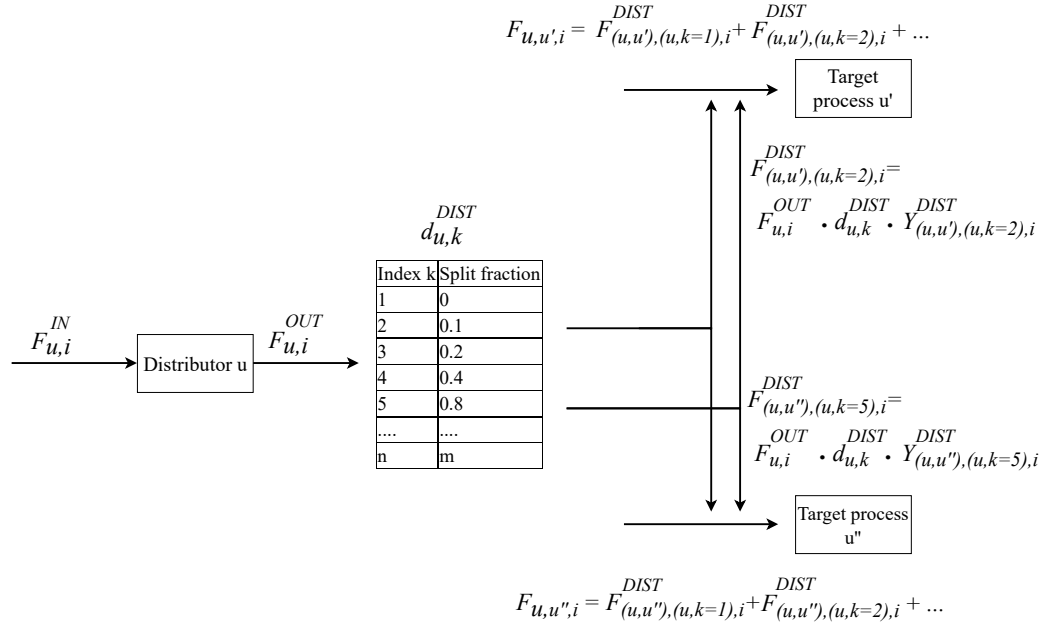
FIGURE 3.2: REPRESENTATION OF DISTRIBUTOR UNIT-OPERATION MASS BALANCE CALCULATION.

$$F_{(u,u'),i} \leq \sum_{(u,k) \in UK, (u,u',u,k) \in UK_D} F_{(u,u'),(u,k),i}^{DIST} + \alpha_u \cdot (1 - Y_{u'}) \quad \begin{aligned} &(u,u') \\ &\in U_{DIST}, \\ &i \in I \end{aligned} \quad (3.22)$$

$$F_{(u,u'),i} \geq \sum_{(u,k) \in UK, (u,u',u,k) \in UK_D} F_{(u,u'),(u,k),i}^{DIST} - \alpha_u \cdot (1 - Y_{u'}) \quad \begin{aligned} &(u,u') \\ &\in U_{DIST}, \\ &i \in I \end{aligned} \quad (3.23)$$

$$\sum_{(u,u') \in U_{DIST}} F_{(u,u'),i} = F_{u,i}^{OUT} \quad (3.24)$$

3.4 HEAT INTEGRATION

The supply of heating and cooling utilities can be dealt with in different ways. The most detailed approach is an extensive heat exchanger network (HEN) optimization, e.g. using the transshipment model method [42], [43], [70]. However, rigorous HEN optimization using MINLP models is computationally expensive. Since OUTDOOR's model aims for early design phase superstructure optimization, it is not practical to invest extensive computational and modeling resources for a detailed HEN optimization, while other aspects, such as capital cost calculations are based on simpler concepts. Hence, rigorous HEN optimization

concepts are simplified in OUTDOOR to keep the model linear, whilst yielding initial estimates on heat integration and network costs.

Prior to optimization, the required heat integration data must be prepared. This is automated inside OUTDOOR's object-oriented superstructure construction framework (for details see chapter 2.3.2). During data preparation, first heating and cooling demands of the different processes are specified by energy demands $\tau_{u,ut}^{HEAT}$ and $\tau_{u,ut}^{COOL}$, as well as given inlet and outlet temperatures. Every process can require up to two heating/cooling demands. This allows for the usage of bigger surrogate models, where different unit-operations (some exothermic others endothermic) are combined into one surrogate unit-operation. It is not necessary to use this feature, but due to the reduced data input, it can come in handy if large superstructures are investigated. Next, OUDOOR defines a temperature grid with fixed heat intervals using the inlet and outlet temperatures of the processes as well as predefined utility temperatures as shown in Figure 3.3. Although it is possible to implement different utilities, it is important to implement at least one hot utility whose temperature can satisfy the heat demand of the unit-operations as well as one cold utility which is able to cool down remaining waste heat. To keep the heat integration simple, it is assumed that only the heat of vaporization is used from external steam.

Based on the temperature grid and the predefined specific energy demand, OUTDOOR partitions the required heating and cooling between the heat intervals as shown in Figure 3.3 and Eq. (3.25) and (3.26). If unit-operation u is a non-isothermal process the ratio $\beta_{u,hi}^{H}$ is calculated using Eq. (3.25), however if the process is designed as an isothermal process ($\Delta T_u = 0$) the ratio for the heat interval of the corresponding temperature is set to 1, using Eq. (3.26).

$$\beta_{u,ut,hi}^{H} = \frac{(T_{hi-1} - T_i)}{\Delta T_u} \qquad u \in U, hi \in HI, ut \in HUT \qquad (3.25)$$

$$\beta_{u,ut,hi}^{H} = 1 \qquad \begin{aligned} & u = \\ & \{u \in U \,|\, u = \\ & Isothermal\}, hi \in HI, \quad ut \in \\ & HUT \end{aligned} \qquad (3.26)$$

The data preparation in terms of heat interval based heating and cooling requirement, as described before, is detached from the actual optimization model. OUTDOOR calculates the heat interval-based heat ratios $\beta_{u,ut,hi}^{H}$ prior to the optimization and feeds them as a parameter to the model itself.

Using the specific heat demand, the heat interval ratio $\beta_{u,ut,hi}^{H}$ and a specific flow $M_{ut,u}^{REF,UT}$ the cooling demand $Q_{u,hi}^{C}$ and the heating demand $Q_{u,hi}^{H}$ of process unit u is calculated using Eq. (3.27) and (3.28). Here the specific flow is determined using

a similar approach as in the concentration calculation, with additional options to link energy demand to either the molar flow through the molecular weight (MW_i) or the heat capacity (cp_i) (ref. Eq. (3.29)).

$$Q^H_{u,hi} = \sum_{ut \in HUT} \tau^{HEAT}_{u,ut} \cdot M^{REF,UT}_{ut,u} \cdot \beta_{u,ut,hi} \qquad \begin{array}{l} u \in U, \\[6pt] hi \in HI \end{array} \qquad (3.27)$$

$$Q^C_{u,hi} = \sum_{ut \in HUT} \tau^{COOL}_{u,ut} \cdot M^{REF,UT}_{ut,u} \cdot \beta_{u,ut,hi} \qquad \begin{array}{l} u \in U, \\[6pt] hi \in HI \end{array} \qquad (3.28)$$

$$M^{REF,UT}_{ut,u} = \sum_{i \in I} \begin{cases} F^{OUT}_{u,i} \\ F^{IN}_{u,i} \\ F^{IN}_{u,i} \big/ mw_i \\ F^{OUT}_{u,i} \big/ mw_i \\ F^{IN}_{u,i} \cdot cp_i \cdot uc \\ F^{OUT}_{u,i} \cdot cp_i \cdot uc \end{cases} \cdot \kappa^{1,UT}_{ut,u,i} \qquad u \in U \qquad (3.29)$$
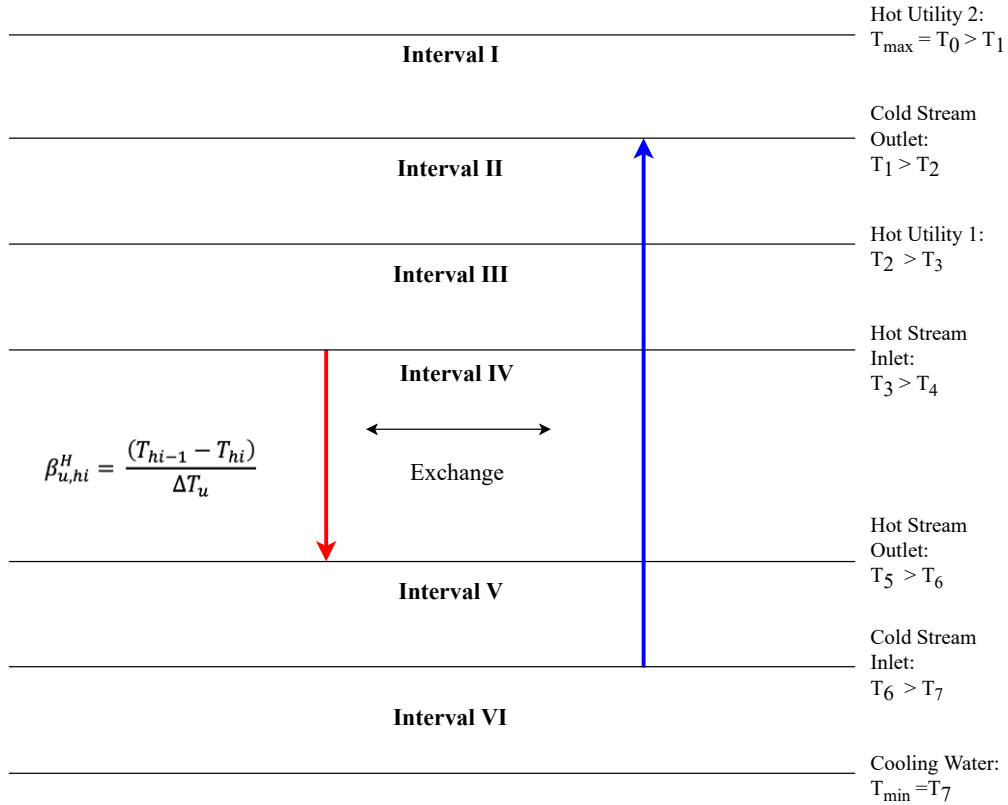
FIGURE 3.3: EXAMPLE REPRESENTATION OF THE TEMPERATURE GRID WITH HEAT INTERVALS.

Additionally, to the interval-based heating and cooling demand, some unit-operations are labelled as furnaces. These units burn combustible components to produce heat at the highest defined temperature interval, generally superheated steam. The usable heat is calculated by the lower heating value lhv_i and an

efficiency coefficient η_u^{HEAT} (cf. Eq. (3.30)). This superheated steam can be used internally or sold to the market, realized by Eq. (3.31).

$$Q_u^{PROD} = \eta_u^{HEAT} \cdot \sum_{i \in I} F_{u,i}^{IN} \cdot lhv_i \qquad\qquad u \in U_{FUR} \qquad\qquad (3.30)$$

$$Q^{PROD,USE} = \sum_{u \in U_{FUR}} Q_u^{PROD} - Q^{PROD,SELL} \qquad\qquad\qquad\qquad (3.31)$$

Based on the calculated heating and cooling demands as well as the produced superheated steam, the energy balances are written for every heat interval for the heating side as shown in Eq. (3.32) and (3.33) as well as the cooling side as given in Eqs. (3.34) - (3.37).

$$\sum_{u \in U} \left(Q_{u,hi}^H \cdot {flh_u}/{hr} \right) - Q_{hi}^{DEFI} - Q_{hi}^{EX} = 0 \qquad \begin{array}{l} hi \in HI \\ \notin HI^{HP,OUT} \end{array} \qquad (3.32)$$

$$\sum_{u \in U} \left(Q_{u,hi}^H \cdot {flh_u}/{hr} \right) - Q_{hi}^{DEFI} - Q_{hi}^{EX} - Q^{HP,USE} = 0 \quad hi \in HI^{HP,OUT} \qquad (3.33)$$

Q_{hi}^{DEFI} depicts the heat deficit in interval hi which cannot be supplied by exchanged heat Q_{hi}^{EX}. hr represents the general, default full load hours of the system. For hot streams, residual heat Q_{hi}^{RESI} is calculated at each interval. This heat can be cascaded down to intervals with lower temperatures. On the inlet temperature heat interval of the defined heat pump ($HI^{HP,IN}$) heat surplus can also be used to provide heat for the defined outlet temperature heat interval ($HI^{HP,OUT}$). On the lowest temperature interval (HI^M) residual heat has to be cooled down by cooling water (Q^{COOL}).

$$\sum_{u \in U} \left(Q_{u,hi}^C \cdot {flh_u}/{hr} \right) - Q_{hi}^{RESI} - Q_{hi}^{EX} + Q^{PROD,USE} \\ = 0 \qquad\qquad\qquad\qquad\qquad\qquad hi = 1 \qquad (3.34)$$

$$\sum_{u \in U} \left(Q_{u,hi}^C \cdot {flh_u}/{hr} \right) - Q_{hi}^{RESI} - Q_{hi}^{EX} + Q_{hi-1}^{RESI} - Q^{HP} \\ = 0 \qquad\qquad\qquad\qquad\qquad\qquad hi \in HI^{HP,IN} \qquad (3.35)$$

$$\sum_{u \in U} \left(Q_{u,hi}^C \cdot {flh_u}/{hr} \right) - Q_{hi}^{RESI} - Q_{hi}^{EX} + Q_{hi-1}^{RESI} = 0 \qquad \begin{array}{l} hi \in HI \\ \notin HI^{HP,IN} \vee 1 \\ \vee HI^M \end{array} \qquad (3.36)$$

$$\sum_{u \in U} \left(Q_{u,hi}^C \cdot {flh_u}/{hr} \right) + Q_{hi-1}^{RESI} - Q_{hi}^{EX} - Q^{COOL} = 0 \qquad hi = HI^M \qquad (3.37)$$

The exchanged heat at the highest temperature interval *hi*=1 can only be lower or equal to the sum of required cooling and internally utilized superheated steam as well as the sum of required heating in this interval. For all other intervals the exchanged heat has to be lower or equal to the required cooling plus the residual heat and lower than the required heating (cf. Eqs. (3.38) - (3.40)). In addition, a binary variable Y_{hi}^{HEX} is introduced to distinguish between heat intervals chosen for heat exchange and those who are not (ref. Eq. (3.41)).

$$Q_{hi}^{EX} \leq \sum_{u \in U} Q_{u,hi}^{C} + Q^{PROD,USE} \qquad hi = 1 \qquad (3.38)$$

$$Q_{hi}^{EX} \leq \sum_{u \in U} Q_{u,hi}^{H} \qquad hi \in HI \qquad (3.39)$$

$$Q_{hi}^{EX} \leq \sum_{u \in U} Q_{u,hi}^{C} + Q_{hi-1}^{RESI} \qquad \begin{aligned} hi = \\ \{hi \in HI \mid hi \\ \neq 1\} \end{aligned} \qquad (3.40)$$

$$Q_{hi}^{EX} \leq Y_{hi}^{HEX} \cdot \alpha^{HEX} \qquad hi \in HI \qquad (3.41)$$

This heat integration framework provides a way to implement a high temperature heat pump, which uses low exegetic heat as well as electricity for generation of low-pressure steam. The ratio of usable steam $Q^{HP,USE}$ and utilized low-ex heat Q^{HP} is determined by the coefficient of performance cop^{HP} as expressed in Eq. (3.42).

$$Q^{HP,USE} = \frac{Q^{HP}}{1 - (1 - cop^{HP})} \qquad (3.42)$$

3.5 UTILITY BALANCES

Besides heating and cooling, electricity and chilling are additional utilities which are included in the model. Chilling describes low temperature cooling which cannot be satisfied by cooling water and therefore is not part of the heat integration. If one of these utilities is consumed in unit-operation *u*, the demand is calculated using a specific utility demand $\tau_{u,ut}^{UT}$ and the corresponding unit specific flow $M_{u,ut}^{REF,UT}$ (ref. Eq. (3.43)) similar to the calculation of heating and cooling demand. If the unit *u* is labelled as an electricity generation unit, e.g. a combined power circle process, the produced electricity is calculated using a process efficiency η_u^{EL} together with the lower heating values LHV_i of the entering compounds as depicted in Eq. (3.44). In addition to unit-operation specific electricity demand and generation, further electricity demand can be generated if

a high-temperature heat pump is utilized for heat integration. This demand depends on the coefficient of performance (COP) and the provided heat, as shown in Eq. (3.45). The total chilling utility demand is derived from the sum of all unit-operations (Eq. (3.46)). The total net electricity demand is determined by the sum of the unit-operations plus the demand of the heat pump and minus the total production by electricity generators (see Eq. (3.47)).

$$E_{u,ut}^{UT} = \tau_{u,ut}^{UT} \cdot M_{u,ut}^{UT} \qquad\qquad u \in U, ut \notin HUT \qquad (3.43)$$

$$E_u^{EL,PROD} = \eta_u^{EL} \cdot \sum_{i \in I} F_{u,i}^{IN} \cdot lhv_i \qquad\qquad u \in U_{TUR} \qquad (3.44)$$

$$E^{EL,HP} = \frac{Q^{HP}}{(cop^{HP} - 1)} \qquad\qquad (3.45)$$

$$E_{ut=Chilling}^{TOT} = \sum_{u \in U} E_{u,ut=Chilling}^{UT} \qquad\qquad (3.46)$$

$$E_{ut=Electricity}^{TOT} = \sum_{u \in U} E_{u,ut=Electricity}^{UT} + E^{EL,HP}$$
$$- \sum_{u \in U_{TUR}} E_u^{EL,PROD} \qquad\qquad (3.47)$$

3.6 COST FUNCTIONS

The total annualized capital costs (CAPEX) are calculated based on major equipment costs (EC_u). These costs are in general non-linearly depending on the capacity of a unit-operation u. Using economy of scale and a reference plant, costs can be calculated using Eq. (3.48). The specific flow M_u^{CAPEX} is again determined during the calculation, using Eq. (3.49).

$$EC_u^{Non-linear} = C_u^{REF} \left(\frac{M_u^{CAPEX}}{M_u^{REF}}\right)^{f_u} \cdot \frac{CECPI}{CECPI_u^{REF}} \qquad\qquad u \in U_c \qquad (3.48)$$

$$M_u^{CAPEX} = \begin{cases} \sum_{i \in I} \begin{cases} F_{u,i}^{OUT} \\ F_{u,i}^{IN} \end{cases} \cdot \kappa_{u,i}^{1,CAPEX} \\ E_u^{EL} \\ Q_u^{PROD} \\ E_u^{EL,PROD} \end{cases} \qquad u \in U_c \qquad (3.49)$$

However, the economies of scale are non-linear and can therefore pose serious computational issues in solving, especially for large superstructures with many unit-operations. To reduce the complexity of the model, the economies of scale

equations can be linearized using piece-wise linear formulation and lambda-constraint programming, as presented in Eq. (3.50) and (3.51) [71].

$$M_u^{CAPEX} = \sum_{p \in P} \lambda_{p,u} \cdot x_{p,u} \qquad\qquad u \in U_c \qquad\qquad (3.50)$$

$$EC_u = \sum_{p \in P} \lambda_{p,u} \cdot f(x)_{p,u} \qquad\qquad u \in U_c \qquad\qquad (3.51)$$

$$\sum_{p \in P^I} Z_{u,p}^{CAPEX} = 1 \qquad\qquad u \in U_c \qquad\qquad (3.52)$$

$$S_{u,p}^{CAPEX} \le Z_{u,p}^{CAPEX} \qquad\qquad u \in U_c, \qquad p \in P \qquad (3.53)$$

$$\lambda_p = Z_{u,p}^{CAPEX} - S_{u,p}^{CAPEX} \qquad\qquad u \in U_c, \qquad p = 1 \qquad (3.54)$$

$$\lambda_p = S_{u,p-1}^{CAPEX} \qquad\qquad \begin{array}{l} u \in U_c, \\ \\ p \in P^M \end{array} \qquad (3.55)$$

$$\lambda_p = Z_{u,p}^{CAPEX} - S_{u,p}^{CAPEX} + S_{u,p-1}^{CAPEX} \qquad \begin{array}{l} u \in U_c, \\ \\ p = \\ \{p \in P \mid P \\ \ne 1 \lor P^M\} \end{array} \qquad (3.56)$$

Here $x_{p,u}$ and $f(x)_{p,u}$ represent pre-calculated reference flows M_u^{CAPEX} and equipment costs $EC_u^{Non-linear}$ of linear interval piece p, as shown in Figure 3.4. Eqs. (3.52) – (3.56) illustrate the implementation of special ordered sets type 2 as presented in [72]. The procedure of linearization is, similar to the heat balance preparation detached from the actual optimization model (see chapter 2.3.2), so that Eqs. (3.50) – (3.56) are the constraints implemented in the model and $x_{p,u}$ as well as $f(x)_{p,u}$ as fed to the model as pre-calculated parameters.
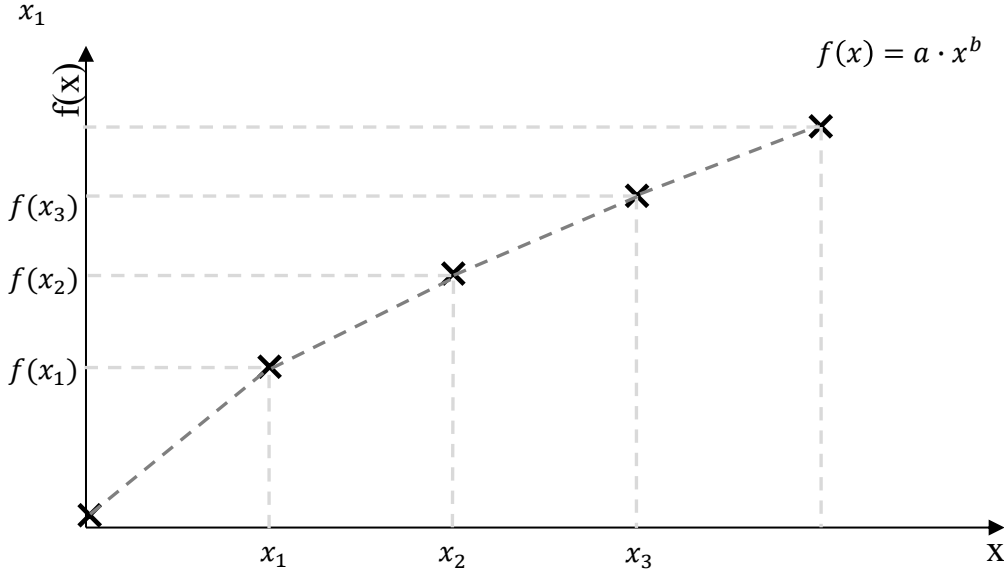
FIGURE 3.4: EXAMPLE OF PIECE-WISE LINEARIZED FUNCTION AS USED FOR CAPITAL COSTS.

Using the calculated major equipment costs, first the fixed capital investment (FCI_u) is determined by linear cost factors for direct (installation, electrics etc.) as well as indirect costs (engineering, legal costs, insurance) based on the approach by Peters et al. (ref. Eq. (3.57)) [73]. Afterwards the annualized capital costs (ACC_u) are computed using a capital recovery factor (crf_u^{UNITS}) which is determined prior to the actual optimization for each process unit to avoid non-linearities (cf. Eqs. (3.58) and (3.59)).

$$FCI_u = EC_u \cdot (1 + f_u^{DC} + f_u^{IDC}) \qquad\qquad u \in U_c \qquad (3.57)$$

$$ACC_u = FCI_u \cdot crf_u^{UNITS} \qquad\qquad u \in U_c \qquad (3.58)$$

$$crf_u^{UNITS} = \frac{ir \cdot (1 + ir)^{lt_u}}{(1 + ir)^{lt_u} - 1} \qquad\qquad u \in U_c \qquad (3.59)$$

Some major equipment have regular recurring investment costs, such as catalysts or electrolysis stacks which must be replaced after a defined time (e.g. years or operating hours). These costs are considered as repeating recurrence costs ACC_u^{RE} (ref Eq. (3.61)). These costs are calculated as a function of the required number of periods n_u^{RE} during the lifetime of a unit-operation and a percentage c_u^{RE} of the raw purchase equipment costs. The number of periods is dependent on the lifetime of the unit-operation as well as the frequency of replacement, which is either given on hourly basis ($lt_u^{RE,h}$) or on yearly basis ($lt_u^{RE,y}$) (Eq. (3.60)). The second case is more relevant if the plant is operated with low occupancy rate.

$$n_u^{RE} = \begin{cases} lt_u \big/ lt_u^{RE} \\ lt_u \cdot flh_u \big/ lt_u^{RE,h} \end{cases} \qquad\qquad u \in U_c \qquad (3.60)$$

$$ACC_u^{RE} = c_u^{RE} \cdot n_u^{RE} \cdot EC_u \cdot crf_u^{UNITS} \qquad\qquad u \in U_c \qquad (3.61)$$

In addition to the costs derived from the major equipment, the capital costs for the heat integration have to be considered. Here two factors have to be calculated. The capital costs for the high temperature heat pump, as well as the heat exchanger network (HEN) itself.

The costs for the heat pump are derived from Eq. (3.62), using the heat supplied by the heat pump as well as a capital recovery factor crf^{HP} and specific costs per kW installed (ec^{HP}).

$$ACC^{HP} = Q^{HP,USE} \cdot crf^{HP} \cdot ec^{HP} \qquad\qquad (3.62)$$

The costs of the HEN are calculated using a simplified approach of the major equipment cost calculation for heat exchangers. Here, it is assumed, that the costs of the simplified HEN are reflected by the costs of one big heat exchanger per heat interval. The costs of the heat exchanger (HEX) are dependent on its heat duty (cf. Eqs. (3.63) - (3.65)). Linearized reference costs of a reference HEX were calculated beforehand using Aspen Plus simulation, resulting in slope m^{HEN} and axis intercept b^{HEN}. To only consider heat exchangers that exchange heat, the costs are derived using the defined binary variable Y_{hi}^{HEX}, written as a Big-M constraint. The total annualized capital expenditures ($CAPEX$) are defined by the sum of all annualized capital costs (ref. Eq. (3.66)).

$$ACC_{hi}^{HEN} \leq m^{HEN} \cdot Q_{hi}^{EX} + b^{HEN} + \alpha^{HEX} \cdot \left(1 - Y_{hi}^{HEX}\right) \qquad hi \in HI \quad (3.63)$$

$$ACC_{hi}^{HEN} \geq m^{HEN} \cdot Q_{hi}^{EX} + b^{HEN} - \alpha^{HEX} \cdot \left(1 - Y_{hi}^{HEX}\right) \qquad hi \in HI \quad (3.64)$$

$$ACC_{hi}^{HEN} \leq \alpha^{HEX} \cdot Y_{hi}^{HEX} \qquad hi \in HI \quad (3.65)$$

$$CAPEX = \sum_{u \in U_c} ACC_u + ACC^{HP} + \sum_{hi \in HI} ACC_{hi}^{HEN} + \sum_{u \in U_c} ACC_u^{RE} \qquad (3.66)$$

The operational costs ($OPEX$) are derived from utility costs, raw material costs as well as costs for operation and maintenance of the process plant. The electricity and chilling costs are calculated from the total net demand of the system and the specific utility price δ_{ut}^{UT} (Eq. (3.67)). The costs for heating are derived from the heat

deficits at the different intervals and the external purchase costs of steam δ_{hi}^{H}, while sold steam is vended for 70 % of the purchase costs. Cooling costs are dependent on the cooling demand and costs for cooling water respectively (Eq. (3.68) and (3.69)). The total costs of utilities are the sum of electricity, chilling, heating and cooling costs (Eq. (3.70)).

$$C_{ut}^{UT} = E_{ut}^{TOT} \cdot \delta_{ut}^{UT} \cdot hr \qquad\qquad \begin{matrix} ut \in UT \\ \notin HUT \end{matrix} \qquad (3.67)$$

$$C^{HEAT} = \left(\left[\sum_{hi \in HI} Q_{hi}^{DEFI} \right] + Q^{PROD,SELL} \cdot 0.7 \cdot \delta_{hi=1}^{H} \right) \\ \cdot hr \qquad (3.68)$$

$$C^{COOLING} = Q^{COOL} \cdot \delta^{COOL} \cdot hr \qquad (3.69)$$

$$C^{UT,TOT} = C^{HEAT} + C^{COOLING} \sum_{ut \in UT \notin HUT} C_{ut}^{UT} \qquad (3.70)$$

Costs for raw materials are derived from the total flows $F_{u_s}^{SOURCE}$ of a source with its respective costs $\delta_{u_s}^{RM}$ (Eq. (3.71)).

$$C^{RM} = \sum_{u_s \in U_S} F_{u_s}^{SOURCE} \cdot \delta_{u_s}^{RM} \cdot flh_{u_s} \qquad (3.71)$$

The costs for operating and maintenance are determined as a linear factor based on the fixed capital investment as shown in Eq. (3.72).

$$C^{O\&M} = \sum_{u \in U_C} f_u^{O\&M} \cdot FCI_u \qquad (3.72)$$

The total operating costs are the sum of utility costs, costs for raw materials as well as operating and maintenance costs $C^{O\&M}$ (Eq. (3.73)). In addition to the costs, revenues can also be generated. These are determined by the total inlets of the defined product pools with their respective market prices (Eq. (3.74)).

$$OPEX = C^{O\&M} + C^{UT,TOT} + C^{RM} \qquad (3.73)$$

$$PROFITS = \sum_{u \in U_{PP}} \left(\sum_{i \in I} F_{u,i}^{IN} \right) \cdot \delta_u^{PP} \cdot flh_u \qquad (3.74)$$

3.7 ENVIRONMENTAL FUNCTIONS

Two types of environmental burdens are modeled in OUTDOOR. This first one describes the greenhouse gas emissions, or global warming potential, the second depicts the fresh water demand of the process.

Emissions that induce global warming can be directly emitted at the plant ($GWP^{EMITTED}$). These are calculated from the waste flows with their respected global warming potential factor (gwp_i), (Eq. (3.75)).

$$GWP^{EMITTED} = \sum_{u \in U} \sum_i F_{u,i}^{WASTE} \cdot gwp_i \cdot flh_u \tag{3.75}$$

However, they can also emerge as indirect emissions from external utility supply. These are derived from the usage of external utilities, such as electricity from the energy grid or renewable sources and steam produced from natural gas (cf. Eq. (3.76) and (3.77). The total emissions from utilities are the sum of heating emissions and other utilities emissions (cf. (3.78)).

$$GWP_{ut}^{UT} = (E_{ut}^{TOT} \cdot gwp_{ut}^{UT}) \cdot hr \qquad \begin{matrix} ut \in UT \\ \notin HUT \end{matrix} \tag{3.76}$$

$$GWP^{HEAT} = \left(\left[\sum_{hi \in HI} Q_{hi}^{DEFI} \right] - Q^{PROD,SELL} \right) \cdot gwp^{HEAT} \cdot hr \tag{3.77}$$

$$GWP^{UT,TOT} = GWP^{HEAT} + \sum_{ut \in UT \notin HUT} GWP_{ut}^{UT} \tag{3.78}$$

Negative emissions can be achieved by captured CO_2 as depicted in Eq. (3.79) or by $GPW^{CREDITS}$ for by-products according to the avoided burden approach [29]. These credits are calculated using the total inlet flow of the given product pools with their respective reference gwp value (Eq. (3.80)). This approach requires knowledge of reference production processes (e.g. oxygen from air separation) as well as the assumption that by-products can be sold and therefore lead to avoided burden.

$$GPW^{CAPTURE} = \sum_{u_s \in U_S} F_{u_s}^{SOURCE} \, gwp_{u_s}^{SOURCE} \cdot flh_{u_s} \tag{3.79}$$

$$GPW^{CREDITS} = \sum_{u \in U_{PP}} \left(\sum_{i \in I} F_{u,i}^{IN} \right) \cdot gwp_u^{POOL} \cdot flh_u \tag{3.80}$$

Fresh water demand is calculated analogous as to the greenhouse gas emissions. Here fresh water demand in terms of direct and indirect raw material demand is

calculated as given in Eq. (3.81). Here if water is used the fresh water factor ($fwd_{u_s}^{SOURCE}$) of source u_s is equal to one. If, on the other hand other sources are used, the factor is equal to the amount of required fresh water to produce this raw material. Additionally, indirect fresh water demand from utilities and heat is generated (Eqs. (3.82) to (3.84)) and credits are calculated for by-products (Eq. (3.86)).

$$FWD^{RM} = \sum_{u_s \in U_S} F_{u_s}^{SOURCE} \cdot fwd_{u_s}^{SOURCE} \cdot flh_{u_s} \tag{3.81}$$

$$FWD_{ut}^{UT} = (E_{ut}^{TOT} \cdot fwd_{ut}^{UT}) \cdot hr \qquad \begin{matrix} ut \in UT \\ \notin HUT \end{matrix} \tag{3.82}$$

$$FWD^{HEAT} = \left(\left[\sum_{hi \in HI} Q_{hi}^{DEFI} \right] - Q^{PROD,SELL} \right) \cdot fwd^{HEAT} \cdot hr \tag{3.83}$$

$$FWD^{UT,TOT} = FWD^{HEAT} + \sum_{ut \in UT \notin HUT} FWD_{ut}^{UT} \tag{3.84}$$

$$FWD^{CREDITS} = \sum_{i \in I, u \in U} F_{u,i}^{IN} \cdot fwd_u^{POOL} \cdot flh_u \tag{3.85}$$

3.8 LOGIC CONSTRAINTS

Normally, OUTDOOR's model does not need additional logic constraints. Mass balances will ensure that a technical feasible solution is generated, while it is possible to combine different process alternatives with each other if this serves the purpose of optimal design. However, in some scenarios it is helpful or desired to regulate different process behaviors. In general, there are two types of cases. The first one is, to ensure that a certain unit-operations u' state is equal to another unit-operations u state. This could be the case if large processes are split into multiple smaller units. Then it is possible to label them as a group G_{G1} where all unit-operations in this group have to have the same state. Eq. (3.86) ensures this. The second case of limited process choices is if at least one from multiple options have to be connected to unit-operation u. This can also be the case for different groups, meaning u has to be connected to at least one alternative from group 1 and one alternative from group 2 etc. This behavior is set into place by Eq. (3.87).

$$Y_u = Y_{u'} \qquad u \wedge u' \in G_{G1} \tag{3.86}$$

$$\sum_{u' \forall \in G_{G2,n}} Y_{u',n} \geq Y_u \qquad u \wedge u' \in G_{G2} \tag{3.87}$$

4 METHODOLOGY DEVELOPMENT

The following chapter presents the developed methodologies for integrated assessment and optimization of sustainable process design. Two methodologies were developed and implemented in OUTDOOR. The first method provides a framework for combined multi-criteria decision-analysis and superstructure optimization. Hence it fills a toolbox for the support of complex decision-making processes in the early design phase, particularly in sustainable process design. The second methodology depicts a special application case of automated two-ways sensitivity analysis. It is especially designed as reaction to data-uncertainty in novel process design. An optimal design screening algorithm is developed which automatically varies chosen parameters over a wide range of values to find feasible operating windows for innovative and competing process alternatives.

Chapter 4.2 is in the process of publication in:

- Kenkel, P., Schnuelle, C., Wassermann, T., & Zondervan, E. (2022) Integrating Multi-Objective Superstructure Optimizationand Multi-Criteria Assessment: A novel methodology for sustainable process design. Physical Science Reviews.

4.1 OUTLINE

OUTDOORs optimization functionalities include different Optimizer classes which serve different types of optimization (ref. chapter2.3.5). Next to the standard SingleOptimizer, three additional optimization modes are included. One performs multi-criteria optimization to consider optimal process design under competing objectives (MCDAOptimizer). The others present varieties of sensitivity analyses (SensitivityOptimizer / TwoWayOptimizer). While the SensitivtiyOptimizer simply adopts the concept of sensitivity analysis, more detailed methodologies were developed for the MCDAOptimizer and TwoWayOptimizer. Although directly implemented and automated in OUTDOOR both methodologies are not exclusive for this software and can be applied in other studies and frameworks. Hence, they are explained in a more general way in the following sections.

4.2 MULTI-CRITERIA OPTIMIZATION FRAMEWORK

The proposed methodology combines concepts from different multi-attribute decision-making- (MADM) and multi-objective decision-making (MODM) approaches. The goal is to provide a method to determine optimal or trade-off process designs from an indefinite solution space for multiple, sometimes conflicting, criteria. To achieve this, the following six-step algorithm is proposed:

  i.   Superstructure model formulation (based on mixed-integer linear programming)

  ii.   Objectives / Criteria definition

  iii. Criteria weighting (based on MADM, optional)

  iv.   Single-criterion optimization (based on MODM)

  v.   Normalization based on step 4 and reference process

  vi.   Reformulation and multi-criteria optimization (based on MADM)

First, the superstructure model has to be set up (step 1). This model is based on mixed-integer linear programing. Afterwards the objectives / criteria have to be selected (step 2) and a weighting is performed. The weighting method proposed here is pairwise comparison inspired by the Analytical Hierarchy Process (AHP) (step 3). Subsequently, the superstructure is optimized for every criterion without taking weights into account, similar to vector optimization (ϵ-constraint optimization) (step 4). Based on the optimization results a normalization and reformulation of the objectives is performed (step 5) and the superstructure is optimized for this reformulated multi-criteria objective (step 6). In the following, step one to six are described in detail.

4.2.1 Superstructure formulation (Step 1)

First, a superstructure model has to be formulated. This model represents a blueprint of the different process flowsheets and is equation based. It includes the mass- and energy balances as well as emission factors and cost functions. If special objectives are to be included into the multi-criteria optimization, it is important that the model itself can represent these objectives in the required detail. For example, if total greenhouse gas emissions are to be minimized, the model has to entail balances for CO_2 and other greenhouse gases, including indirect emissions for e.g. utility usage. Superstructure models can be formulated in various ways, using mixed-integer linear programming (MILP) or non-linear formulations (MINLP) [36], [38], [74]. Next to the correct formulations also all process data such as reaction parameters, energy demands, split factors etc. have to be provided for the investigated processes. The provided data should be in line with the level of detail of the formulated model and vice versa. Therefore, the data collection and preprocessing can require a substantial amount of work and time.

4.2.2 Criteria definition and weighting (Step 2 and 3)

When the superstructure model is written, the objectives of interest have to be formulated and integrated into the model. After the criteria are defined, they are weighted. The easiest way is to use equal weighting [75]. Other weighting methods can be divided into objective and subjective approaches [75]. Subjective approaches like direct ranking, point allocation and SMART (Simple Multi-attribute Ranking Technique) use the preferences of the decision-maker (DM) [75], [76]. However, this process becomes more complicated for a rising number of criteria, which ultimately decreases the accuracy. To counter this effect, objective weighting methods like Entropy method, Standard Deviation method or MEREC (Method based on the Removal Effects of Criteria) calculate preferences based on the initial data of the decision matrix and therefore on the characteristics of the criteria and data itself [76]. Their biggest advantage is also their biggest disadvantage, since the preferences of the DM are not considered anymore.

In this work a subjective method, the pairwise comparison with adjustments for inconsistencies also known from the Analytical Hierarchy Process is proposed [77]. In conventional pairwise comparison n given criteria are compared in their importance with respect to each other in a $n \times n$ decision matrix. This can be done by using intuitive linguistic terms like "equally important" or "extremely important" [77], [78].

TABLE 4.1: SAATY SCALE FOR ASSESSMENT OF CRITERIA IMPORTANCE [77], [79].

Linguistic term	Score
Equally important	1
Moderately more important	3
Strongly more important	5
Very strongly more important	7
Extremely more important	9
Intermediate values	2,4,6,8

Using the scale of Saaty (cf. Table 4.1) these linguistic terms can be translated into numbers. Through this pairwise comparison of criteria importance, matrix A with $a_{i,i} = 1$ and $a_{i,j} = {}^{1}/{a_{j,i}} \neq 0$, where i depicts the row and j the column, is constructed [78]:

$$A = \begin{pmatrix} a_{1,1} \, a_{1,2} \ldots a_{1,n} \\ a_{2,1} \, a_{2,2} \ldots a_{2,n} \\ \ldots \quad \ldots \quad \ldots \quad \ldots \\ a_{n,1} \, a_{n,2} \ldots a_{n,n} \end{pmatrix} \qquad (4.1)$$

Due to the direct relation $a_{i,j} = {}^{1}/{a_{j,i}}$ of pairwise comparison, it is only necessary to fill out the upper right triangle of matrix A. This can be explained simply by an example. If criterion 1 is classified as "strongly more important" than criterion 2 (score of 5), than automatically criterion 2 has to be classified as the reciprocal value "strongly more unimportant" (score = 1/5). As already mentioned before, this approach has the advantages of considering the DM's preferences, but it also has the disadvantage of increasing inaccuracy and inconsistencies for large decision-matrixes. This is also easily explained using another example. It is possible, while going through the matrix that the DM classifies criterion 1 as "extremely more important" (score = 9) than criterion 2, and criterion 2 "strongly more important" (score=5) than criterion 3. However, deciding on importance of different criteria with respect to each other is a highly subjective process, which is done, more or less based on intuition. Therefore, it could happen, that the DM classifies criterion 3 as "moderately more important" (score=3) than criterion 1. This is obviously an inconsistency, because criterion 1 is more important than 2 and criterion 2 more than 3, therefore, criterion 3 cannot be more important than criterion 1 [78], [79].

There are two ways to deal with inconsistency in the decision matrix. The first one is proposed by Saaty: A consistency index is calculated based on the eigenvalues of the matrix A, if this value is lower than a given threshold the matrix is still considered consistent enough to be used. If the value is higher than the given threshold, the matrix has to be adjusted [79].

The second approach avoids inconsistencies directly by restricting the pairwise comparison to the first row of matrix A and filling in all other values by logic afterwards [78]. This approach has two direct advantages: Firstly, the initial effort in filling a decision matrix is reduced to the first row. Secondly, additional effort of adjusting inconsistence matrices afterwards is prevented. Therefore, the second approach is applied, where the remaining values of A are calculated from the values of the first row based on the transitivity rule in Eq. (4.1) [78]:

$$a_{i,j} = \frac{a_{1,j}}{a_{1,i}} \tag{4.2}$$

Utilizing matrix A the weighting factors of the different criteria i are calculated using the expanded geometric mean and linear sum normalization as shown in Eqs. (4.3) and (4.4) [78]:

$$w_i = \sqrt[n]{\prod_{j=1}^{n} a_{i,j}} \tag{4.3}$$

$$w_i^{norm} = \frac{w_i}{\sum_{i=1}^{n} w_i} \tag{4.4}$$

4.2.3 Single criterion optimization (Step 4)

After the different criteria are set up and weighting factors are calculated, a single criterion optimization for every criterion is conducted. This approach is similar to ϵ-constraint optimization, where single-criterion optimization runs are used to locate the boundaries of the pareto-front. Here it is also used to find boundary values. In total n process configurations are calculated for n criteria, while the optimal value for each criterion is set as the upper boundary, the worst value from the n given configuration for every criterion is set as lower boundary. These results are still independent from the subjective weighting and depict a small share of a possible pareto front. Figure 4.1 shows the graphical concept of this approach for two antagonistic criteria. If both criteria are to be minimized, alternative A_1 will be the solution of optimizing criterion 1 and A_2 will be the process design of the optimization of criterion 2. Both alternatives lie on a potential pareto-front and depict the upper and lower boundaries for the given criteria.
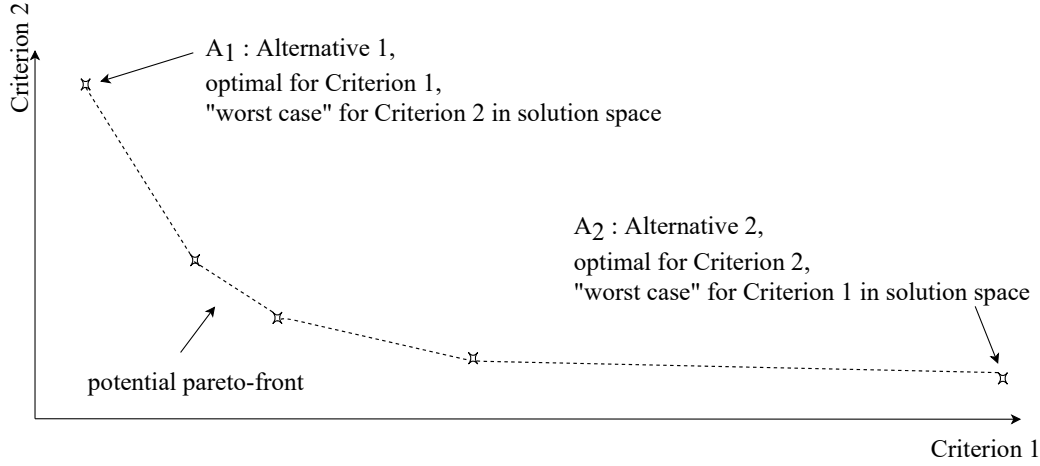
FIGURE 4.1: EXAMPLE PARETO-FRONT WITH DEPICTED OPTIMAL AND "WORST CASE" ALTERNATIVES PROCESS OPTIONS.

4.2.4 Normalization (Step 5)

Normalization is a crucial step in every MCDA method. Goal of this step is to calculate a value $v_{t,i}$ of every technology t and criterion i which enables the direct comparison of criteria with different units. Different normalization methods are available [80], [81]. Common techniques are linear, linear-sum, vector and linear-min-max normalization. Linear normalization refers to the maximum value for beneficial criteria and either to the maximum or minimum value for non-beneficial (cost) criteria [80], [81]. Linear-sum normalization refers to the sum and reciprocal sum of the given values for beneficial and non-beneficial criteria [80], [81]. The vector normalization concept uses the vector distant calculation [80], [81]. Finally, the linear-min-max approach uses the maximum and minimum value to map all other solutions between those values as shown in Eqs. (4.5) and (4.6) [80], [81]. While all methods are valid for normalization, the last approach is proposed for this framework to avoid sign change problems.

$$v_{t,i} = \frac{\left[x_{t,i} - x_i^{MIN}\right]}{\left[x_i^{MAX} - x_i^{MIN}\right]} \tag{4.5}$$

$$v_{t,i} = \frac{\left[x_i^{MAX} - x_{t,i}\right]}{\left[x_i^{MAX} - x_i^{MIN}\right]} \tag{4.6}$$

Since superstructure optimization models are designed to answer questions in process systems engineering in the domain of production and this framework is built to improve the design of sustainable process alternatives it is assumed that conventional reference processes are always known. Thus, an additional conventional reference process is considered during normalization, potentially, expanding the range of minimum and maximum values.

4.2.5 Reformulation and multi-objective optimization (Step 6)

With the given single-criterion optimization solutions and the chosen normalization approach including a conventional reference process in total $m = n + 1$ process configurations are known. The different objectives can be reformulated and integrated to one overall multi-criteria optimization (MCO) function using the Technique for Order Preference by Similarity to Ideal Solution (TOPSIS) [66]. First the known normalized objective values $v_{t,i}$ are multiplied with the weighting factors w_i^{norm} generated in step 3 to calculate the weighted value score $V_{t,i}$ for each known process configuration t and criterion i (ref. Eq. (4.7)).

$$V_{t,i} = v_{t,i} \cdot w_i^{norm} \tag{4.7}$$

Afterwards the best and worst weighted value scores V_i^+ and V_i^- are identified from the given number of $V_{t,i}$. Now the objective variables $V_{t,i}^O$ are reformulated to implement the normalization approach and weighting factor. This is shown exemplary for a dummy non-beneficial criteria function in Eq. (4.8).

With Eqs. (4.9) and (4.10) two additional variables are introduced into the model, which are the Manhattan distances (D_t^+ and D_t^-) to the ideal and anti-ideal solution (also called utopia and nadir point). The Manhattan distance is not as commonly used as the Euclidean distance in TOPSIS, however it avoids non-linear quadratic constraints in the reformulated optimization problem, which cause major challenges for MILP solvers [66]. Using these new variables, the relative closeness ratio (C_t) is defined as new objective function as presented in Eq. (4.11). Normally this function would also lead to non-linearities, but in consequence of linear min-max normalization and Manhattan distance utilization, the sum of $D_t^+ + D_t^-$ will always equal to 1, therefore canceling out the non-linearities.

$$V_{t,i}^O = \frac{\left[x_i^{MAX} - f(y_1, y_2, \dots y_n) \right]}{\left[x_i^{MAX} - x_i^{MIN} \right]} \cdot w_i^{norm} \tag{4.8}$$

$$D_t^+ = \sum_i \left| V_i^+ - V_{t,i}^O \right| \tag{4.9}$$

$$D_t^- = \sum_i \left| V_i^- - V_{t,i}^O \right| \tag{4.10}$$

$$max \, C_t = \frac{D_t^-}{D_t^+ + D_t^-} \tag{4.11}$$

4.2.6 Implementation in OUTDOOR

OUTDOOR's MCDAOptimizer automates most of the six-step algorithm. It uses OUTDOOR's integrated SuperstructureModel class which already includes the three objectives minimal NPC, NPE and NPFWD. The user only has to perform the weighting in beforehand and input the resulting weights as well as data (costs, emissions, water demand) for a conventional reference process. Afterwards, OUTDOOR will perform single-criterion optimization, reformulation and multi-criteria optimization automatically and return all results back to the user. From there on the user can use the AdvancedMultiModelAnalyzer class to investigate and print different results like the relative closeness ratio C_t of the resulting process flowsheets.

4.3 OPTIMAL DESIGN SCREENING ALGORITHM

The proposed screening algorithm is based on a two-way sensitivity analysis combined with automated graph drawing. Its goal is to present graphs which offer a quick way to check operating windows of competing process alternatives. It is developed as a reaction of data-uncertainty for novel processes. One major example could be the comparison of two novel processes in an overall superstructure, without detailed knowledge on their total costs. Using the proposed screening algorithm, the costs are defined variable and operating windows are identified based on the declared parameter range. The optimal design screening algorithm generally consists of seven steps as depicted below, which will be described in detail in the following sections.

i.   Superstructure model formulation (based on mixed-integer linear programming)

ii.   Sensitive parameter definition including value spectrum

iii. Two-way sensitivity optimization

iv.   Mapping of technology choice and objective to heatmap and contour lines

v.   Definition of investigated (competing) process alternatives

vi.   Translation of technology choice to binary number system

vii. Graph drawing for inspection

4.3.1 Modeling, parameter definition, optimization (Step 1 – 3)

First the superstructure model has to be formulated and setup (step 1). This process step is similar to the one in the multi-criteria optimization framework (ref. chapter 4.2) [36], [38]. It builds the basis for the further procedure and has to include all important balances as well as parameters and objective functions.

Afterwards a set of two parameters has to be declared as sensitive and their value range has to be defined (step 2). Based on the given optimization model and initial data of the two sensitive parameters, a two-way sensitivity analysis is performed (step 3). Such a sensitivity analysis calculates the optimal process design for each parameter value-pair. Given n values of parameter one and m values of parameter two, the procedure leads to $n \times m$ possible process flowsheets.

4.3.2 Data postprocessing (Step 4 – 7)

Depending on the value range n and m, a two-way sensitivity analysis can produce a significant amount of results data. In order to read and analyze certain data intuitively, postprocessing is crucial. The proposed methodologies goal is to present two results for the vast amount of results. The first is the actual optimized value of the objective function for each parameter value pair. The second is the design of the flowsheet with particular respect to certain unit-operations. These will be in general the novel processes which are competing with each other. Nonetheless, the methodology is not bound to this definition. To extract the required data the procedure uses a three-step post-processing. The first step describes the parsing of the objective function values for all parameter value-pairs and setting them up on a mesh grid using the sensitive parameters as x- and y-axis (step 4, ref. Figure 4.2 left hand side). For the second step, first the process alternatives of interest have to be defined. Using the defined alternatives, the flowsheets are scanned and the technology choice is translated into a numerical system (step 5 + 6) as follows. Using a scale based on the binary number system as presented in Table 4.2, the investigated (competing) alternatives, single-choices are assigned an ascending number. A combination of different technologies is affiliated with their corresponding sum. This leads to an unambiguously numerical scale for the technology choice (ref. Table 4.2).

TABLE 4.2: EXAMPLE NUMERICAL SCALE FOR TECHNOLOGY CHOICE MAPPING.

Technology	Numeric mapping value
Alternative 1	1
Alternative 2	2
Alternative 3	4
Alternative 4	8
Combination example: Alternative 1 and 3	1+4 = 5
Combination example: Alternative 1,2 and 4	1+2+8 = 11

The numeric scale is afterwards mapped to the same mesh grid as the objective function values (ref. Figure 4.2 right hand side). While the objective function values are in general real floating points, the numeric technology choice mapping is based on integers. Hence, both scales are drawn differently on the same graph.

The objective function is drawn using contour-lines, while the technology choice is drawn using a heat map (ref. Figure 4.2). In the end both graphs are brought together. The resulting two-dimensional graph depicts an intuitive way to discover optimal process alternatives for wide parameter ranges with their affiliated optimal objective values.
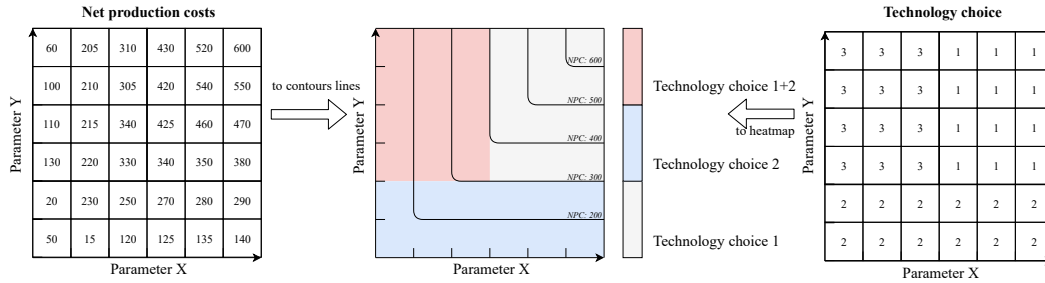
FIGURE 4.2: MAPPING OF OBJECTIVE FUNCTION (E.G. NPC) AND TECHNOLOGY CHOICE TO
GRAPH.

4.3.3 Implementation in OUTDOOR

Similar to the multi-criteria optimization framework OUTDOOR includes an Optimizer class (TwoWayOptimizer) which automates most of the presented algorithm. The user has to define the objective function as well as the two sensitive parameters with their minimum and maximum value as well as number of data points. OUTDOOR afterwards automatically calculates the linear vector of the parameters, performs the two-way sensitivity analysis and returns the complete data structure of the optimization. Subsequently, the included AdvanvedMultiModelAnalyzer class contains a method to automatically generate the two-dimensional graph based on the optimization data and the process alternatives list, which is an input from the user.

5   MULTI-CRITERIA DESIGN OPTIMIZATION OF RENEWABLE METHANOL PRODUCTION

This chapter presents a detailed case study of renewable methanol production as one major exemplary petrochemical. It includes an integrated Power-to-Methanol and biogas-reforming process utilizing carbon capture, water electrolysis, methanol synthesis by direct hydrogenation of CO_2 and reforming of biogas to H_2/CO_2 mixtures as feedstock for methanol synthesis. A multi-criteria optimization is performed to investigate renewable methanol production in terms of net production costs, greenhouse gas emissions and freshwater demand compared to conventional methanol production based on natural gas.
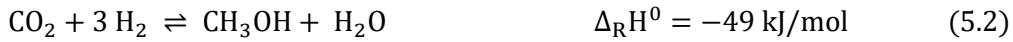
Parts of this chapter are in the process of publication in:

- Kenkel, P., Schnuelle, C., Wassermann, T., & Zondervan, E. (2022) Integrating multi-objective superstructure optimization and multi-criteria assesment: A novel methodology for sustainable process design. Physical Science Reviews.

5.1 OUTLINE

Methanol is an important petrochemical which is used in various applications like production of formaldehyde, acetic acid or methyl methacrylate [15]. Additionally, methanol can be used as energy carrier in combustion engines and is often discussed as major renewable base chemical due to the possibility to serve as intermediate for other important platform chemicals like olefins, aromatics or hydrocarbon fuels like gasoline, diesel or kerosene [15]. Next to its versatile applicability it also has the advantage of large-scale existing infrastructure and safe and simple handling [15].

Conventional methanol production utilizes synthesis gas, a mixture of hydrogen and carbon monoxide in a catalytical reaction under pressure of 50 – 100 bar and temperatures of 220 – 280°C based on Eq. (5.1) and (5.2) [38]. CO_2 content in classic methanol synthesis is low with 3 – 10 mol.-% which is why Eq. (5.1) is the prominent conversion route [15], [38]. Next to methanol synthesis also water-gas shift (Eq.(5.3)) occurs which links Eq. (5.1) to Eq. (5.2).

$$CO + 2\,H_2 \;\rightleftharpoons\; CH_3OH \qquad\qquad \Delta_R H^0 = -91\ kJ/mol \qquad (5.1)$$

$$CO_2 + 3\,H_2 \;\rightleftharpoons\; CH_3OH + H_2O \qquad\qquad \Delta_R H^0 = -49\ kJ/mol \qquad (5.2)$$

$$CO + H_2O \;\rightleftharpoons\; H_2 + CO_2 \qquad\qquad \Delta_R H^0 = -41.2\ kJ/mol \qquad (5.3)$$

Synthesis gas from fossil fuels is produced from natural gas. The most prominent production ways are steam methane reforming (SMR), partial oxidation (POX) and autothermal reforming (ATR) [15], [38]. SMR converts methane with high excess of steam to synthesis gas (cf. Eq. (5.4)). It is a highly endothermic reaction and relies on external heating. Partial oxidation is an exothermic reaction of methane with limited oxygen (cf. Eq. (5.5)). ATR depicts a combination of SMR and POX which leads to an autothermal process with higher H_2/CO ratio than POX [15], [38].

$$CH_4 + H_2O \;\rightleftharpoons\; 3\,H_2 + CO \qquad\qquad \Delta_R H^0 = 206\ kJ/mol \qquad (5.4)$$

$$CH_4 + {}^1\!/_2\,O_2 \;\rightleftharpoons\; 2\,H_2 + CO \qquad\qquad \Delta_R H^0 = -35\ kJ/mol \qquad (5.5)$$

Howbeit, methanol can also be synthesized directly from CO_2 and H_2 by direct hydrogenation (Eq. (5.2)) utilizing adjusted catalysts and operating conditions [15], [82]. Both required raw materials can be produced from either Biomass-to-X (BtX) or electricity-based (PtX) pathways [83]–[85]. The conceptual process design of combined BtX and PtX processes for methanol production under multiple criteria will be elaborated in the upcoming sections.

5.2 CASE STUDY DESCRIPTION

Figure 5.1 depicts the general layout of the renewable methanol plant. Its BtX pathway consists of biogas reforming technologies which provide H_2 and CO_2 as raw materials for methanol synthesis. The PtX pathway includes different carbon capture as well as water electrolysis processes to produce CO_2 and H_2 respectively. The integration of both concepts leads to a combined bio- and electricity-based methanol production. In the following sections the different process steps and possible process alternatives are described in detail.
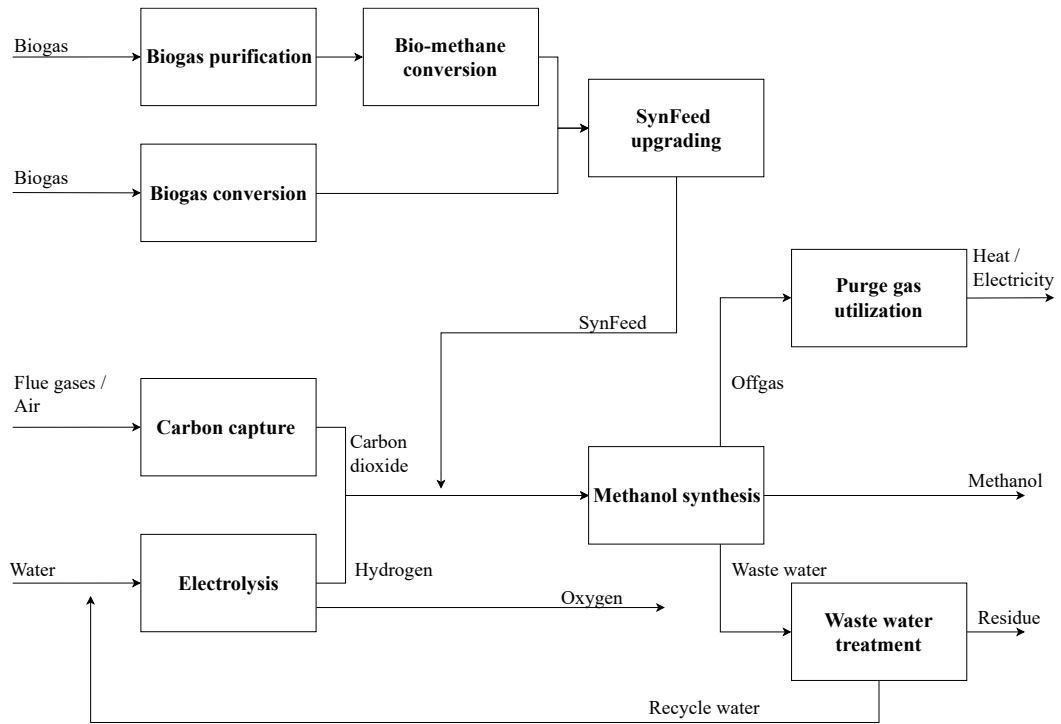
FIGURE 5.1: SIMPLIFIED METHANOL PRODUCTION PLANT REPRESENTATION (DETAILED SUPERSTRUCTURE REPRESENTATION WITH ALL UNIT-OPERATIONS CAN BE FOUND IN APPENDIX A, TABLE A.1 AND FIGURE A.1).

5.2.1 Power-to-X process

The PtX process utilizes SynFeed for MeOH production. SynFeed contains a mixture of CO_2 and H_2 with a mass ratio of 7.33 (molar H_2/CO_2 ratio = 3) which depicts the optimal value for direct hydrogenation of CO_2.

Carbon capture

Carbon capture is considered with three different sources. One way to acquire CO_2 is utilizing low temperature direct air capture (LT-DAC) based on the technology by Climeworks [86]. Another way is to use concentrated sources from industry. In this study two different industrial carbon sources are implemented, namely cement factory flue gases and a mixed flue gas from a crude oil refinery. The

cement factory is assumed to be operated as oxyfuel combustion plant (OXY), therefore CO_2 capture is performed by flue gas chilling and water separation [87], [88]. The refinery flue gases are mixed flue gases from an internal power plant as well as the catalytic reformer and steam cracker. The gas composition is depicted in Table 5.1 [82]. The carbon capture technology applied is chemical absorption using monoethanolamine (MEA-CC). Data for MEA-based carbon capture is taken from Wassermann et al. [82].

TABLE 5.1: REFINERY FLUE GAS COMPOSITION [82].

Component	Nitrogen (N_2)	Carbon dioxide (CO_2)	Oxygen (O_2)	Water (H_2O)
Mass-fraction	0.732	0.139	0.041	0.088

Figure 5.2 displays the different options this process step. While CO_2 from the cement factory is automatically prepared at high pressures, CO_2 from LT-DAC and MEA-CC is captured at low pressures of around $1-2$ bar. It is mixed with potential CO_2 from the bio-SynFeed upgrading section. The CO_2 is afterwards compressed to high pressures and used for methanol synthesis. Techno-economic model data is extracted from literature and processed for application in the superstructure model.
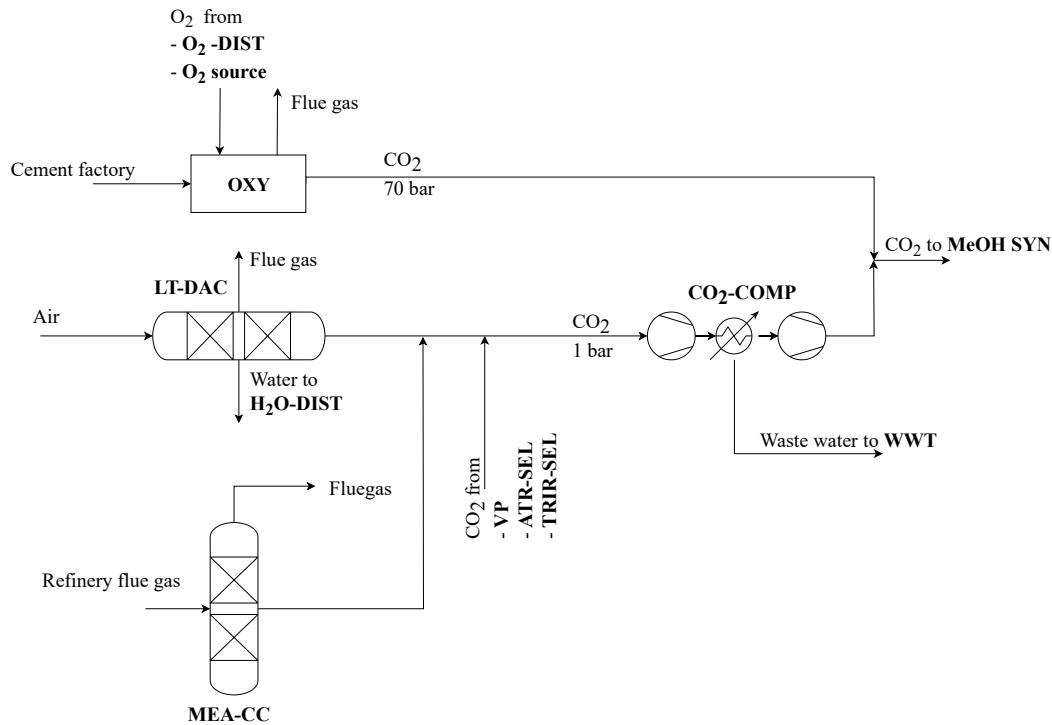

FIGURE 5.2: CARBON CAPTURE PROCESS SECTION OF METHANOL PRODUCTION SUPERSTRUCTURE.

Water electrolysis

H_2 is provided by water electrolysis, which splits water molecules into H_2 and oxygen (O_2) using electricity. This superstructure implements an alkaline electrolyzer (AEL) and a solid oxide electrolyzer (SOEL) operating at ambient pressure as well as a polymer electrolyte membrane (HP-PEMEL) and alkaline electrolyzer (HP-AEL) at elevated pressure of 30 bar [89]–[91] (ref. Figure 5.3). While PEMEL and AEL operate at low temperatures of around 70°C and are powered solely by electricity, SOEL operates at elevated temperatures up to 1000°C where part of the energy input is introduced as steam. Therefore, electricity demand varies from 4.4 kWh/Nm³ to 4.9 kWh/Nm³ and capital costs from 700 €/kW$_{el}$ to 3000 €/kW$_{el}$. [89]–[91]. It is assumed, that all electrolyzer technologies achieve total conversion, meaning that one kg of water is converted to 0.112 kg of H_2 and 0.888 kg of O_2 (ref. Eq. (5.6)).

$$H_2O \rightarrow 0.112\ H_2 + 0.888\ O_2 \tag{5.6}$$
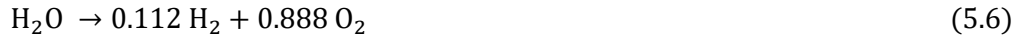
Raw H_2 is either pressurized to MeOH synthesis operating pressure of 70 bar by single-stage compression (H_2-MH-COMP) or multi-stage compression (H_2-LH-COMP) for high pressure electrolyzers and ambient pressure electrolyzers, respectively [74]. Oxygen can be sold as by-product or used as raw material e.g. in the oxyfuel cement factory or included biomass reforming processes.
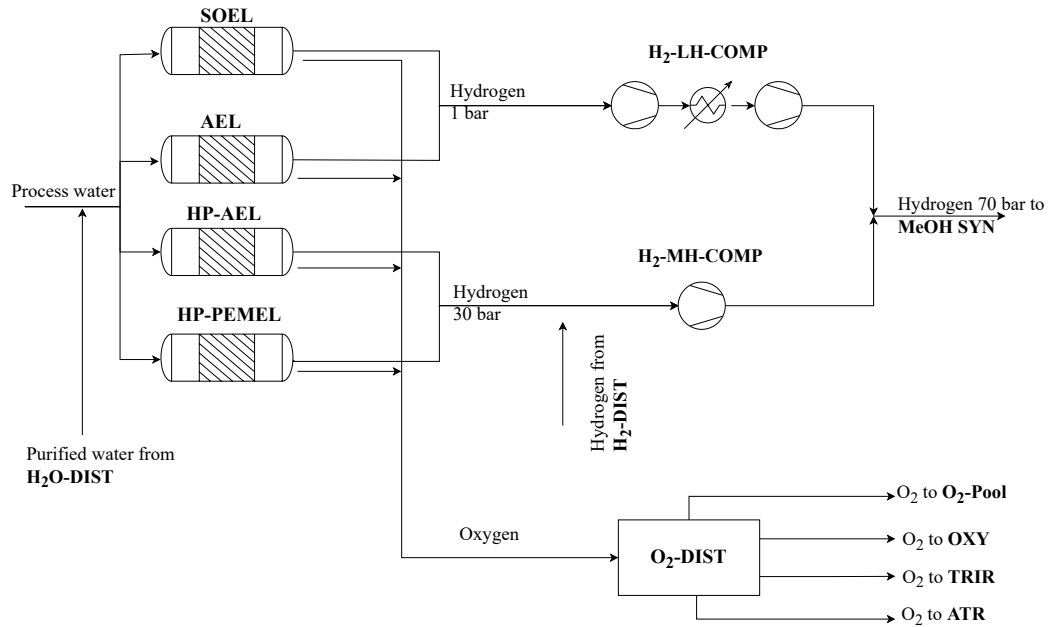

FIGURE 5.3: WATER ELECTROLYSIS PROCESS SECTION OF METHANOL PRODUCTION SUPERSTRUCTURE.

Methanol synthesis

The direct hydrogenation of CO_2 to MeOH is modeled as a three-step process (Figure 5.4). First the actual methanol synthesis is implemented as a yield reactor operating at 250°C and 70 bar (MEOH SYN) [82]. Table 5.2 shows the derived yield factors for methanol synthesis step.

TABLE 5.2: PRODUCT DISTRIBUTION OF METHANOL SYNTHESIS PROCESS, DERIVED FROM WASSERMANN ET AL. [82].

--	MeOH	CO_2	O_2	H_2O	CO	H_2
Yield factor	0.619	0.023	0.002	0.35	0.002	0.002

Afterwards the raw product is purified in two steps. The first step is a flash drum (MEOH FLASH) to separate purge gas and the second one is a distillation column (MEOH DC) to purify MeOH and separate water. The model data for equipment costs, utility demand, operating conditions and split factors is extracted from a detailed simulation provided by Wassermann et al. and converted into a fitting data format [82].
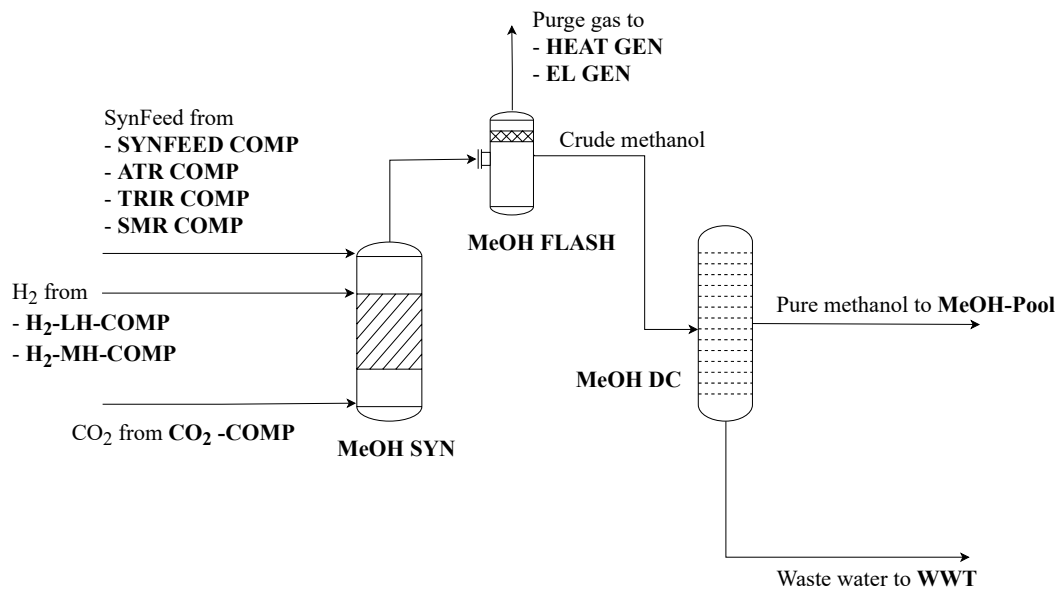
FIGURE 5.4: METHANOL SYNTHESIS PROCESS SECTION OF METHANOL PRODUCTION SUPERSTRUCTURE.

5.2.2 Biomass-to-X process

The considered BtX process route uses biogas with a composition of 65 vol. -% methane (CH_4) and 35 vol. -% CO_2 as raw material. Biogas is converted to SynFeed by a series of pretreatment, reforming and upgrading steps. Biogas is assumed to be produced in a typical biogas plant by anaerobic digestion. These facilities are rather small compared to methanol production plants. Therefore, the maximal

input of biogas is limited to 3.5 t/h which corresponds to 3,000 Nm^3/h and depicts a German large-scale biogas plant operating for bio-methane production [92].

Biogas can either be converted to SynFeed directly, or in purified bio-methane form (ref. Figure 5.5). If direct conversion is chosen, biogas pretreatment is omitted. Otherwise, CO_2 is separated by pressure swing adsorption and vacuum pump (BG-PSA and VP) [24]. The separated CO_2 can still be used in methanol synthesis with previous compression. This leads to smaller equipment sizes in the reforming technology, which may be beneficial.
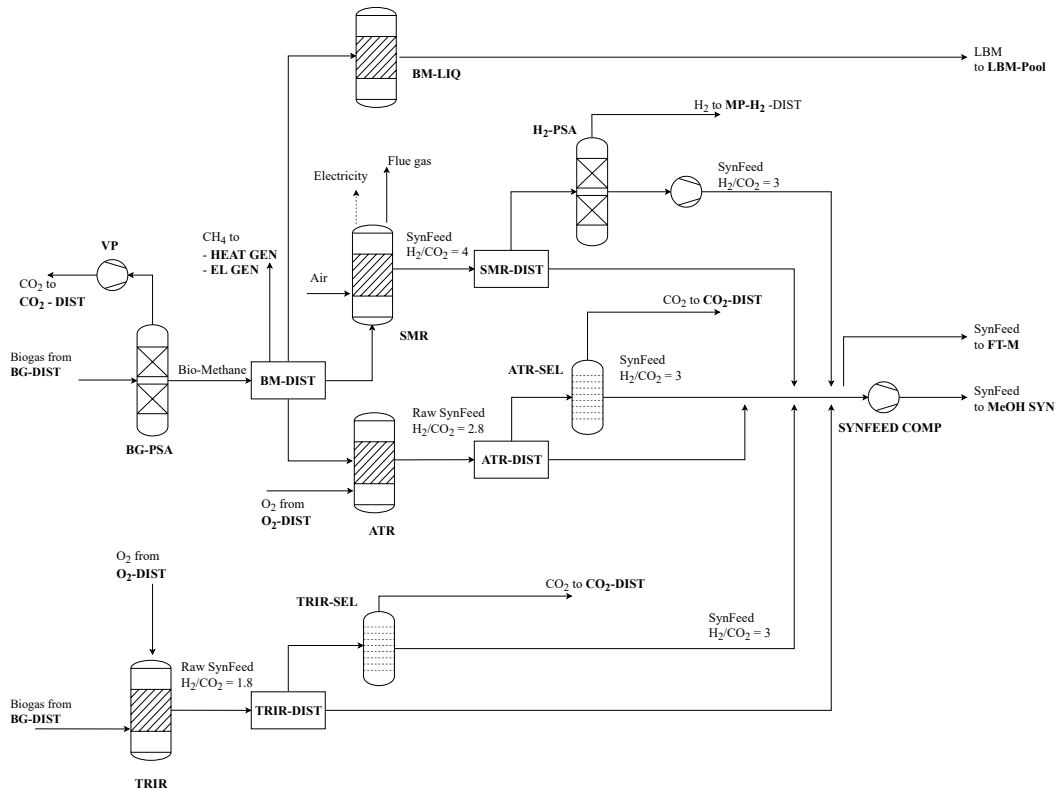
FIGURE 5.5: BIOGAS PRETREATMENT, REFORMING AND UPGRADING PROCESS SECTION OF METHANOL PRODUCTION SUPERSTRUCTURE.

Biogas/ bio-methane reforming

Three different reforming technologies are included in the superstructure: Steam methane (SMR) and autothermal reforming (ATR) of bio-methane as well as direct biogas tri-reforming (TRIR). All three processes are similar in that matter that they include a series of reforming steps, namely pre-reforming at 500°C, main reforming to syngas as well as two-stage water-gas-shift reaction at 350°C and 210°C to convert CO and H_2O to H_2 and CO_2 according to Eq. (5.3). In the end the raw SynFeed is available at approx. 23 bar and cooled down to 40°C for compression to 70 bar. Differences in the process design arise in the main synthesis reaction. The SMR unit uses an externally fired isothermal reactor at 890°C, where

heat supply is provided by combustion of a share of the inlet bio-methane. Hot flue gas is used in heat recovery and steam generation to produce excess electricity. ATR and TRIR both utilize partial oxidation at temperatures around 1000°C. Due to internal heat supply, no excess heat is produced.

Independently on the reforming technology the raw SynFeed has to be compressed to operating pressure of the methanol synthesis. This is ensured by a product compressor (depicted as SMR, - ATR, - and TRIR-COMP in Figure 5.5). However, this step is skipped if SynFeed upgrading is selected (see next section), where final compressing is taking place after the upgrading (SYNFEED COMP). In that case the raw SynFeed at 40°C and approx. 23 bar is fed to the upgrading technology.

The integrated techno-economic models of the reforming technologies are based on detailed models and simulation using Aspen Plus. By modeling different plant capacities (small-, medium-, large-scale), non-linear economies-of-scale equations were derived with the aid of the Aspen Economic Analyzer. Additionally, linear-dependent utility and raw material demands as well as conversion rates were extracted from the simulation results and converted to the level of detail included in the superstructure model. Table 5.3 presents the calculated product distribution in wt. -%. Further details on modeling assumptions as well as resulting flowsheets, stream data and additional techno-economic results of the Aspen Plus models can be found in Appendix C.

TABLE 5.3: PRODUCT DISTRIBUTION OF DIFFERENT REFORMING TECHNOLOGIES; FURTHER INFORMATION IN APPENDIX C.

–	CH_4 (wt. -%)	CO_2 (wt. -%)	H_2O (wt. -%)	CO (wt. -%)	H_2 (wt. -%)
SMR	1.6	82.2	0.5	0.6	15.1
ATR	0.3	86.3	0.4	1.6	11.4
TRIR	0.2	90.6	0.3	1.3	7.6

SynFeed upgrading

All three conversion processes do not produce SynFeed with a fitting H_2/CO_2 ratio for methanol synthesis (see Table 5.3 and Figure 5.5). Matching of raw SynFeed H_2/CO_2 and required ratio can be done in two ways. The first is to simply supplement the missing component to the stream. Hence, SMR-SynFeed would be mixed with additional CO_2 from biogas pretreatment or carbon capture processes, and ATR/TRIR-SynFeed would be mixed with additional H_2 from water electrolysis.

The second possibility is to separate the excess components. Excess H_2 from SMR can be separated by pressure swing adsorption (H_2-PSA in Figure 5.5). Techno-

economic model data was generated using Aspen Plus as described further detail in Appendix D. The total PSA train includes the PSA unit itself as well as subsequent vacuum pump and compression to the initial pressure of the entering SynFeed. The PSA unit itself was modeled as a black-box using the hydrogen recovery factor of 89 % given by Spallina et al. [93]. Calculated energy demand as well as capital costs from the Aspen Economic Analyzer were translated into unit-operation data on superstructure model level afterwards.

CO_2 excess from ATR and TRIR can be separated by physical absorption using the industrial Selexol process (ATR-SEL and TRIR-SEL in Figure 5.5). To gain the necessary model data, this process was also simulated using Aspen Plus prior to optimization. The concept utilizes CO_2 absorption into a mixture of different polyethylene glycols as solvent at the outlet pressure of the raw SynFeed and temperatures at around –1°C. CO_2 recovery is achieved by pressure reduction where a CO_2 recovery factor of 90 % is reached. Details on the developed flowsheets with their primary assumptions as well as major techno-economic results are given in Appendix D. Utilizing three modeled capacities, again non-linear economies-of-scale equations as well as linear dependent utility and raw materials demand were extracted from the model and simplified for the superstructure model as presented in Table 5.4.

TABLE 5.4: MAJOR TECHNO-ECONOMIC DATA FOR SYNFEED UPGRADING TECHNOLOGIES; FURTHER INFORMATION IN APPENDIX D.

–	Hydrogen / CO_2 recovery factor (%)	Electricity (MWh/t$_{SynFeed}$)	Cooling (MWh/t$_{SynFeed}$)	Chilling (MWh/t$_{SynFeed}$)
H2-PSA	89	0.107	0.107	–
ATR-SELEXOL	90	0.02	0.009	0.03
TRIR-SELEXOL	90	0.02	0.006	0.02

5.2.3 Purge gas and waste water treatment

The purge gas from the methanol purification includes remaining H_2, CO and MeOH. This gaseous stream is combusted to produce either steam (HEAT GEN) or electricity (EL GEN) which can either be used internally or be sold to the market (cf. Figure 5.6) [24]. Additionally, biogas or bio-methane can be co-combusted with purge gas to produce heat or electricity. This way biogas also be used to only provide CO_2 by BG-PSA and VP, depicting an additional fourth carbon source technology. Separated H_2 from H_2-PSA can either be used as additional input for methanol synthesis, energy production or sold as by-product.

Waste water streams that arise in the chemical plant cannot be emitted to the environment without pretreatment. Additionally, it could be economically and environmentally favorable to recycle water for water electrolysis or steam/autothermal/tri- reforming. To achieve waste water purification a waste

water treatment (WWT) is implemented, which is not modeled in detail but only implemented with a fixed cost factor of 2.5 €/t [94].
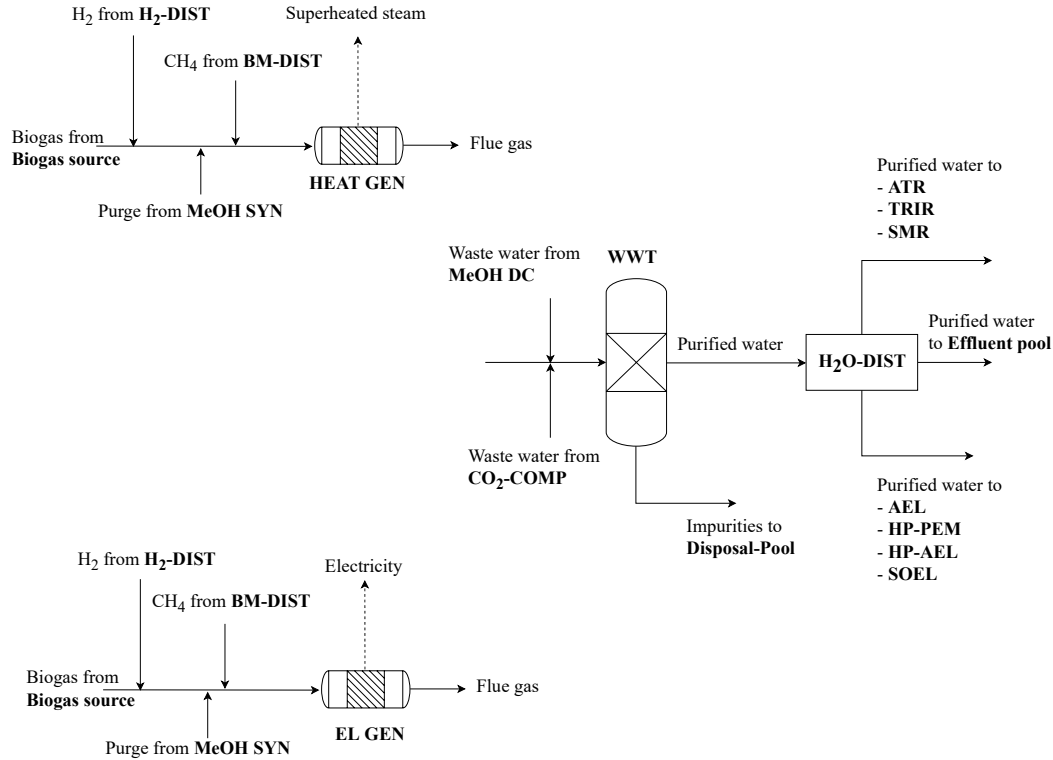
FIGURE 5.6: WASTE WATER AND PURGE GAS TREATMENT PROCESS SECTION OF METHANOL PRODUCTION SUPERSTRUCTURE.

5.2.4 Raw materials, product pools and distributors

Next to biogas the available raw material sources include freshwater, refinery flue gas, cement factory flue gas, air, pure oxygen and monoethanolamine. Except for biogas none of the raw material sources are limited to a maximum amount. Pure oxygen is assumed to be produced by a cryogenic air separation unit.

The main product is the methanol. However, oxygen from electrolysis as well as hydrogen from H_2-PSA can be sold as by-products.

Seven distributor units are included in the superstructure. They ensure a free, optimization-depending, distribution of different intermediates like O_2, H_2, CH_4, SynFeed or purified waste water. Their given inlet unit-operations as well as target processes are listed in Table 5.5.

TABLE 5.5: DISTRIBUTOR NAMES AND PROCESS CONFIGURATION OF METHANOL PRODUCTION SUPERSTRUCTURE.

Distributor name	Inlets	Targets
O_2-DIST	O_2 from AEL/HP-PEM/SOEL/HP-AEL	O_2-Productpool, OXY, ATR, TRIR
H_2-DIST	H_2 from H_2-PSA	HEAT GEN, EL GEN, H_2-Productpool, H_2-MH-COMP
BM-DIST	BM-PSA	SMR/ATR, HEAT GEN, EL GEN
H_2O-DIST	WWT	AEL/HP-PEM/SOEL/HP-AEL, ATR, TRIR, Effluent-Pool
SMR-DIST	SMR	H_2-PSA, SMR-COMP, SYNFEED COMP
ATR-DIST	ATR	ATR-SEL, ATR-COMP
TRIR-DIST	TRIR	TRIR-SEL, TRIR-COMP

5.2.5 General assumptions and key parameters

The flowsheet synthesis is investigated based on generic assumptions. However, relevant data like electricity or natural gas costs and emission factors are modeled after the German energy system. Table 5.6 depicts main input parameters. Full load hours were derived from a H_2 supply optimization case study by Wassermann et al. [95]. Electricity greenhouse gas (GHG) emissions and fresh water demand (FWD) were calculated based on data from the ecoinvent database [95], [96]. They reflect direct electricity purchase from offshore wind farms at the German North Sea with the FLH derived from Wassermann et al.. Electricity costs for offshore wind energy are taken from a study published by the Fraunhofer ISE [97]. Steam costs were derived using Aspen Plus simulation and its integrated economic analyzer. The approach assumes natural gas combustion with a cascade of four heat exchangers to produce superheated, high-, medium- as well as low-pressure steam. Natural gas at costs were assumed to be 2.785 ct/kWh [74]. Costs of unit-operations, natural gas and final cooling were allocated to the different steam types based on their energy content. Table 5.7 presents costs, GHG emissions and FWD of major raw materials and (by)products. Additionally, costs and emissions of conventional methanol are presented as they are used as reference in the multi-criteria optimization framework.

TABLE 5.6: ASSUMPTIONS ON KEY PARAMETERS [74], [82], [92], [94]–[99].

Parameter	Value	Unit	Parameter	Value	Unit
Interest rate	0.05	-	Waste treatment costs	2.5	€/t
Costs of electricity	72	€/MWh	Chilling costs	19.06	€/MWh
GHG emissions of electricity	0.0085	$t_{CO_2-eq.}$/ MWh	Chilling GHG	0.4	$t_{CO_2-eq.}$/ MWh
FWD of electricity	0.0997	t_{H_2O}/ MWh	Chilling FWD	3.17	t_{H_2O}/ MWh
Steam GHG emissions	0.294	$t_{CO_2-eq.}$/ MWh	Superheated Steam at 600°C	37.1	€/MWh
Steam FWD	0.485	t_{H_2O}/ MWh	High pressure saturated steam at 330°C	37	€/MWh
Product load cap^{PROD}	200	kt_{MeOH}/a	Medium pressure saturated steam at 230°C	36.8	€/MWh
Full load hours per year	4777	h/a	Low pressure saturated steam at 135 °C	32.2	€/MWh
Process water	2	€/t	Biogas availability	3.5	t/h

TABLE 5.7: COSTS, GREENHOUSE GAS EMISSIONS AND FRESH WATER DEMAND FOR RAW MATERIALS AND BY-PRODUCTS [94], [96], [98], [100].

--	Methanol	Oxygen purchase (from ASU)	Biogas	Hydrogen product	Oxygen product
Costs (€/t)	325	21	350	2000	14.7
GHG emissions ($t_{CO_2-eq.}$/ t)	0.586	0.585	-1.21	12.13	0.585
FWD (t_{H_2O}/ t)	4.272	3.57	0.605	4.5	3.57

5.3 RESULTS

The described case study is investigated for multiple criteria utilizing the algorithm proposed in chapter 4.2. In the following the results for the criteria weighting process as well as the single- and multi-objective process design optimization are presented.

5.3.1 Objective weighting by pairwise comparison

A weighting is performed using the pairwise comparison method proposed: The importance of the total costs compared to the other criteria is estimated using linguistic values as presented in Table 5.8. Costs of the methanol are considered as the most important criterion. This is reasoned with the argument, that renewable methanol will not be produced if it is not cost competitive, also currently in industries costs will always be the final decision parameter on technology choice. However, costs are also only slightly more important than NPE due to the urgency

of the climate change. NPFWD is not as important as NPE and NPC are moderately more important than NPFWD. This is especially true for Germany where fresh water supply is not overall critical to the current date. The conversion of these linguistic values to numbers according to the Saaty-scale is shown in Table 5.9. Based on the first row of the comparison matrix the rest of the matrix is built using Eq. (4.2). The resulting complete matrix is shown in Table 5.10.

TABLE 5.8: PAIRWISE COMPARISON OF CRITERIA IMPORTANCE IN LINGUISTIC VALUES.

-	NPC	NPE	NPFWD
NPC	Equally important	Equally to moderately more important	Moderately more important

TABLE 5.9: PAIRWISE COMPARISON OF CRITERIA IMPORTANCE TRANSLATED INTO NUMERIC VALUES.

-	NPC	NPE	NPFWD
NPC	1	2	3

TABLE 5.10: PAIRWISE COMPARISON OF COMPLETE CRITERIA MATRIX IN NUMERIC VALUES.

-	NPC	NPE	NPFWD
NPC	1	2	3
NPE	1/2	1	3/2
NPFWD	1/3	2/3	1

Utilizing Eq. (4.4) and Table 5.10 the resulting weights as shown in Eqs. (5.7) to (5.9) are calculated to be 55 % for NPC, 27 % for NPE and 18 % for NPFWD. If no weighting is applied all criteria obtain the same weighting which would result in weights of 1/3 or 33.33 %.

It should be noted, that the performed weighting is only an example of the general weighting process and highly subjective. Depending on the DM, these preferences could vary. To further increase the quality of the weighting process additional steps like surveys, the Delphi-method and average value calculation could be considered.

$$w_{NPC}^{norm} = 0.55 \qquad (5.7)$$

$$w_{NPE}^{norm} = 0.27 \qquad (5.8)$$

$$w_{NPFWD}^{norm} = 0.18 \qquad (5.9)$$

5.3.2 Single-criterion optimization

The consecutive calculation of single-criterion optimization, reformulation and integrated MCO is automated in OUTDOOR. The pre-calculated weights as well

as reference values for conventional fuels are handed over to OUTDOOR. Based on these values, OUTDOOR sets up the mathematical model and solves this model for the single-criterion objective functions. Afterwards the best and worst values as well as weights are gathered automatically and a reformulation is executed as presented in the algorithm. The resulting reformulated model is solved and all results are presented to the user.

The implementation of the case study in the OUTDOOR software results in a MILP model with 42,427 variables, of which 1030 are binary and 111,135 constraints. This model was solved on a MacBook Pro with a 2 GHz Dual-Core Intel Core i5 processor and 8 GB RAM utilizing Gurobi Version 9.1. With this configuration, a single-criterion optimization takes 24 – 28 seconds and the total multi-criteria optimization process including pre- and postprocessing in OUTDOOR takes approximately 111 seconds.

The three different non-weighted single-criterion optimizations result in three different process designs. The derived NPC, NPE. And NPFWD are presented in Table 5.11 for all three process concepts and the conventional reference product. It can be observed, that all renewable concepts outperform the reference process in terms of NPE and NPFWD by far. The negative values, depicting GHG and FWD savings, arise from carbon capture and avoided burdens, respectively. However, none of the process concepts is economically competitive to the reference process.

TABLE 5.11: KEY PERFORMANCE INDICATORS OF DIFFERENT SINGLE-CRITERION METHANOL PRODUCTION OPTIMIZATIONS.

-	NPC-optimized	NPE-optimized	NPFWD-optimized	Reference
Calculated *NPC* (€/t)	1282	1408	1635	325
Calculated *NPE* (t_{CO_2}/ t)	–1.92	–2.29	–2.01	0.59
Calculated *NPFWD* (t_{H_2O}/ t)	–2.62	–2.99	–4.17	4.27

NPC-Optimization

The process layout of the cost-optimized design is depicted in Figure 5.7. This configuration utilizes an integrated PtX and BtX concept. Biogas is used to the maximum amount of 3.5 t/h to produce raw SynFeed by TRIR. The raw SynFeed is fed to the methanol synthesis step. Due to limited amount of biogas, the major share of H_2 and CO_2 supply are provided by carbon capture from refinery flue gases by MEA-CC and low-pressure alkaline electrolysis with subsequent multi-stage compression. About 2.25 t/h of purge gas are produced during the methanol synthesis, which are used to produce about 7.18 MWheat of superheated steam for internal utilization. 24.76 t/h of waste water arise mainly from raw methanol

distillation as well as from CO_2 compression. This water is purified in waste water treatment and recycled to decrease fresh water demand. The process requires about 422 MW_{el} of electricity of which about 98 % is consumed by the AEL and subsequent H_2-LH-COMP. Only one unit-operation requires heat, which is the absorption-based carbon capture process. This process needs about 54 MW_{heat} of which 13 % are provided by purge gas combustion and about 33 % from heat integration by recovering waste heat from methanol synthesis and multi-stage H_2 compression. A high temperature heat pump for further waste heat utilization does not seem to be economically beneficial. Methanol is produced at costs of approx. 1282 $€/t_{MeOH}$ which is nearly four times the price of conventional methanol. With CO_2 emissions of –1.92 t_{CO_2}/t_{MeOH} CO_2 abatement costs are about 381.27 $€/t_{CO_2}$.
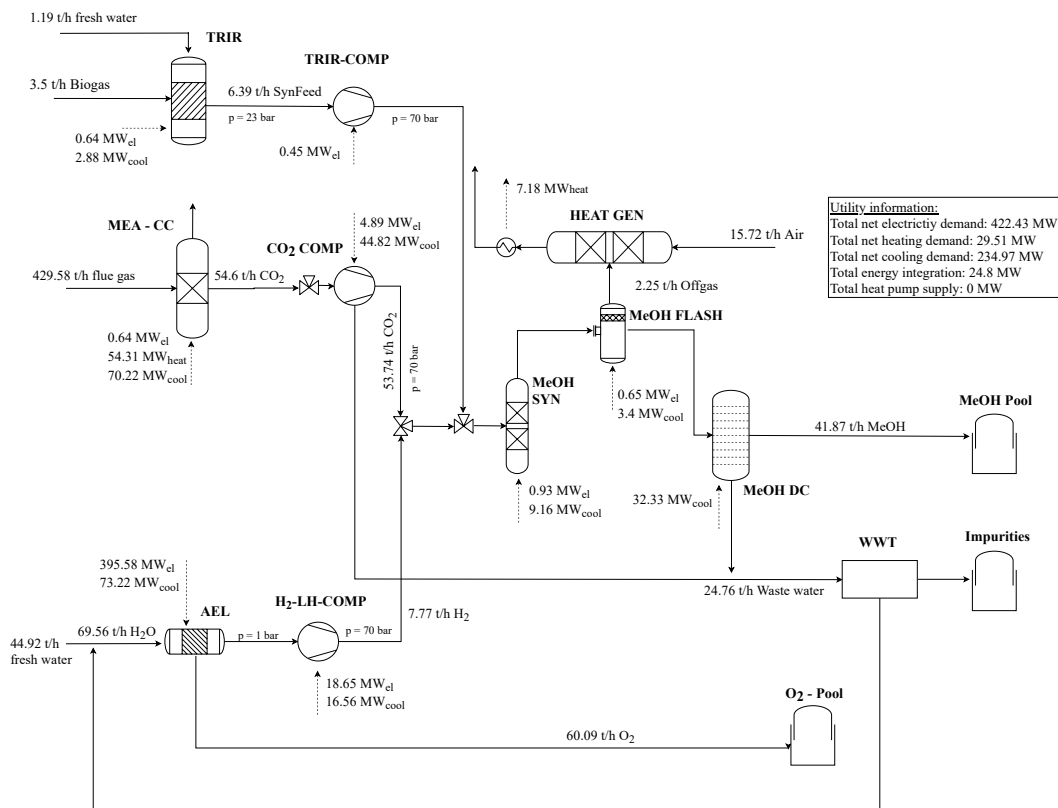

FIGURE 5.7: PROCESS FLOW DIAGRAM OF NPC-OPTIMIZED RENEWABLE METHANOL PRODUCTION.

NPE-Optimization

If optimized for minimal GHG emissions the process layout changes drastically (cf. Figure 5.8). Biogas is not anymore used as raw material for methanol synthesis but rather used for the production of steam, which is sold to the market in order to gain economic as well as GHG credits. CO_2 is supplied by a combination of MEA-CC and low temperature direct air capture. H_2 is solely produced by low-pressure alkaline electrolysis. Water for electrolysis is provided by fresh water as well as captured water in LT-DAC and purified waste water. The process

consumes about 464 MW_el of electricity of which 95 % are required by the electrolyzer and multi-stage H2-LH-COMP. To reduce the net heating demand to zero, thus saving external utility-based GHG emissions, about 30 MW_heat is recovered and used in the MEA-CC and LT-DAC units. Additionally, a high temperature heat pump utilizes low exergetic waste heat to supply additional 37.2 MW_heat while consuming about 14.88 MW_el. The given process produces methanol at costs of 1400 €/t_MeOH, while presenting higher negative GHG emissions of –2.26 t_{CO_2}/t_{MeOH} compared the the NPC-optimized design. CO2 abatement costs of this route are 377.19 €/t_{CO_2}.
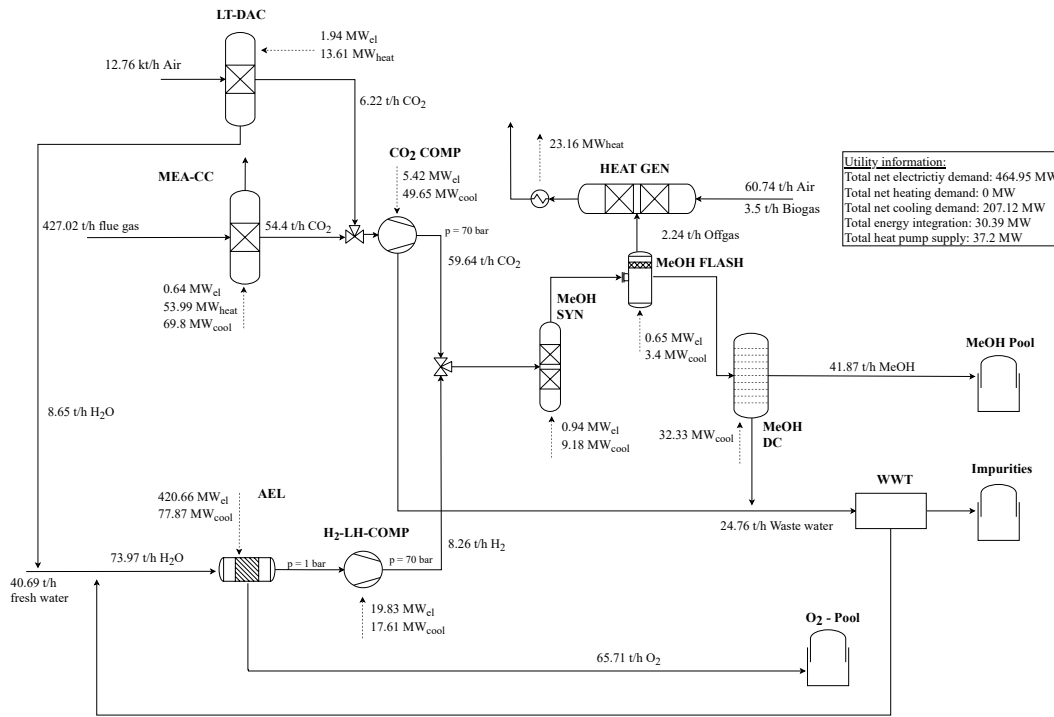

FIGURE 5.8: PROCESS FLOW DIAGRAM OF NPE-OPTIMIZED RENEWABLE METHANOL PRODUCTION.

NPFWD-Optimization

The optimized design for fresh water demand is depicted in Figure 5.9. The general layout is similar to the NPE-optimized design. However, the shares of CO2 and heat integration differ. CO2 is provided by MEA-CC and LT-DAC, with LT-DAC having a share of ca. 60 % compared to 10 % if optimized for NPE. The LT-DAC unit is scaled up to provide low impact water for electrolysis to the point that the low pressure alkaline electrolyzer is operated solely by water from air and recycled water from waste water treatment. Biogas is still combusted together with purge gas to produce steam. However, this steam is now internally used to lower external heat demand. Nonetheless, the process still requires about 25 MW_heat of net heating due to higher energy demand from LT-DAC compared to MEA-CC. Overall the process is the most electricity intensive of the three configurations, requiring up to 469 MW_el of electricity. Once again, most electricity (94 %) is consumed by the

electrolyzer plus the compressor. However, now 2 % are supplied to the direct air capture unit. In total, this configuration produces methanol at costs of 1635 €/t_{MeOH} with negative GHG emissions of –2.01 t_{CO_2}/t_{MeOH}. With 503.85 €/t_{CO_2} CO2 abatement costs are the highest of the three option. However, fresh water savings are 40 – 60 % higher than in NPE and NPC optimized flowsheets.
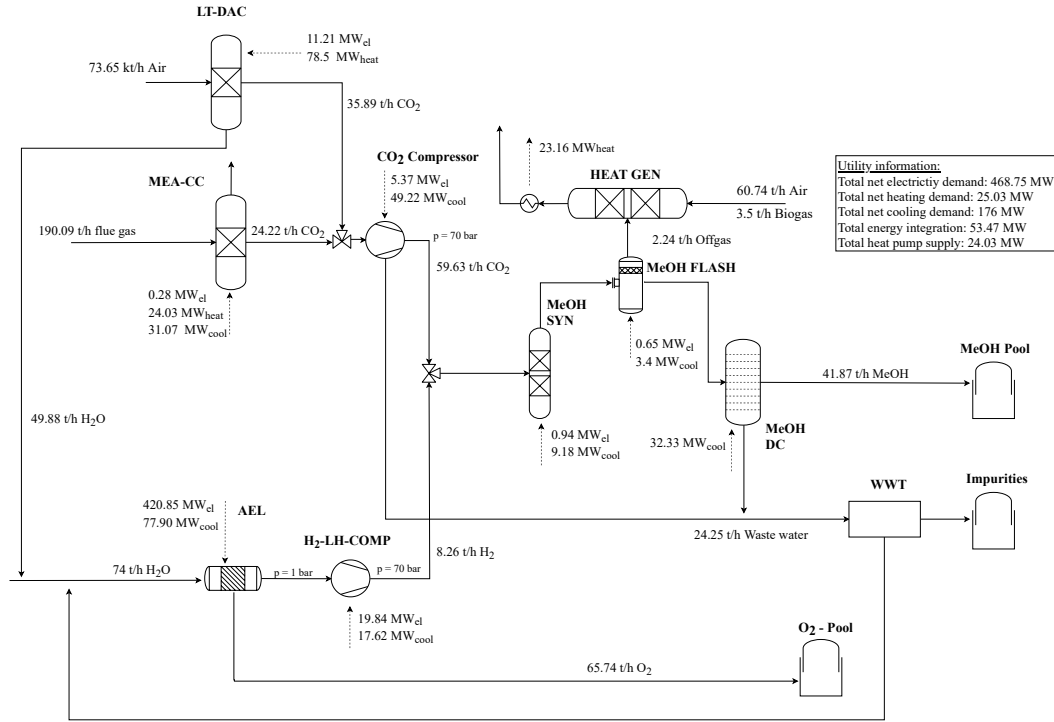

FIGURE 5.9: PROCESS FLOW DIAGRAM OF FWD-OPTIMIZED RENEWABLE METHANOL PRODUCTION.

5.3.3 Multi-criteria optimization

Reformulation and multi-criteria optimization

From the three single-criterion optimization results as well as the reference values, the best and worst values x_i^{MIN} and x_i^{MAX} are derived and presented in Table 5.12. Based on x_i^{MAX} and x_i^{MIN} and Eq. (10) normalized values $v_{t,i}$ are calculated (cf. Table 5.13).

TABLE 5.12: BEST- AND WORST-CASE NPC, NPE AND NPFWD OF SINGLE-CRITERION OPTIMIZATION AND REFERENCE PROCESS.

-	NPC (€/t_{MeOH})	NPE (t_{CO_2}/ t_{MeOH})	NPFWD (t_{H_2O}/ t_{MeOH})
x_i^{MIN}	325	-2.26	-4.17
x_i^{MAX}	1635	0.586	4.27

TABLE 5.13: NORMALIZED VALUE $v_{t,i}$ OF SINGLE-CRITERION OPTIMIZATION AND REFERENCE PROCESS.

-	NPC-Optimized	NPE-Optimized	NPFWD-Optimized	Reference
NPC	0.27	0.18	0	1
NPE	0.88	1	0.91	0
NPFWD	0.82	0.94	1	0

Decision-makers weights optimization

Using the derived $v_{t,i}$ values and the weights calculated in chapter 4.2 a multi-criteria optimization and assessment is performed. As presented in Figure 5.10, the resulting process is simpler than the prior layouts. CO_2 is solely provided by MEA-CC, while H_2 is still produced by AEL. Biogas is not utilized anymore. Purge gas from the methanol synthesis is combusted to produce steam, which is sold to the market to generate economic, GHG and FWD credits. However, the required net heating demand is still zero, due to the use of heat recovery (27.9 % of required heat) and a high temperature heat pump (72.1 % of required heat). External cooling demand is approx. 225 MW_{cool} and electricity demand sums up to 466 MW_{el}.
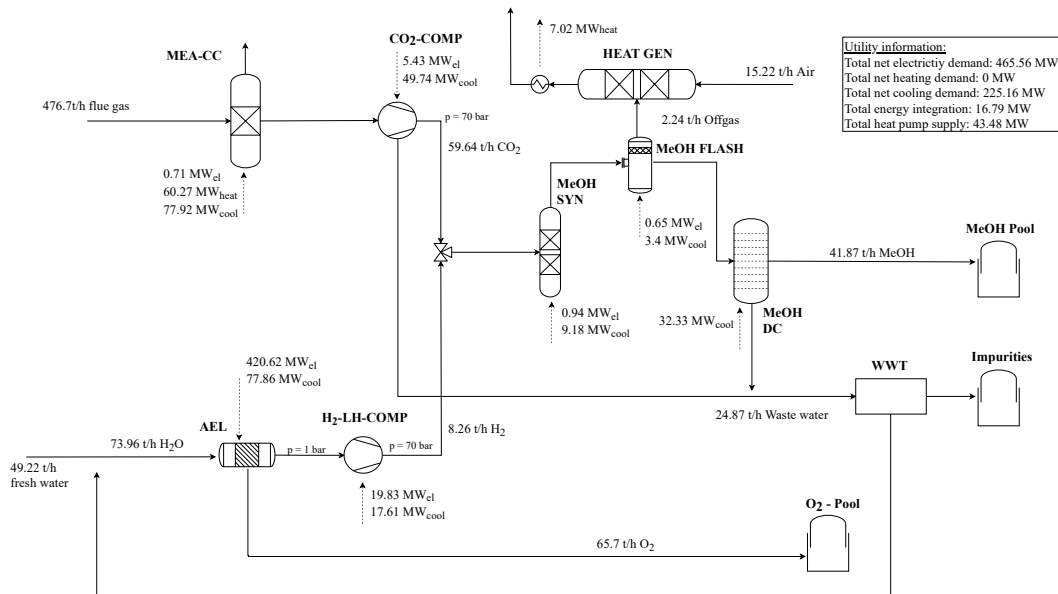

FIGURE 5.10: PROCESS FLOW DIAGRAM OF MULTI-CRITERIA-OPTIMIZED RENEWABLE METHANOL PRODUCTION.

The total annualized costs of this process are 261 M€ of which 27.7 % are capital investment costs (CAPEX) and the rest operational costs (OPEX) as shown in Table 5.14. Major cost driver is the H_2 supply system (AEL + H_2-LH-COMP), which account for 79 % of the CAPEX and over 90 % of the electricity demand as presented in Figure 5.11. In combination with costs for operating and maintenance the H_2 supply accounts for approx. 73 of the total operational costs.

TABLE 5.14: NET PRODUCTION COST DISTRIBUTION OF METHANOL.

Position	Share (%)	€/t$_{MeOH}$
Capital costs	27.7	362
Raw materials	0.5	6.5
Electricity	61.3	801.2
Operating & Maintenance	12.2	159.5
Heat integration /Refrigeration	0.1	1.3
Profits	–1.8	–23.5

This design produces methanol at costs of 1307 €/t$_{MeOH}$ with GHG emissions of – 2.23 t$_{CO_2}$/t$_{MeOH}$ and FWD of –3.42 t$_{H_2O}$/t$_{MeOH}$, representing a good trade-off compared to the single-criterion optimization layouts. CO₂ abatement costs are at 348.23 €/t$_{CO_2}$ presenting the minimum of the considered cases. Overall the results are in good agreement with similar studies given in Literature. Adnan et al. calculated methanol costs of 900 €/t$_{MeOH}$ for lower electricity costs of 4 ct/kWh [101]. The approx. 900 €/t$_{MeOH}$ are also achieved in this study if electricity costs are reduced (ref. chapter 5.3.5). A detailed study from Wassermann et al. determines methanol costs of 1146 €/t$_{MeOH}$ with –1.97 t$_{CO_2}$/t$_{MeOH}$ with slightly higher electricity costs but lower electrolyzer invest as well as higher full load hours. In their study the H₂ supply system contributed about 88 % of the total costs compared to 89 % calculated in this study [82].

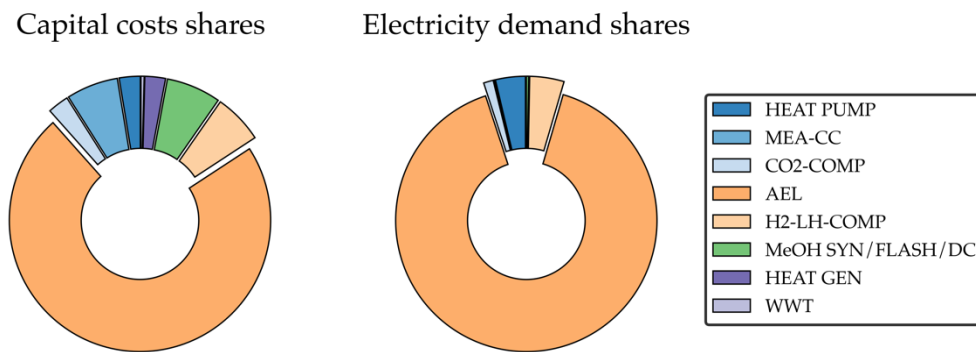FIGURE 5.11: CAPITAL COST AND ELECTRICITY DEMAND BREAKDOWN FOR RENEWABLE METHANOL PRODUCTION.

Table 5.15 and Table 5.16 show the normalized weighted value scores and the relative closeness ratio. The multi-criteria optimized process layout outperforms the single-criterion optimized renewable processes as well as the reference process slightly. All relative closeness ratios are in the same region.

TABLE 5.15: NORMALIZED WEIGHTED VALUE SCORES $V_{t,i}$ OF DIFFERENT PROCESS CONFIGURATIONS FOR DECISION-MAKERS WEIGHTING.

-	NPC-Optimized	NPE-Optimized	NPFWD-Optimized	Reference	MCO
NPC	0.149	0.098	0	0.55	0.138
NPE	0.238	0.27	0.247	0	0.268
NPFWD	0.147	0.17	0.18	0	0.164

TABLE 5.16: RELATIVE CLOSENESS RATIO C_t FOR DECISION-MAKERS WEIGHTING OPTIMIZATION.

-	NPC-Optimized	NPE-Optimized	NPFWD-Optimized	Reference	MCO
C_t	0.533	0.538	0.427	0.55	0.57

Equal weights optimization

In addition to the DM's weighting optimization, a second MCO run is performed to investigate the influence of weighting. In this setup, all three criteria have a weight of 33.3 %. When optimized for this weighting profile the process layout does not change compared to the DM's weighting profile, which could be a first indication of a rather robust trade-off optimum of the PtX process.

Table 5.17 shows the normalized and weighted value scores $V_{t,i}$ of this multi-criteria optimization. Table 5.18 shows the relative closeness ratio C_t. It can be seen, that the reference process is now the least favorable process design. The MCO configuration outperforms the other concepts more dominantly than in the DM's weighting choice.

TABLE 5.17: NORMALIZED WEIGHTED VALUE SCORES $V_{t,i}$ OF DIFFERENT PROCESS CONFIGURATIONS FOR EQUAL WEIGHTING.

-	NPC-Optimized	NPE-Optimized	NPFWD-Optimized	Reference	MCO
NPC	0.09	0.06	0	0.333	0.084
NPE	0.29	0.333	0.304	0	0.33
NPFWD	0.27	0.314	0.333	0	0.303

TABLE 5.18: RELATIVE CLOSENESS VALUE C_t FOR EQUAL WEIGHTS OPTIMIZATION.

-	NPC-Optimized	NPE-Optimized	NPFWD-Optimized	Reference	MCO
C_t	0.66	0.71	0.64	0.33	0.72

5.3.4 Variation analysis

The preceding analysis gives a first indication of a steady trade-off process using flue gas carbon capture, alkaline electrolyzers and intense heat integration as well as utilization of high temperature heat pumps to reduce external heating and cooling utilities. To further investigate the trade-off between PtX and BtX process

routes, major parameters are varied as part of a variation analysis. The availability of biogas is changed from 3.5 t/h (depicting a large German biogas plant) to 60 t/h, which would suffice to provide the total SynFeed input for methanol synthesis. The electricity price, which is the major influence in the costs of the PtX route is reduced to zero. Hence, three additional scenarios are defined as shown in Table 5.19 and optimized for an equal weighting.

TABLE 5.19: MAIN PARAMETERS FOR ADDITIONAL SCENARIOS IN METHANOL PRODUCTION CASE STUDY.

-	Base scenario	Variation scenario 1	Variation scenario 2	Variation scenario 3
Maximum biogas input (t/h)	3.5	3.5	60	60
Electricity price (€/MWh)	72	0	72	0

The simulation of all three variations (plus the base scenario) strengthens the impression that stand-alone Power-to-Methanol is the best trade-off when costs, greenhouse gas emissions and fresh water demand are considered simultaneously. If the electricity price is reduced to 0 €/MWh (variation scenario 1), the NPE- and NPFWD- optimization process layouts do not change. The NPC-optimized layout changes to a purely electricity-based facility where CO_2 is provided by MEA-CC and H_2 is provided by high-pressure alkaline electrolysis due to the assumption of similar capital costs compared to low-pressure AEL. The MCO process layout is similar to the NPE-optimized process, resulting in NPC of about 500 €/t_{MeOH}.

Variation scenario 2 presents changed process layouts for NPE- and NPFWD- optimization, in both cases biogas intake is increased to produce more steam, which is sold. NPE-optimization sells steam to full extend while NPFWD- optimization still provides internal heat. Cost optimization leads to a purely bio-based process using bio-methane in tri-reforming with lower costs of ca. 805 €/t_{MeOH} compared to electricity-based production. However, the MCO trade-off depicts again a PtX route as presented in the base scenario without the utilization of biogas.

The last scenario leads to similar results as scenario one and two. The layout of NPE- and NPFWD- optimization is consistent, while biogas is used to the maximum amount for steam production. Lowest costs are still achieved by electricity-based production as in scenario one. Additionally, the MCO process configuration is again similar to the NPC-optimized layout. The key performance indicators for all three scenarios are displayed in Table A.2 – A.4.

5.3.5 Sensitivity analysis

Due to the fact that the electricity-based methanol production displays a steady trade-off in multi-criteria optimization, a simple, one-dimensional, sensitivity analysis is conducted for the most influencing parameter. As shown in chapter 5.3.3 electricity costs for H_2 provision take up over 40 % of the total costs. Therefore, the influence of the electricity price is investigated further in Figure 5.12. It can be observed, that depending on the electricity price the methanol production costs vary from 500 – 1500 €/t_{MeOH}, while GHG emissions and FWD are constant. Also, the ratio of C_t for the MCO design and the reference process is only slightly decreasing for rising electricity costs. This indicates that the process design of the trade-off solution stays constant for varying electricity prices, once again depicting a steady trade-off. However, together with the preceding variation analysis this clarifies that even with free electricity, renewable methanol production is not economically competitive to conventional methanol production. Remarkably, at rather low costs of 500 €/t_{MeOH} and negative GHG emissions of – 2.23 t_{CO_2}/t_{MeOH} the CO_2 abatement costs decrease to 62.06 €/t_{CO_2}.
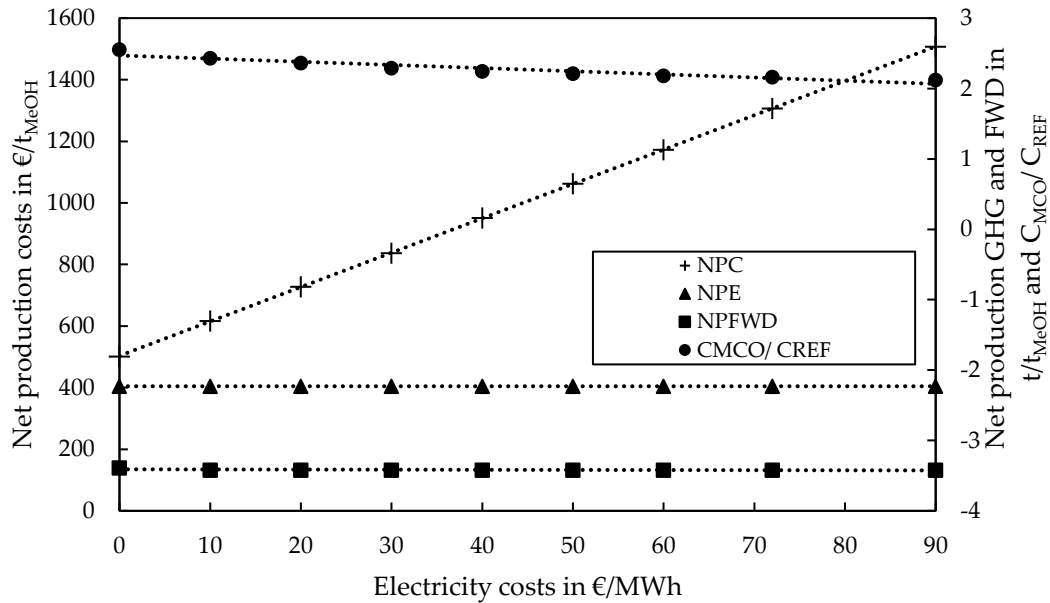

FIGURE 5.12: NET PRESENT COSTS (NPC), GREENHOUSE GAS EMISSION (NPE), FRESH WATER DEMAND (NPFWD) AND RELATIVE CLOSENESS RATIO OF MULTI-CRITERIA OPTIMUM (C_{MCO}) AND REFERENCE PLANT (C_{REF}) IN RELATION TO ELECTRICITY PRICE.

5.4 DISCUSSION

The presented case study provides a deep insight on renewable methanol production using a combination of PtX and BtX processes. Conceptual process design was optimized for multiple objectives. However, a final discussion regarding feasibility and sustainability should be carried out.

The total plant capacity is set to 200,000 t/a of methanol, which depicts 14 % of the German production capacity and is in the region of an average methanol plant with 40,000 – 1,000,000 t/a [102], [103]. The NPC-optimized flowsheet uses a combination of biogas-reforming and electrolysis/carbon capture to provide SynFeed. The size of the biogas provider is set to a single large-scale biogas plant. To have such a plant in co-location of the methanol plant seems more believable than having a larger network of biogas plants deliver gas combined in Germany. The resulting biogas-reforming technology produces around 8,000 Nm^3 of H_2 which is at the lower end of commercial reforming technologies that are normally designed for outputs of 1,000 – 200,000 Nm^3 of H_2 based on natural gas [104]. Additionally, the process requires 430 t/h of refinery flue gas which depicts approx. 65 % of the actual production of the Heide refinery in Schleswig-Holstein, that was used as data basis for the amine scrubbing process [105]. However, the PtX process only operates for 4777 h/a, therefore the total CO_2 demand only displays 40 % of the total available CO_2. The NPE- and NPFWD-optimized processes combine amine scrubbing of flue gases with direct air capture. The calculated DAC-CO_2 streams of ca. 6 and 36 t/h would require land space of 0.7 and 4 ha when the container units of Climeworks are utilized [106]. Consequently, with 36 t/h being approx. 60 % of the total CO_2 input, a fully DAC-based supply would lead to an area demand of ca. 6.7 ha [106]. Considering Germanies total methanol production capacities, a total area of 47 ha (0.47 km^2) would be required for CO_2 supply, which depicts 0.0001 % of Germanies total land space. Although this still is feasible, further increasing the CO_2 demand for the production of fuels or further chemicals could pose a problem for densely populates countries like Germany. Anyhow, this issue is not the case for low-density countries as they exist in the MENA region. Here, the additional benefit of excess H_2O from LT-DAC could be used for other applications like farming or drinking water, leading to added-value of Power-to-X processes.

The scope of the multi-criteria optimization is restricted to NPC, NPE and NPFWD on the one hand and to a cradle-to-gate approach on the other hand. Although a complete sustainability analysis would include further metrics like land use, eutrophication or social aspects, it was decided that the implemented objectives display the most relevant in the discussion of PtX and BtX. Use- and end-of-life phases are not included in the calculations because it can be assumed, that these

phases are independent of the production pathway (including conventional methanol production), thus they can be neglected in comparisons.

Utilization of flue gases by amine scrubbing is the preferred technology, but this source cannot be considered sustainable. Using this approach carbon dioxide is merely recycled, which provides a good start, but should not lead to extending the operating of non-renewable processes. Additionally, processes that are designed now are supposed to operate for the upcoming $20 - 25$ years. If the carbon source is to be chosen as flue gas, but this source vanishes at some point, the CO_2 acquisition has to be redesigned. Therefore CO_2-supply should be designed to be adaptable, from the start. The combination of MEA-CC, LT-DAC and TRIR could be such a design. Initially CO_2 could be provided by MEA-CC and TRIR, while also small shares of H_2 are produced by TRIR. Due to the combination the MEA-CC process can initially designed in smaller scale. With increasing transformation of the energy sector, the flue gas availability will decrease. During that time the modular LT-DAC technology can be included. Its capacity is increased step-by-step to replace amine scrubbing.

In conclusion, the developed conceptual designs of this study are feasible to build and operate. Mature technologies like flue gas scrubbing have the upper hand compared to novel technologies like DAC. However, the upcoming transformation of the energy sector should be considered as well. Therefore, a design, which is adaptable to further adjustments in the future should be considered. The design of such optimized systems however, is dependent on many variables such as development of energy prices, maximal operating timeframe of conventional industries, availability of renewable energy carriers and issued policies.

6 INTEGRATED POWER-TO-X AND BIOREFINERY OPTIMIZATION FOR FUELS PRODUCTION

This chapter presents a detailed case study on the renewable production of liquid fuels. Focus is set on jet fuel, which will be required on mid- and long-term due to the lack of suitable alternatives. An integrated biomass- and electricity-based refinery is set up. It combines electricity-based pathways of methanol- and Fischer-Tropsch synthesis with an algae-based biorefinery for production of hydroprocessed esters and fatty acids and biogas for further biogas reforming. As response to uncertain data the renewable refinery is optimized for costs using the optimal-design screening algorithm, identifying operational windows for methanol-to-jet and algae refinery as well as their potential integration.

6.1 OUTLINE

Fuels like motor-gasoline, diesel and jet fuel make up about 56 % of oil-refinery outputs in Germany to this date [6]. Although electrification of cars in individual traffic is rising, it is assumed that especially shipping and aviation cannot be electrified easily [107]. Additionally, with rising demand in emerging countries like Africa as well as increasing globalization, liquid fuels will stay an important energy carrier in the upcoming years [107].

The different fuels each depict a mixture of complex hydrocarbons, which is produced from crude oil by distillation and hydrotreating among other processes [5]. They are not defined specifically by their component mixture but rather by standardized designated properties such as boiling and freeze point, density, cetane or octane number or viscosity [5]. This ensures a standardized application of the different fuels. In general, gasoline is made up from light and heavy naphtha and contains rather short hydrocarbons with carbon numbers of C_5 to C_{12} [5]. Slightly heavier hydrocarbons ($C_8 - C_{16}$) are used for jet fuel [5]. Diesel fuel is mainly produced from gas oils and (pre-treated) vacuum gas oils and depicts a general carbon range of $C_8 - C_{21}$ [5].

Nonetheless, liquid fuels can also be produced by various renewable processes, based on both electricity and biomass [9], [15], [19]. Such process pathways include Fischer-Tropsch synthesis as well as methanol synthesis with subsequent methanol-to-jet production (Power-to-X), as well as bio-based processes like hydroprocessing of bio-oils or alcohol-to-jet using bio-based ethanol [9], [15], [19]. The upcoming sections will discuss the optimization of a conceptual process design to produce a mixture of fuels based on renewable and integrated PtX and BtX processes, with a focus on jet fuel.

6.2 CASE STUDY DESCRIPTION

The general layout of the superstructure is depicted in Figure 6.1. It includes 11 main processing steps. The bio-based pathway includes a biorefinery using algae biomass as raw material to produce hydroprocessed esters and fatty acids (HEFA) as main product, with minor shares of gasoline and diesel as by products. The Power-to-X pathway includes different water electrolysis and carbon capture technologies to produce H_2 and CO_2 with subsequent methanol- or Fischer-Tropsch synthesis including their respective upgrading to jet fuel and further by-products. A combination of PtX and BtX is realized by integrating algae residue conversion to SynFeed (H_2/CO_2 mixture) as input for thermochemical synthesis as well as combined waste water management, purge gas utilization and heat integration. The detailed processing steps and considered technology options of the renewable refinery are described in detail in the following section.
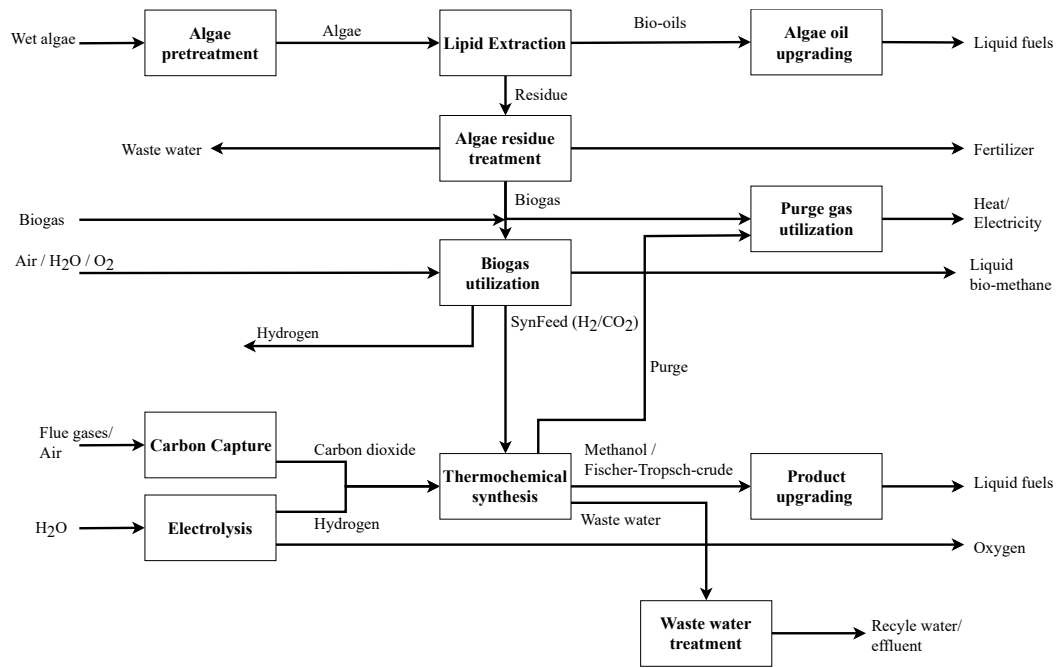
FIGURE 6.1: SIMPLIFIED RENEWABLE REFINERY REPRESENTATION (DETAILED SUPERSTRUCTURE REPRESENTATION WITH ALL UNIT-OPERATIONS CAN BE FOUND IN APPENDIX B, TABLE B.1 AND FIGURE B.1).

6.2.1 Power-to-X process

Electricity-based fuel production uses carbon capture processes for pure carbon dioxide production as well as water electrolysis for hydrogen production with oxygen by-product. Hydrogen and carbon dioxide are consumed in thermochemical synthesis by either methanol synthesis or Fischer-Tropsch synthesis. Produced intermediates are afterwards upgraded depending on the primary synthesis to liquid fuels.

Carbon capture

The carbon capture section provides CO_2 as raw material for thermochemical synthesis. Technology options and used models are similar to the ones described in chapter 5.2.1. Three different technologies, namely low temperature direct air capture (LT-DAC), oxyfuel fired cement factory with subsequent cooling and water separation (OXY) as well as refinery flue gas scrubbing using monoethanolamine are included in the superstructure [82], [87], [88]. As shown in Figure 6.2 the low-pressure CO_2 streams are mixed with potential flows from a CO_2-disributor (CO2-DIST) and compressed to high pressure for thermochemical synthesis.
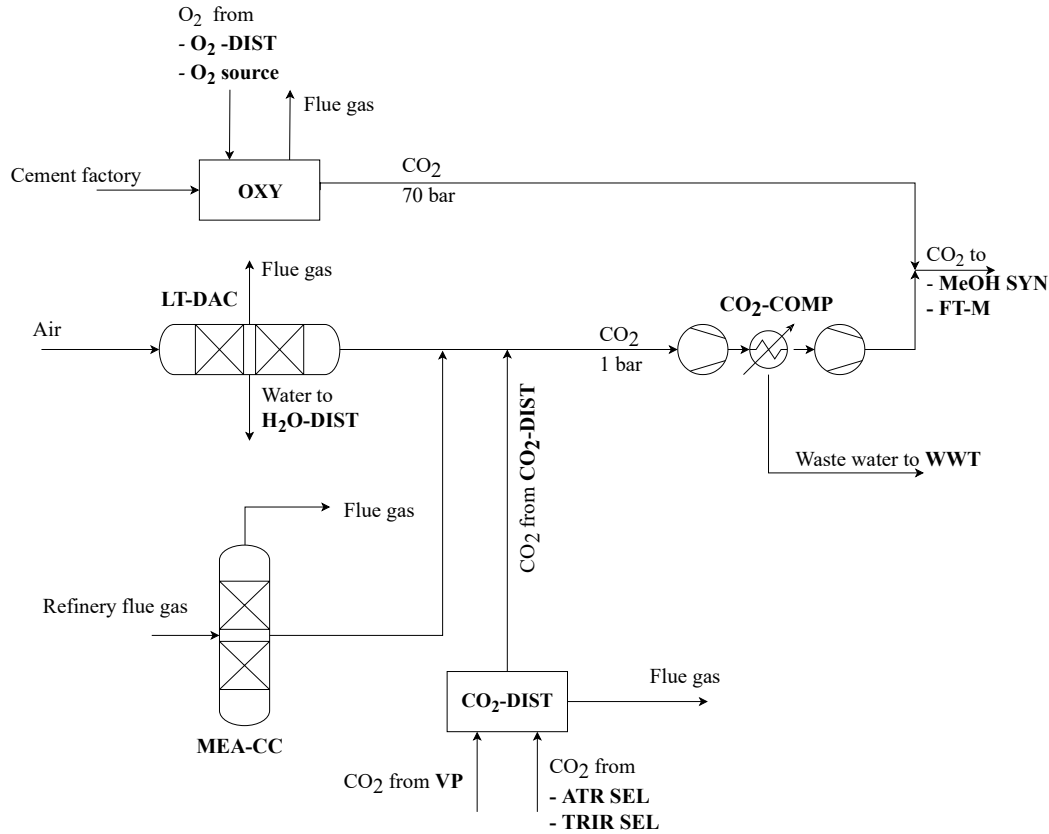
FIGURE 6.2: CARBON CAPTURE PROCESS SECTION OF RENEWABLE REFINERY SUPERSTRUCTURE.

Water electrolysis

Water electrolysis provides the H_2 feedstock for thermochemical synthesis as well as hydrotreating processes. Similar to the carbon capture section, the technology options and models are equivalent to chapter 5.2.1. Included technologies are high- and low-pressure alkaline electrolysis (HP-AEL / AEL), high-pressure proton exchange membrane electrolysis (HP-PEMEL) and solid oxide electrolysis (SOEL) (cf. Figure 6.3).

Three types of H_2 compressors are included in this superstructure. A first one compresses ambient-pressure H_2 to methanol operating pressure of 70 bar (H_2-LH-COMP). A second compressor provides a single-stage compression from 30 bar to 70 bar (H_2-MH-COMP) in order to connect HP-AEL and HP-PEMEL to methanol synthesis. A third compressor depicts a single-stage compression of ambient-pressure H_2 to medium pressure of 30 bar (H_2-LM-COMP). High-pressure hydrogen at 70 bar is solely used in methanol synthesis. However, medium- (30 bar) and low- (1 bar) pressure H_2 has several applications in the process structure. Therefore, both streams are connected to the distinct distributors MP-H_2-DIST and LP-H_2-DIST, respectively. Low-pressure H_2 can be distributed to the H_2-LM-COMP and H_2-LH-COMP as well as used in energy integration where it is combusted with other purge gases to produce either steam (HEAT GEN) or electricity (EL GEN). Next to compression to 70 bar, medium-pressure hydrogen

is the electricity-based raw material for Fischer-Tropsch synthesis. However, it is also used in deoxygenation of bio-oil (BIO-U), hydrotreating of methanol-to-jet intermediates (MTJ) and Fischer-Tropsch crude hydrocracking (FT-C). Additionally, it can also be used in HEAT GEN and EL GEN as well as sold as by-product (H_2-Pool).

Similar to the case study described in chapter 5, O_2 can either be sold as by-product or used in processes like oxyfuel cement factory carbon capture and autothermal as well as TRI reforming.
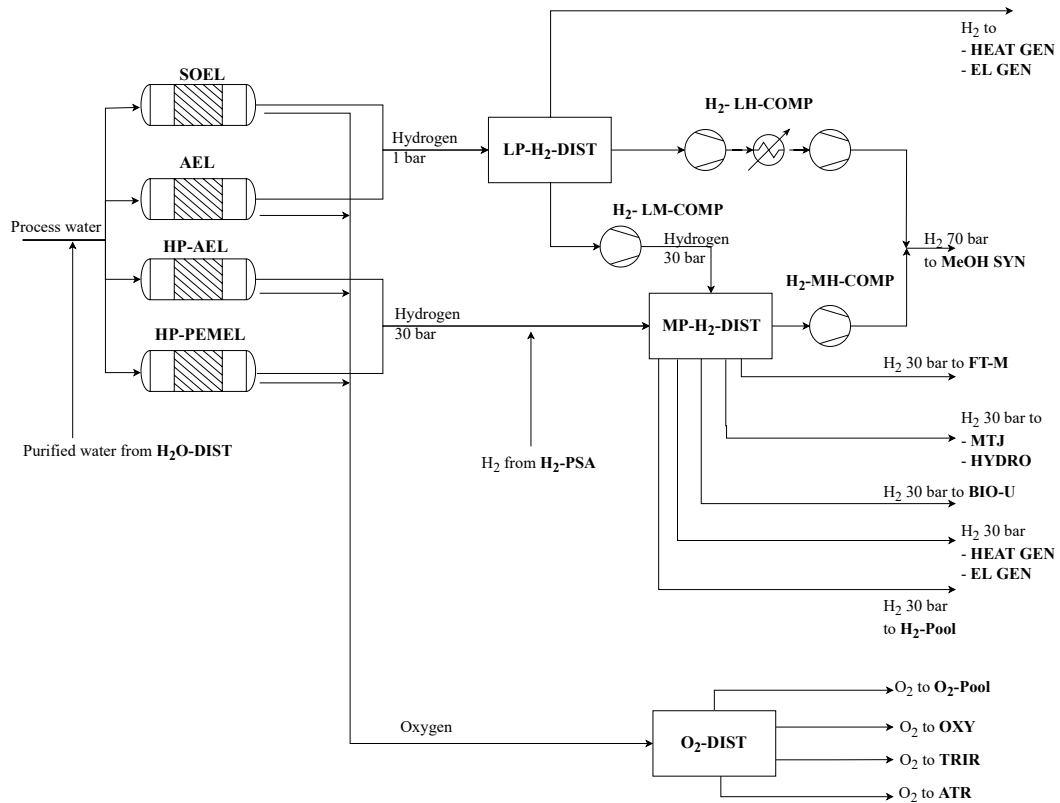

FIGURE 6.3: WATER ELECTROLYSIS PROCESS SECTION OF RENEWABLE REFINERY SUPERSTRUCTURE.

Thermochemical synthesis and upgrading

The thermochemical product synthesis is either chosen as methanol synthesis or as Fischer-Tropsch-Synthesis route (cf. Figure 6.4).

The methanol synthesis implemented in the superstructure is similar to the one described in chapter 5.2.1 and depicts direct hydrogenation of CO_2 at 250°C and 70 bar operating conditions. Equivalent to the case study from chapter 5, the process is modeled as a three-step process with synthesis, purge stream separation and distillation. Purge is sent to either steam or electricity production (HEAT GEN / EL GEN) and waste water to waste water treatment (WWT).

Meanwhile the pure methanol is upgraded using the general concept of methanol-to-jet (MTJ) based on consecutive methanol-to-olefins, olefins oligomerization and

hydrofinishing. The product distribution (given in Table 6.1) as well as hydrogen demand in hydrotreating are based on the MtSynfuels process described by Liebner et al. [18]. The hydrofinishing step requires ca. 0.004 t H_2/t MeOH. Here again waste water is separated and treated in WWT for recycling or disposal.

The Fischer-Tropsch route is modeled after the work of König and depicts a conversion with jet fuel as main product [108]. The detailed model was again consolidated to a limited number of unit-operations. First the raw materials are mixed (FT-M), afterwards CO_2 and H_2 are converted to synthesis gas by reverse water-gas-shift reaction at temperatures of 900°C (RWGS). The required heat is provided internally by fuel gas combustion and small amounts of steam. The synthesis gas is afterwards converted to Fischer-Tropsch crude, waxes, waste water and fuel gas in a FT-reactor at 225°C and approx. 25 bar (FT-R). The fuel gas produced is used as heating agent of the RWGS in a burner (FT-B). The waste water generated in the FT synthesis is sent to the waste water treatment plant. Crude and waxes are afterwards upgraded. Crude is sent directly to product splitting via distillation. Waxes are first hydrocracked with H_2 demand of 0.006 t_{H_2}/t_{Waxes}. Afterwards the produced intermediate is also sent to the distillation column. Here liquid fuels are again separated and a small share of additional fuel gas is generated which is sent to the FT-B. The yield factors of the main Fischer-Tropsch reaction as well as FT-upgrading and MTJ process are given in Table 6.1.

The capital costs for the MTJ are between 300-700 €/t_{Jet} (if scaled down to small scale) [18]. Capital costs for small scale FT synthesis are reported to be between 270 and 800 €/$_{Jet}$. Additionally, Liebner states that MTJ can deliver a 15 % cost reduction in comparison to FT synthesis in small scale. Considering König's rather conservative data for Fischer-Tropsch synthesis of approx. 780 €/t_{Jet}, costs for MTJ are assumed to be roughly 85 % of this value, leading to base case capital costs of 660 €/t_{Jet}. Considering 20 years plant lifetime and 5 % interest to calculate the capital recovery factor and assuming 10 % of yearly operational costs based on the fixed capital investment, total processing costs of ca. 1500 €/t_{Jet} are taken as base value (ref. Eq. (6.1)).

$$C_{MTJ} = 660 \frac{€}{t} + \left(\frac{660 \text{ €/t}}{CRF} \cdot 10\,\% \right) = 1485 \approx 1500 \text{ €/t}_{Jet} \tag{6.1}$$

TABLE 6.1: YIELD FACTORS FOR FISCHER-TROPSCH REACTION + UPGRADING AS WELL AS METHANOL-TO-JET PROCESS [18], [108].

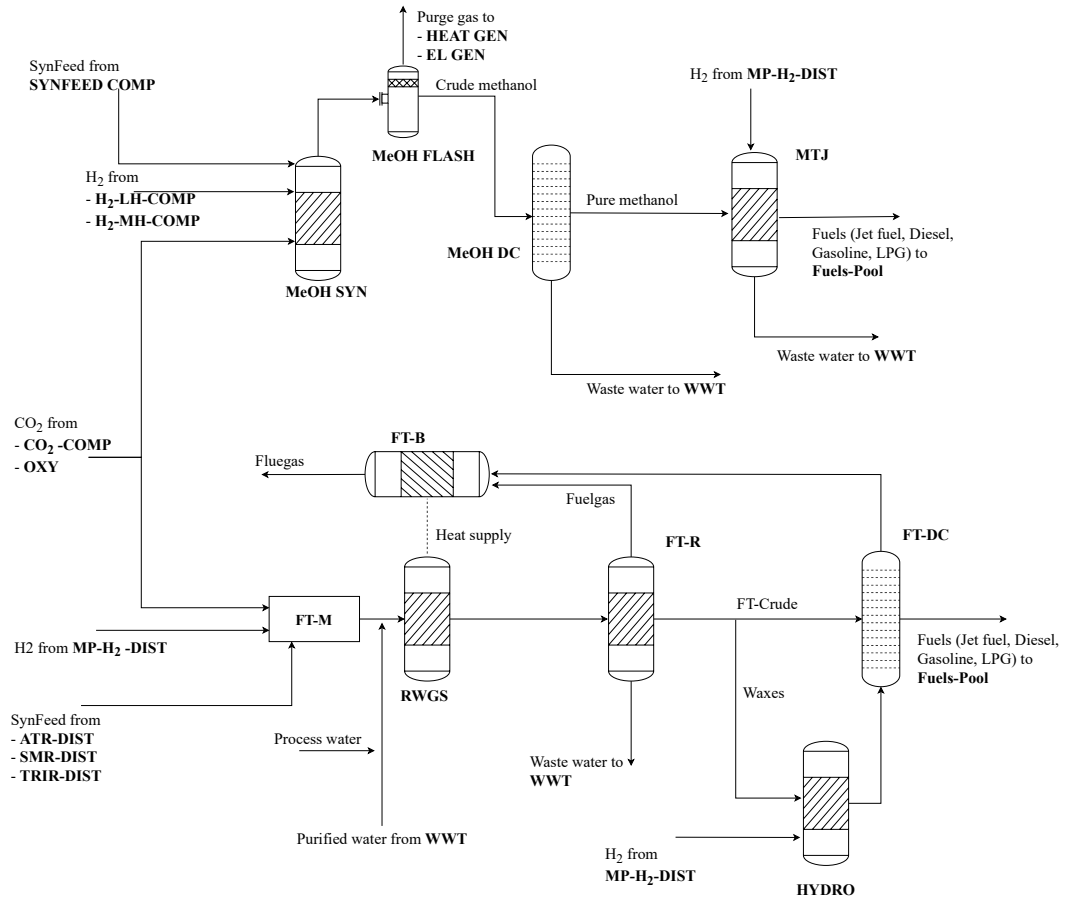| Component	Jet fuel	Diesel	Gasoline	LPG	Fuel gas	CO_2	H_2O	Crude	Waxes
Yield Factor MTJ	0.2	0.163	0.046	0.039	-	-	0.552	-	-
Yield Factor FT-Syn	-	-	-	-	0.668		0.111	0.16	0.062
Yield Factor FT-U	0.71	0.03	0.24	-	0.02	-	-	-	-

FIGURE 6.4: THERMOCHEMICAL SYNTHESIS AND UPGRADING PROCESS SECTION OF RENEWABLE REFINERY SUPERSTRUCTURE.

6.2.2 Biomass-to-X process

The BtX process pathway is two-fold in this superstructure. The first path utilizes biogas with a composition of 65 vol. -% CH_4 and 35 vol. -% CO_2 for the production of SynFeed in thermochemical synthesis, similar to the case study described in chapter 5.2.2. The second pathway depicts an algae-based biorefinery to produce hydroprocessed esters and fatty acids (HEFA). While biogas input is again limited to 3.5 t/h (ca. 3,000 Nm^3/h), the capacity of the biorefinery is unlimited.

Algae raw material

The biorefinery-pathway uses microalgae biomass to produce liquid fuels from the algae-oil as well as biogas, recycle water and solid fertilizer from the remaining carbohydrates, protein and water shares. Industrial algae cultivation is a process that is still under development and subject to a broad scientific discussion. Different cultivation reactor concepts from open ponds, over photo-bioreactors and thin-layered cascade reactors exist. Additionally, different strains of algae differ greatly in terms of productivity, lipid content or even applied culture broth. Literature reports productivity values from 5 to a maximum of 60 $g/m^2/d$, while lipid content can rise up to 50 or even 70 wt.-% [109], [110]. On top of that, micro

algae can be clustered into freshwater and saline strains, where the first one can also be used to treat municipal waste water, while the other is not dependent on fresh water reserves [111], [112]. Typical primal harvesting and dewatering technologies are settling tanks, filter presses and centrifugation [113], [114]. Due to this broad spectrum of raw material and processing alternatives, literature reports algae production costs between 145 and 1315 €$_{2020}$/t$_{Dry-mass}$ [109].

Due to the wide variety of technology options as well as scarcely available detailed techno-economic models in literature wet algae biomass is modeled as raw material which is produced on-site. The biomass has a dry matter concentration of 10 wt.-%, which is often described in literature. Algae costs of 265 €$_{2020}$/t$_{Dry-mass}$ based on results from Davis et al. serve as base case costs [109]. These costs can be affiliated with a large-scale production with cultivation productivity of 25 g/m^2/d [109]. Assuming 10 wt.-% dry biomass this leads to 26.5 €/t$_{Algae-sludge}$ which is rounded to 25 €/t$_{Algae-sludge}$. Table 6.2 gives an overview of the key parameters of the algae raw material.

TABLE 6.2: KEY ASSUMPTIONS OF ALGAE BIOMASS RAW MATERIAL [109], [112].

Base costs	CO_2 factor	Fresh water demand	Lipid content	Dry biomass content
25 €/t$_{Algae-sludge}$	-1.8 kg/kg	45.9	25 wt.-%	10 wt.-%

Biomass pretreatment and lipid extraction

Typical micro algae for fuels production exhibit lipid contents of 25 wt.-%. However, only a certain share of those oils is directly available. Some extent is mixed with other components and stored in cell walls, which reduces the amount of extractable oil. To break intercellular walls and increase the available oil content, a pretreatment step can be included. In this superstructure a sonication process (SONIC) is implemented (cf. Figure 6.5). It is assumed that 50 % of the lipids are available without pretreatment. Using sonication, the available share can be increased to 96 % [24].

To separately use the lipids and algae residue, an extraction step is necessary. Oil extraction is commonly performed by chemical extraction using non-polar solvents. Two process alternatives are implemented: The commonly known hexane extraction (HEX-EXT) and the more advanced supercritical CO_2 extraction (SUP-CO_2-EXT) (cf. Figure 6.5). While the hexane extraction only extracts 35 % of the available oils, supercritical CO_2 extraction has an efficiency of 100 % [24]. However, the energy consumption of this alternative is also substantially higher.
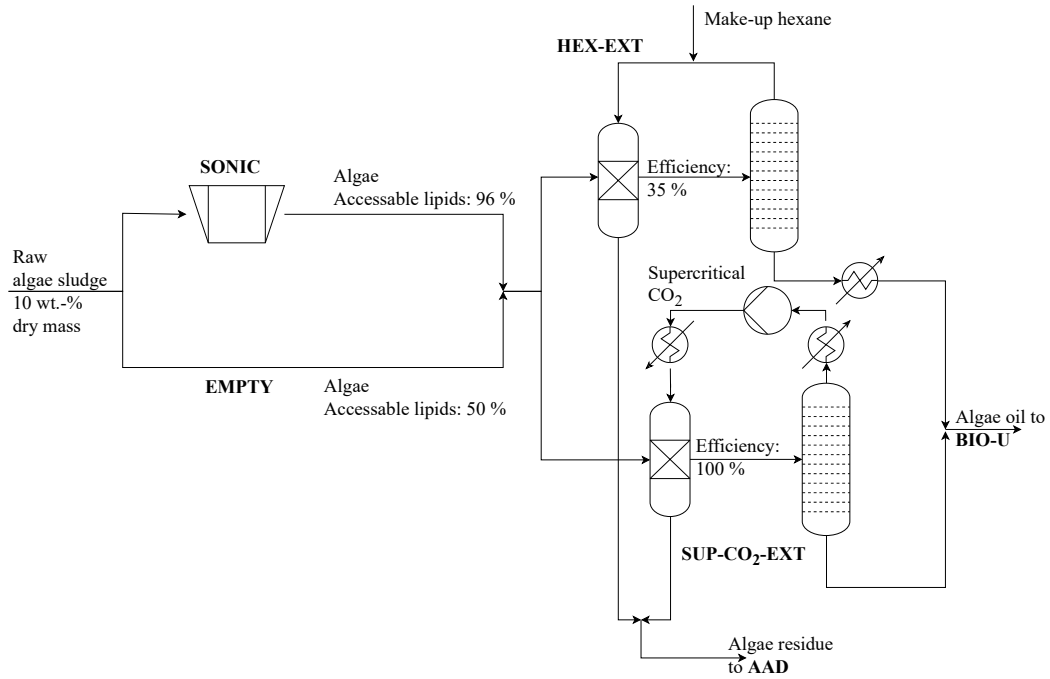
FIGURE 6.5: ALGAE PRETREATMENT AND LIPID EXTRACTION PROCESS SECTION OF RENEWABLE REFINERY SUPERSTRUCTURE.

Lipid upgrading

The extracted bio-oil is upgraded based on the UOP refining process (BIO-U). This process includes hydrotreating, hydrocracking and isomerization as well as product distillation. The data of the techno-economic model is extracted from Klein-Marcuschamer et al. [115]. His process design considers a three-stage hydrodeoxygenation reactor at 350°C to produce saturated alkanes and propane. Afterwards, the alkanes are further treated by hydrocracking and hydro-isomerization. Unreacted hydrogen is recovered and cleaning using amine scrubbing, before internal recycling. The product distribution of the process is depicted in Table 6.3. The total hydrogen demand is 0.158 $t_{H_2}/t_{Bio-oil}$. During amine scrubbing high purity CO_2 is produced. Because capital cost data was only based on rough estimates, the complete process design is modeled as one surrogate unit-operation in the superstructure model. This unit-operation includes the complete data such as yield factors, energy demand and capital costs.

TABLE 6.3: YIELD FACTORS FOR THE UPGRADING OF BIO-OIL [115].

Component	Jet fuel	Gasoline	Diesel	Fuel gas	H_2O	CO_2	LPG
Yield Factor	0.41	0.22	0.06	0.08	0.04	0.06	0.13

Algae residue treatment

After lipid extraction remaining algae biomass and water can be further exploited (cf. Figure 6.6). The wet residue is converted into biogas by anaerobic digestion (AAD). Afterwards gaseous stream and liquid stream are separated. The liquid

stream contains water with diluted salts and remaining solid compounds. The solid compounds are separated from the liquid using centrifugation (CENTR) and can be sold as fertilizer [24]. The water can be purified and used as raw material for electrolysis or directly used as cultivation medium in algae cultivation. The second option suggests a co-location of algae biomass production and renewable refinery as it is assumed in this work. The gaseous product of anaerobic digestion is raw biogas with a composition of 65 vol. -% CH_4 and 35 vol. -% CO_2 [24]. This biogas can be further utilized. Therefore, a biogas distributor (BG-DIST) can be used to distribute among the biogas utilization or the purge gas treatment section.
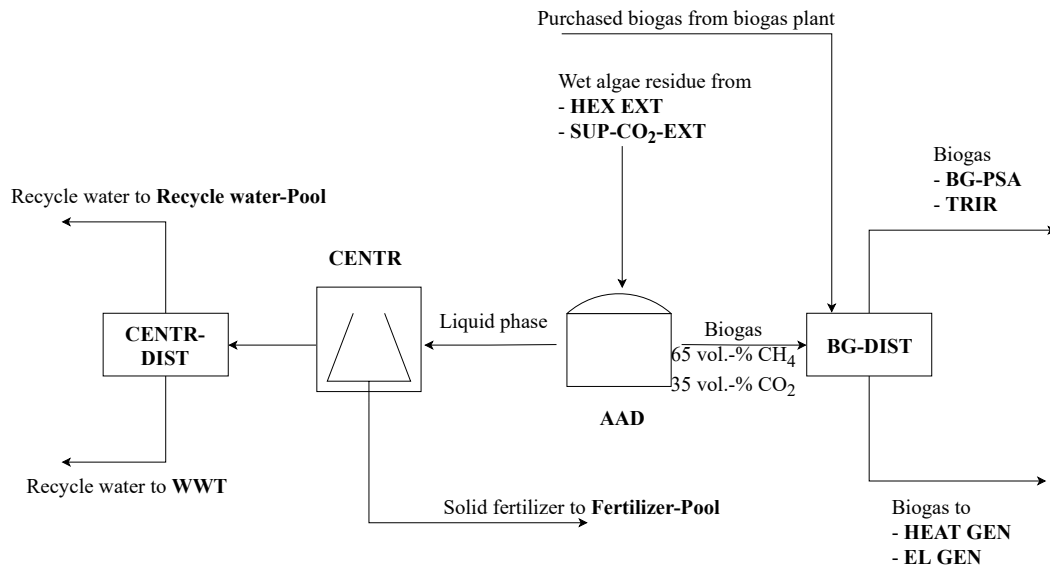

FIGURE 6.6: ALGAE RESIDUE TREATMENT PROCESS SECTION OF RENEWABLE REFINERY SUPERSTRUCTURE.

Biogas utilization and SynFeed upgrading

Biogas from anaerobic digestion of algae residue can be utilized in similar ways as the raw material biogas from the biogas plant. The technology options and used models are mostly similar to the ones presented in chapter 5.2.2 and 5.2.3 (cf. Figure 6.7). The simplest way to use biogas is to produce steam or electricity by combustion with other purge gases (HEAT GEN/ EL GEN). Additionally, biogas reforming to SynFeed (TRIR) as well as biogas-purification to bio-methane by pressure swing adsorption and vacuum pump (BG-PSA and VP) are implemented. The pure CO_2 stream can be mixed with low-pressure CO_2 from carbon capture to provide raw material for thermochemical synthesis, or just vented to environment. The pure bio-methane is either converted to SynFeed by steam methane (SMR) or autothermal reforming (ATR), combusted to produce steam or electricity (STEAM / EL GEN) or liquified to –152°C by a reversed Rankine process (BM-LIQ). The resulting liquefied biomethane depicts a liquid fuel. However, it is only considered as a by-product in this work due to the major difference in handling and transportation compared to the other fuels. Additionally, the liquifying process

does not produce aviation fuel (shares), which is the main goal of the process layout. Data for biogas and biomethane reforming processes are taken from the detailed Aspen Plus study, similar to chapter 5.2.2. Data for pressure swing adsorption and vacuum pump is extracted from Hasan et al. and data for the liquefication of biomethane is taken from Capra et al. [116], [117].

Equivalent to chapter 5.2.2, the raw SynFeed has to be upgraded to meet the H_2/CO_2 ratio of the different thermochemical synthesis process options. Therefore, H_2-PSA, ATR-SEL and TRIR-SEL are implement for SMR, ATR and TRIR processes, respectively. These options depict H_2- and CO_2 separation processes with H_2- and CO_2 recovery factors of 89 % and 90 % as described in chapter 5.2.2. Independent on the decision on reforming technology and upgrading, the different SynFeed streams are distributed by a set of distributors to Fischer-Tropsch synthesis or compression for methanol synthesis. The given case study is much more complex than the one described in chapter 5. In order to save computational effort and reduce calculation time the compression of SynFeed for methanol synthesis is modeled by one overall SYNFEED COMP which was predesigned for a H_2/CO_2 ratio of 3. Depending on the conversion technology, this ratio can be under- or overestimated leading to slightly under- and overestimation of capital costs and electricity demand. Nonetheless, the deviations are sufficiently small considering the total impact of the SynFeed compressor in the overall process design, and the gained computational efficiency.
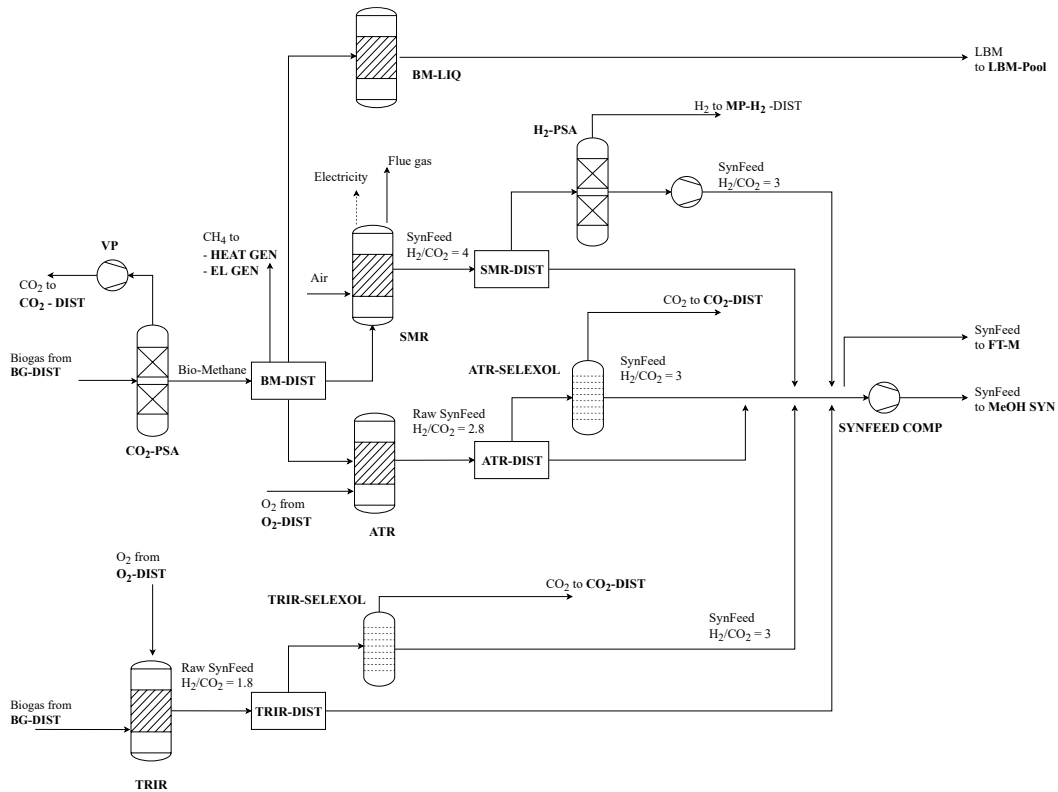

FIGURE 6.7: BIOGAS UTILIZATION AND SYNFEED UPGRADING PROCESS SECTION OF RENEWABLE REFINERY SUPERSTRUCTURE.

6.2.3 Purge gas and waste water treatment

Depending on the final process layout, different combustible gases arise which have to be burned in order to keep emissions of unreacted hydrocarbons to a minimum as well as to increase the overall energy efficiency of the process. These gases are the purge stream from methanol synthesis, raw biogas from either algae remnant treatment or raw material (biogas plant) as well as H_2-by-products. Gases can either be burned to produce steam for internal heat supply (HEAT GEN) or electricity by application of a combined cycle power plant (EL GEN) (cf. Figure 6.8) [24].

Arising waste water from distillation columns, compression intercooling or from wet algae biomass can be recycled and used again in processes like electrolyzers or as steam input for biogas reforming processes. Another option is to release remaining water into the environment as effluent. Anyway, in both cases waste water has to be purified first in order to reduce impurities and potential remaining hydrocarbons. Waste water treatment is not modeled in detail but considered with specific costs of 2.5 €/t [94].
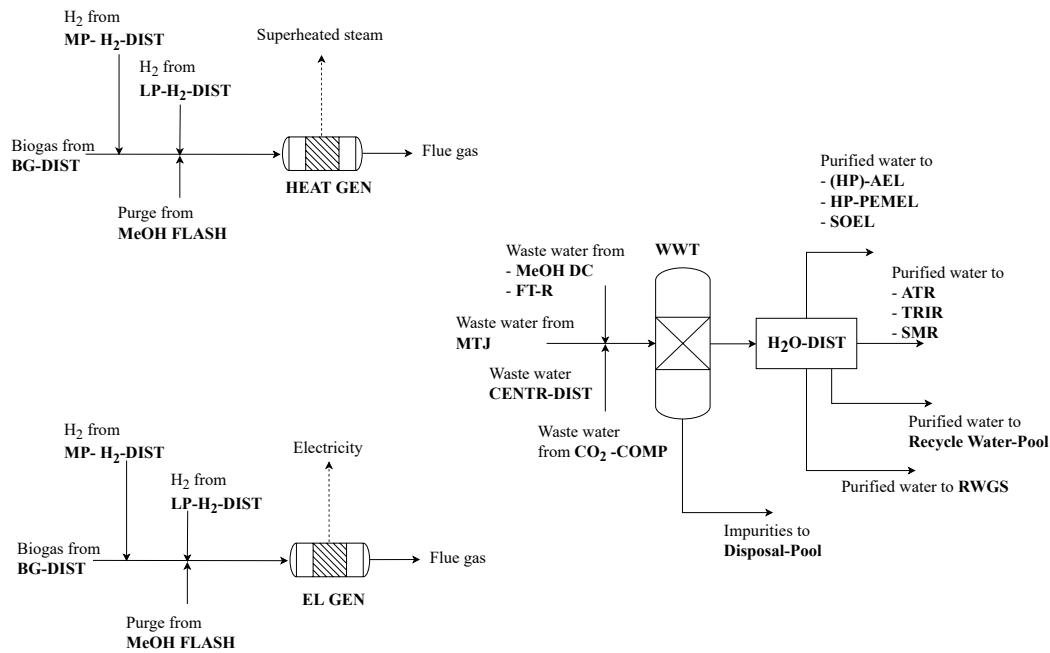

FIGURE 6.8: WASTE WATER AND PURGE GAS TREATMENT PROCESS SECTION OF RENEWABLE REFINERY SUPERSTRUCTURE.

6.2.4 Raw materials, product pools and distributors

Raw materials include biogas from the biogas plant with an input limit of 3.5 t/h, as well as different flue gases, pure O_2, wet algae sludge, process water, air, monoethanolamine and hexane. Similar to the case study described in chapter 5, none of the raw materials are limited except for biogas, and O_2 is assumed to be produced using cryogenic air separation.

The main product of the process system are the fuel products. Main products are jet fuel, gasoline, diesel and LPG. The process alternatives derive the exact distribution of fuels. However, in the end they are summarized under one final product "fuels" with their respective lower heating value. Due to this approach costs as well as emissions can be easily allocated to the different main products depending on their energy content. Next to the main fuel pool, by-products include medium-pressure hydrogen, oxygen, solid fertilizer, liquified bio-methane and recycle water for algae cultivation.

A set of 10 distributor units are implemented in the superstructure, which distribute streams according to Table 6.4.

TABLE 6.4: DISTRIBUTOR NAMES AND PROCESS CONFIGURATION OF RENEWABLE REFINERY SUPERSTRUCTURE.

Distributor name	Inlets	Targets
O_2-DIST	O_2 from AEL/HP-PEM/SOEL/HP-AEL	O_2-Productpool, OXY, ATR, TRIR
MP-H_2-DIST	H_2 from H_2-PSA	HEAT /EL GEN, H_2-Productpool, H_2-MH-COMP, FTS, BIO-U, MTJ
BM-DIST	BM-PSA	SMR/ATR, HEAT GEN, EL GEN
H_2O-DIST	WWT	AEL/HP-PEM/SOEL/HP-AEL, ATR, TRIR, SMR, Recycle water pool
SMR-DIST	SMR	H_2-PSA, SYNFEED COMP
ATR-DIST	ATR	ATR-SEL, SYNFEED COMP
TRIR-DIST	TRIR	TRIR-SEL, SYNFEED COMP
BG-DIST	Biogas from AAD	BG-PSA, TRIR, HEAT/ EL GEN
LP-H2-DIST	H_2 from AEL, SOEL	H_2-LM-COMP, H_2-LH-COMP, HEAT/ EL GEN
CENTR-DIST	Waste water from CENTR	Recycle water Productpool, Waste water treatment

6.2.5 General assumptions and key parameters

The general data basis is the same as in presented in chapter 5. Key parameters can be found in Table 5.6 and Table 5.7. The yearly amount of produced main product is set to 240,000 MWh/a. This translates to ca. 20,000 t/a of liquid fuels with different shares of jet fuel, diesel, gasoline and LPG depending on the actual chosen technology pathway. Table 6.5 presents additional key parameters of the investigated fuels.

TABLE 6.5: KEY PARAMETERS OF DIFFERENT FUELS PRODUCED IN THE RENEWABLE REFINERY [6], [96], [118], [119].

Parameter	Jet fuel	Gasoline	Diesel	LPG
Lower heating value (MJ/kg)	42.8	42.3	42.7	43.1
Reference GHG emissions ($t_{CO_2-eq.}$/t)	0.44	0.6	0.53	0.58
Reference H_2O demand (t_{H_2O}/t)	1.35	1.56	1.54	1.84
Costs of reference (€/t)	630	637	566	555

Model data for two processes are especially uncertain. For once these are the costs of the raw algae sludge, which can vary greatly depending on location, reactor concept, used strain etc.. Secondly, the MTJ process is still in development and not commercially available at the moment. The uncertainty of the model data was also noticed during data collection. Here OUTDOOR's optimal design screening algorithm comes into play. Based on the defined base scenario values, raw algae costs as well as total MTJ processing costs are varied with the screening algorithm to gain a broader overview on operating windows of the competing processes. The screening algorithm screens cost optimal process designs for 11 x 11 = 121 data points as given in Table 6.6 in order to find optimal topologies.

TABLE 6.6: PARAMETER RANGE OF OPTIMAL DESIGN SCREENING ALGORITHM.

Parameter	Algae sludge costs (€/t)	MTJ processing costs (€/t_{Jet})
Min	5	680
Max	105	2800
Number of data points	11	11

Additionally, 4 different scenarios are considered with the screening algorithm as shown in Table 6.7.

TABLE 6.7: SCENARIO DEFINITION FOR RENEWABLE REFINERY SUPERSTRUCTURE CASE STUDY.

Parameter	Scenario 1	Scenario 2	Scenario 3	Scenario 4
Electricity price (€/MWh)	72	72	36	36
Lipid content of algae biomass (wt. -%)	25	50	25	72

6.3 RESULTS

The given process design study is investigated for minimal net production costs in two steps. First the base scenario is evaluated in detail, afterwards the screening algorithm, presented in chapter 4.3, is utilized to investigate different operating windows of the competing conversion technologies.

6.3.1 Computational results

The superstructure model consists of 685,497 constraints and 244,823 variables of which 1600 are binary. The base case optimization was performed on a server using four 2.2 GHz cores with a total RAM of 300 GB available. Utilizing Gurobi 9.1.2 as optimization solver the base case takes a total 2033 seconds resulting in an optimal solution with 0.01% remaining optimality gap, which is Gurobis default threshold. Of those 2033 seconds 11 % are required by OUTDOOR's automated superstructure construction and model building, 35 % are invested in transferring the python model to the Gurobi solver and 53 % are actually required by the solver. It is notable that, roughly 16 % of the solver time is required in order to reduce the optimality gap from 1 % to 0.01 %.

The screening algorithm requires numerous sequential optimizations. Therefore, the different scenarios were calculated in parallel on an external server, where each scenario was assigned a maximum number of four 2.2 GHz cores, with a total RAM of 300 GB. During the screening, the single-run solver times vary, depending on the parameter set, and can consume considerably more time (up to >19,000 seconds) than the base case optimization. In order to reduce calculation time a remaining optimality gap of 0.1 % was allowed for the screening algorithm, leading to total computing times of 42,044 to 87,514 seconds, depending on the scenario.

6.3.2 Base case results

For the given base case: Electricity costs 72 €/MWh, algae lipid content 25 wt.-%, algae sludge costs 25 €/t and MTJ costs 1500 €/t_{Jet} an optimal process design depicts a highly integrated Biomass-to-X and Power-to-X process. The detailed flowsheet is depicted in Figure 6.9. In total 240,000 MWh/a (approx. 20 kt fuels/a) are produced at net production costs of 253 €/MWh_{LHV} (approx. 2993 €/t_{Fuel}). The fuels shares are 47 % jet fuel, 23 % diesel, 18 % gasoline and 12 % LPG. Fuels are produced to 52 % based on methanol-to-jet using algae residue and additional biogas and 48 % using hydrotreating of algae bio-oil. Additional CO_2 is not used and H_2 from electrolysis is only used in hydrotreating and not as main feed. Algae sludge is used as raw material and pretreated by sonication. Subsequent lipids extraction is designed as supercritical CO_2 extraction. Lipids are afterwards refined to HEFA using hydrodeoxygenation. Algae residue is converted to biogas by anaerobic digestion. Liquid remnant is treated by centrifugation which separates solid fertilizer as by-product and remaining water for usage in the co-located algae farm. The remaining biogas is mixed with additionally bought biogas from a biogas plant and converted to raw SynFeed by TRIR. Part of the raw SynFeed is upgraded with selexol-based CO_2 capture. The captured CO_2 is not required anymore and vented. The low-detail model of algae cultivation did not

include the acquisition of CO_2. However, in the proposed flowsheet, vented CO_2 from the TRIR-SEL, BIO-U and HEAT GEN process could provide approx. 30 % of the cultivation CO_2 demand. The purified SynFeed is mixed with the remaining SynFeed to meet the specification of methanol synthesis. The produced SynFeed is compressed to 70 bar and converted to methanol, and methanol is upgraded to fuels by MTJ. A high-pressure alkaline electrolysis unit produces small amounts of H_2 which are utilized in hydrodesoxygenation of bio-oil (BIO-U) and hydrotreating in MTJ. The O_2 by-product of the HP-AEL is used in TRIR to produce the required heat via partial oxidation. Purge gas from the methanol synthesis is combusted to produce superheated steam, which is used to decrease the external steam demand. Waste water from methanol distillation, MTJ and BIO-U is treated in WWT first, and afterwards used as raw material in TRIR and HP-AEL.

Heat integration reduces the external heat demand from ca. 6.49 MW to 0.02 MW. Ca 18 % of the recovered heat is produced in purge gas treatment and further 82 % are gained from waste heat of methanol synthesis and flash as well as hydrodeoxygenation of bio-oils and intercooling of the TRIR process. The model does not include detailed HEX-matching. However, based on the given temperature levels a first indication of matches can be provided. In such a matching high temperature heat from HEAT GEN, MeOH SYN, TRIR and BIO-U would be used for medium temperature demand in BIO-U. Heat from cooling in MeOH FLASH and TRIR would be coupled with the distillation column of the SUP-CO2-EXT. Finally waste heat from BIO-U or TRIR would be used in the AAD. Additionally, 18.11 MW of cooling utility are required. The total electricity demand is ca. 30 MW of which 20 MW are required by the HP-AEL.
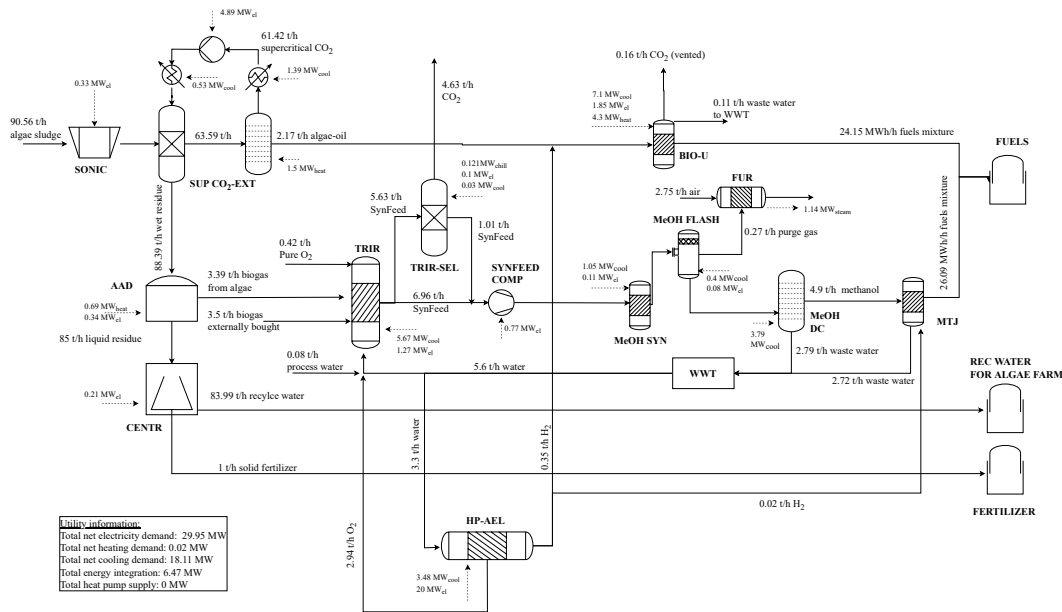

FIGURE 6.9: PROCESS FLOW DIAGRAM OF NPC-OPTIMIZED RENEWABLE REFINERY BASE CASE.

Table 6.8 presents the cost breakdown of the NPC. It can be seen, that the major cost drivers are capital costs with 43.3 % and raw materials with 27.5 %; third and fourth largest share are electricity costs (17 %) and operating & maintenance (16.6 %).

TABLE 6.8: NET PRODUCTION COST DISTRIBUTION OF FUEL MIXTURES IN BASE CASE OPTIMIZATION.

Position	Share (%)	€/MWh	€/t$_{Fuel}$
Capital costs	43.3	110	1299
Raw materials	27.5	70	823
Electricity	17	43	509
Operating & Maintenance	16.6	42	497
Heat integration /Refrigeration	0.3	1	9
Profits	–4.7	12	141

Figure 6.10 shows the breakdown of capital costs (left) and electricity demand (right). Largest capital cost shares are generated by MTJ (24.3 %), TRIR (15.6 %), anaerobic digestion (16.6 %) and BIO-U (17.8 %).

Electricity is mainly consumed by the high-pressure alkaline electrolysis and the H$_2$ compressor (66.8 %) as well as the supercritical CO$_2$ extraction (16.3 %). Raw materials costs mainly arrive from raw algae sludge purchase (64.7 %) and raw biogas (35 %).
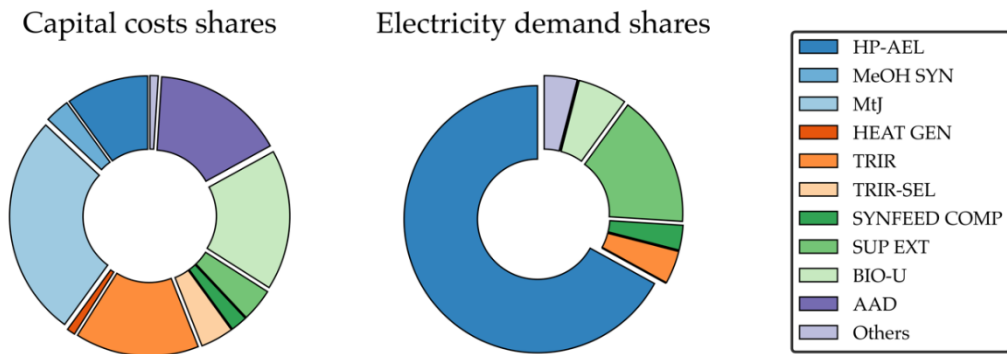

FIGURE 6.10: CAPITAL COST AND ELECTRICITY DEMAND BREAKDOWN OF RENEWABLE REFINERY BASE CASE OPTIMIZATION.

When comparing the combined refinery with a purely electricity-based MTJ or FTJ refinery a cost reduction ca. 21 % and 28 % can be achieved, respectively. If compared to a stand-alone biorefinery, where algae residue is converted to a liquid bio-methane by-product a cost reduction of 11.5 % is achieved. A comparison to literature is not as simple due to the numerous assumptions. Wassermann et al. reported lower MTJ-based jet fuel costs of ca. 2225 €/t$_{Jet}$ [120]. However, they also used reduced electricity costs of 50 €/MWh and lower MTJ process costs of about 400 €/t$_{Jet}$ based on large scale applications [120]. If both factors are included in the

comparison the total costs of fuel are again in the same region. König calculated FT-based jet fuel prices of 3380 €/t$_{Fuel}$ [108]. He however had increased electricity costs of 104 €/MWh but a substantially larger plant with 526 kt$_{Jet}$/a output and high full load hours of 8760 h/a, leading to reduced capital cost shares [108]. In general, all of the results are in the same region depending on the chosen assumptions.

In terms of environmental impacts, the optimal base case comes with negative greenhouse gas emissions of –3.7 t$_{CO_2}$/t$_{Fuels}$, while requiring 960 t$_{H_2O}$/t$_{Fuels}$ of water. When compared to the stand-alone options, greenhouse gas emissions are in the same region for all options. Water demand on the other hand is another matter. Algae cultivation requires substantially more water than water electrolysis and carbon capture. Due to avoided burdens for by-products, electricity-based processes even generate negative water demands of ca. –7.5 t$_{H_2O}$/t$_{Fuels}$. Table 6.9 presents costs and GHG emissions of conventional production of the given yearly product loads considering the actual product distribution and reference GHG emissions and costs from Table 6.5. Based on these values and the calculated costs and emissions of the renewable refinery, CO₂ abatement costs of ca. 561 €/t$_{CO_2}$ arise (ref. Table 6.10).

TABLE 6.9: CALCULATED YEARLY PRODUCTION, GREENHOUSE GAS EMISSIONS AND COSTS OF CONVENTIONAL FUELS PRODUCTION.

–	Jet fuel	Diesel	Gasoline	LPG	Total
Yearly production (t/a)	9,564	4,566	3,705	2,457	20,292
GHG of conventional production (t/a)	4,227	2,402	2,216	1,432	10,277
Costs of conventional production (€/a)	6,025,039	2,584,356	2,360,085	1,363,635	12,333,396

TABLE 6.10: CALCULATED CO₂ ABATEMENT COSTS OF RENEWABLE REFINERY BASE CASE.

Costs of conventional production (€/a)	Costs of renewable refinery (€/a)	GHG emission of conventional production (t$_{CO_2}$/a)	GHG of renewable refinery (t$_{CO_2}$/a)	CO₂ abatement costs (€/t$_{CO_2}$)
12,333,396	60,696,977	10,277	–75,979	561

6.3.3 Optimal design screening algorithm results

Figure 6.11 and Figure 6.12 present the results of the optimal design screening algorithm for the electricity price of 72 €/MWh. Figure 6.11 depicts an algae lipid content of 25 wt. -% and Figure 6.12 depicts a lipid content of 50 wt. -%.

It can be seen that, for 72 €/MWh$_{el}$ and 25 % lipids, fuel costs vary between ca. 177 and 331 €/MWh$_{LHV}$ (2092–3912 €/t) for algae costs between 5 and 105 €/t$_{Algea-sludge}$ and MTJ costs between 680 and 2800 €/t$_{Jet}$. Four distinct operating windows appear for different algae costs and total MTJ processing costs. For low algae and MTJ costs, a combination such as presented in the base case is most profitable. For MTJ

costs higher then 1500 €/t$_{Jet}$, this step is replaced by Fischer-Tropsch synthesis. If algae costs exceed approximately 40 €/t$_{Algae-sludge}$, a purely electricity-based production is chosen based on methanol synthesis for MTJ costs up to ca. 2400 €/t$_{Jet}$. For even higher costs a FTS-based production is most economic.
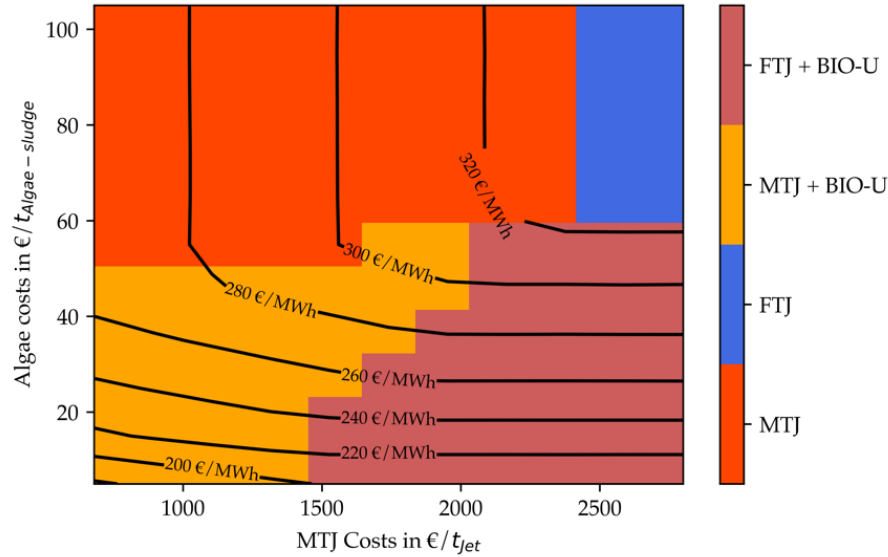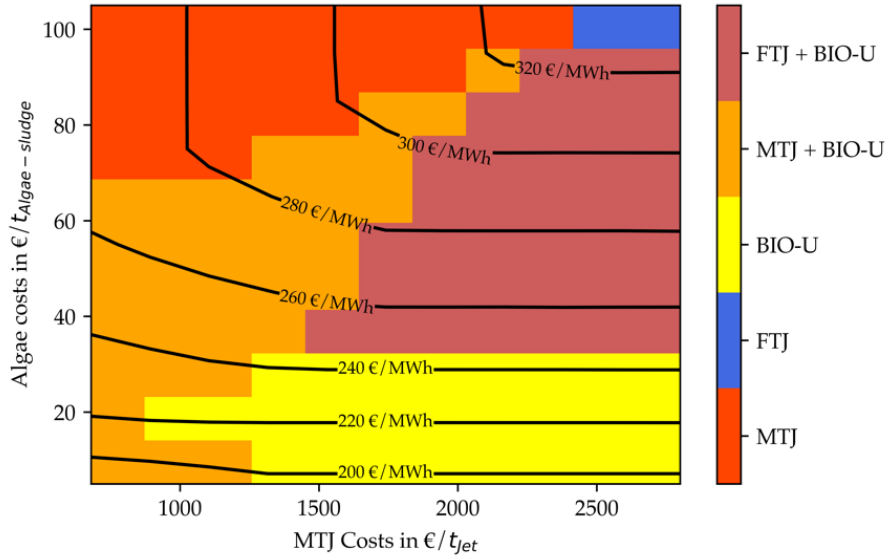

FIGURE 6.11: NET PRODUCTION COSTS (CONTOUR LINES) AND TECHNOLOGY CHOICE (HEATMAP) OF OPTIMIZED RENEWABLE REFINERY DEPENDING ON ALGAE COSTS AND MTJ COSTS IN SCENARIO 1.

If the lipid content in the raw algae is elevated (Figure 6.12) the total fuel costs range changes to 2150 – 3912 €/t. The maximum cost value is still associated with a purely electricity-based production; hence it is independent of the lipid content. The minimal price is slightly elevated compared to a lower lipid content. Nonetheless the costs for combined process concepts are in average about 10 % cheaper compared to the case with 25 % lipids. This can be explained by the bio-based nature of the combined process: While alkaline electrolysis plays a role in the overall process scheme, the main feedstock for the products is based on algae. If the content of lipids which can be converted directly to fuels rises, this leads to smaller capacities in anaerobic digestion, biogas reforming and MTJ. These processes are the most expensive ones in the total process design, which makes capacity reduction a good cost saver.

Additionally, to the four operating windows recorded previously, now a purely bio-based production is most economic for low algae costs of up to 35 €/t$_{Algae-sludge}$ and MTJ costs of 1000 – 1250 €/t$_{Jet}$. Furthermore, the operating window for an integrated design is increased for higher algae costs up to 70 – 95 €/t$_{Algae-sludge}$ depending on the MTJ costs.
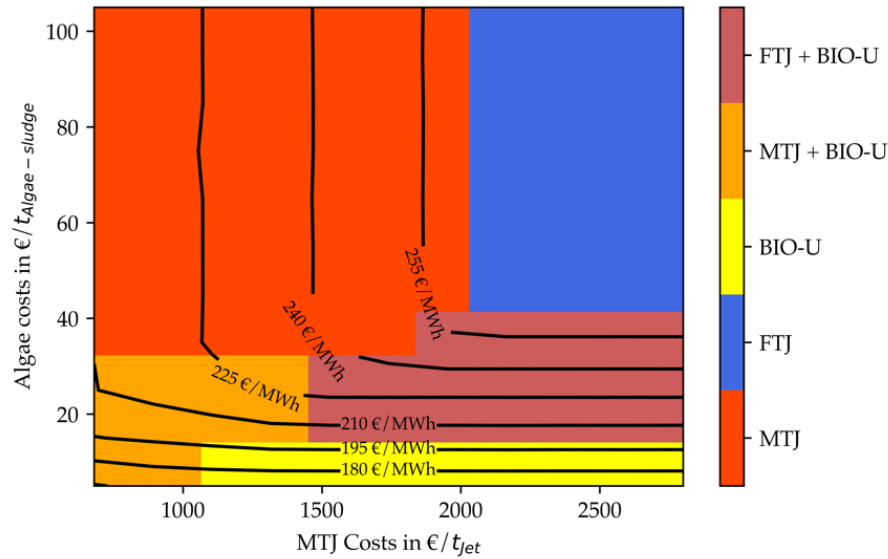
FIGURE 6.12: NET PRODUCTION COSTS (CONTOUR LINES) AND TECHNOLOGY CHOICE
(HEATMAP) OF OPTIMIZED RENEWABLE REFINERY DEPENDING ON ALGAE COSTS AND MTJ COSTS
IN SCENARIO 2.

Figure 6.13 and Figure 6.14 display the screening results for an electricity price of
36 €/MWh. Figure 6.13 again depicts an algae lipid content of 25 % while Figure
6.14 depicts a lipid content of 50 %. Evident from Figure 6.13 is, that the total costs
range for decreased electricity price also decreases to ca 165– 263 €/MWh (1950 –
3109 €/t$_{Fuel}$). This is equivalent of 10 % to 20 % cost reduction compared to the
higher electricity price. Especially for purely electricity-based production, the
share of electricity costs is high, explaining the increased cost reduction at the high-
end of the price range. In general, it can be seen, that the operating windows for
stand-alone MTJ and FTJ production processes are increased compared to the cases
with higher electricity price. Nonetheless, for low algae costs up to 30 – 40 €/t$_{Algae-sludge}$ a combination with methanol or Fischer-Tropsch synthesis is still beneficial.
As shown in Figure 6.13, an operating window for a stand-alone biorefinery also
emerges for very low algae costs of 5 €/t$_{Algae-sludge}$ and MTJ costs above 1000 €/t$_{Jet}$.

FIGURE 6.13: NET PRODUCTION COSTS (CONTOUR LINES) AND TECHNOLOGY CHOICE (HEATMAP) OF OPTIMIZED RENEWABLE REFINERY DEPENDING ON ALGAE COSTS AND MTJ COSTS IN SCENARIO 3.

Figure 6.14 shows the results for a lipid content of 50 % for a decreased electricity price. It follows the logic of the other graphs. Bothe stand-alone electricity-based and bio-based production operating windows are increased. For low algae costs, pure algae-based production is most economic. Due to high lipid content this is the case for algae costs up to 40 €/t. The optimal region for integrated process design is very small. Due to the low electricity price, stand-alone MTJ or FTJ is quickly more economic than a combined process. The total cost range is between 156 and 262 €/MWh (1844 – 3109 €/t). The maximum cost value is again similar to scenario 3, due to the independency of the FTJ process from the algae lipid content. The minimum value is slightly lower, due to more economic usage of algae-oil and lower CAPEX for algae residue treatment, similar to scenario 1 and 2.
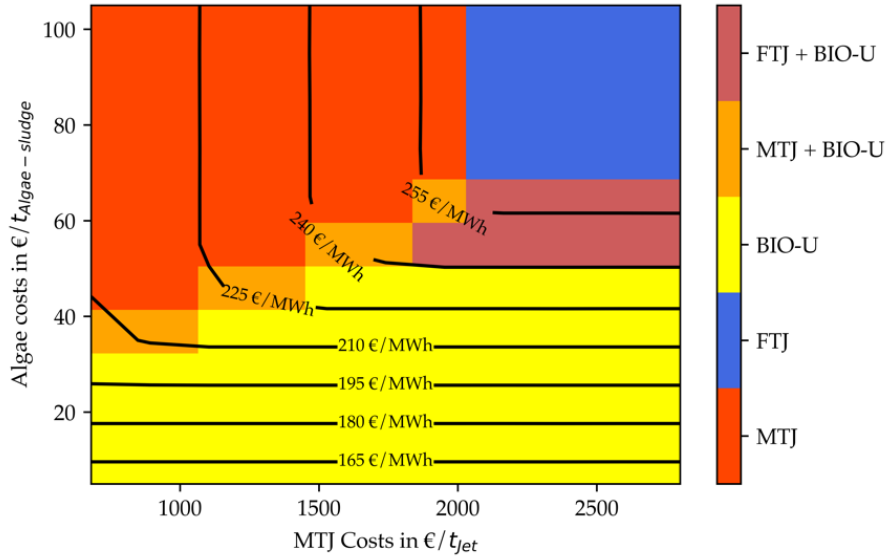
FIGURE 6.14: NET PRODUCTION COSTS (CONTOUR LINES) AND TECHNOLOGY CHOICE (HEATMAP) OF OPTIMIZED RENEWABLE REFINERY DEPENDING ON ALGAE COSTS AND MTJ COSTS IN SCENARIO 4.

All four figures indicate, that for stand-alone PtX processes MTJ is more economic up to MTJ costs of 2000 – 2300 €/t$_{Jet}$. Although the Fischer-Tropsch synthesis produces fuels at 1160 €/t$_{jet}$ at this capacity it possesses a smaller efficiency. The reduced efficiency originates from the large usage of internally produced fuel gas for the reverse water-gas-shift reactor. Hence, only 22 % of the FT inlet is converted into usable fuels compared to ca. 28 % in MTJ. Due to this efficiency disadvantage and an increased H$_2$ demand for synthesis and upgrading compared to MTJ the electrolyzer capacity is about 16 % higher for FTJ. This difference can explain the allowed increased costs of MTJ. A reversed effect, that strengthens this hypothesis can be observed if Figure 6.11 is compared to Figure 6.13. With reduced electricity costs, also its general share of the total costs is decreasing. This effect leads to a smaller allowed operating window of MTJ compared to FTJ.

6.4 DISCUSSION

The presented case study provides an overview on different renewable refinery concepts, including algae-based HEFA production and electricity-based methanol-to-jet and Fischer-Tropsch synthesis.

With a product capacity of roughly 20,000 t$_{Fuels}$/a, the refinery can be considered small scale compared to conventional oil refineries [82]. Optimal costs of approx. 3000 €/t$_{Fuel}$ (for the base case) are about five times as high as conventional products [118]. The individual components of the integrated process are in well-known size ranges. The anaerobic digestion of algae residue produces 3.39 t/h of biogas which is still in the range of large scale bio-methane plants, the subsequent tri-reforming process produces up to 10,500 Nm^3/h of H$_2$. This depicts a small- to medium-scale

reforming unit which are in average designed for capacities around 50,000 Nm³/h [104]. The connected carbon capture unit separates ca. 22 kt_{CO_2}/a. Selexol-based acid gas removal plants are well-known processes that are normally designed for large-scale applications. Hence, a small-scale plant also seems very feasible.

One major challenge in the process design is the algae cultivation plant. To grow the calculated 43,000 $t_{Dry-mass}$/a algae with conventional open ponds up to 520 ha would be required even for well suited locations with growth rates of 25 g/m²/day and 330 days of cultivation time per year [109]. With 1.8 kg_{CO_2}/kg_{algae} the plant captures roughly 77,500 t_{CO_2}/a. If realized by LT-DAC such a plant would only require 2 ha of land size [106]. Even with included land requirements for the remaining plant as well as indirect usage for energy production it seems unlikely for an algae-based plant to require less total area compared to electricity-based production. Additionally, the complete plant is a complex system including biomass cultivation, extraction, upgrading as well as anaerobic digestion a reformer, methanol synthesis and a complete waste water treatment plant. In reality, the technical and financial risk affiliated with such complexity could outweigh the economic benefits. This could be even more the case for special locations. Densely populated countries with medium solar radiation like Germany will face land problems as well as higher algae costs, which could lead to lower or no economic benefits of an integrated refinery compared to a pure MTJ / FTJ process. Sun-rich countries like Morocco or Algeria on the other will have sufficient space and solar radiation for algae cultivation. If saline strains with higher lipid content are cultivated this could lead to the economic superiority of stand-alone biorefineries. It is plain, that for every plant a detailed and location-specific engineering is necessary. Nonetheless, integrated processes as presented in this work should not be dismissed from the start, due to possible cost-reductions.

Renewable refineries that are designed to this date should decrease their environmental impacts, but they are also supposed to work for the upcoming 20 – 25 years. Therefore, their design as well as utilized raw materials and produced good should already have in mind the upcoming changes. If for example renewable electricity becomes more expensive or cheaper due to increased installed capacities or usage restrictions this could have a massive effect on electricity-based processes. Similarly, the further development of novel processes like MTJ, algae cultivation or even electrolysis plants can change the economic feasibility of different process designs in the future.

Gasoline as a transportation fuel will probably lose its importance due to massive electrification. If gasoline prices are decreasing, a well-designed plant should be able to adjust the shares of products to a certain degree. Another opportunity would be to design processes that are easily modified or expanded, e.g. including a steam cracker to produce light olefins from the naphtha fraction. In such terms a

methanol-based production has great potentials, due to its versatility. By-products in MTJ include H_2, methanol, olefins and DME, all important chemicals which allow the refinery to adjust its product portfolio in the future, making it a good trade-off choice [18].

In conclusion the provided case study indicates the feasibility and environmental benefits of integrated renewable refineries. However, land requirement for algae cultivation is large and therefore probably only interesting for non-densely populated countries. The consideration of integrated PtX and BtX concepts exposed cost benefits of such designs, however at the price of increase plant complexity, fresh water demand and land requirement compared to stand-alone PtX processes. Furthermore, designing renewable refineries at the beginning of the upcoming transformation of the energy system should also consider changes in raw material acquisition and product demand. A deliberate design would be adaptable to such changes in the future. Thus, specific detailed engineering is necessary to design optimal processes for specific location while including a transformative mindset to regard for the upcoming changes in the energy system and its varying boundary conditions.

7   CONCLUSION AND OUTLOOK

This chapter delivers a final conclusion for the whole thesis. Based on the defined research questions the accomplished output is evaluated and positioned in the larger picture of climate change and the energy transition. Furthermore, an outlook for possible further research is presented. This outlook includes proposals for further investigations in process design considering the petrochemical industry, as well as methodic development concerning open-source superstructure optimization and optimization in general.

7.1 CONCLUSION

The goal of this thesis was two-fold:

i.   Overcome the restrictions in process synthesis given by highly specified and closed-source frameworks by developing an open-source tool for multi-criteria conceptual process design optimization.

ii. Support the defossilization of the carbon intensive petrochemical industry by identifying optimal renewable process alternatives which provide significant greenhouse gas emission reduction potentials, while considering multiple sustainability criteria.

To reach the first goal, this thesis introduced OUTDOOR (**O**pen s**U**pers**T**ructure mo**D**eling and **O**ptimizati**O**n f**R**amework), the first fully open-source software solution, especially designed for superstructure optimization. It is a Python-based framework including easy modeling capabilities, as well as a detailed mathematical model and extensive pre- and postprocessing tools. Compared to other frameworks like ProCAFD, Pyosyn or COMANDO it focusses on multi-criteria process synthesis, uses a mixed-integer linear model and provides an all-in-one approach of data-collection and storage, modeling, optimization and analysis [55], [60], [61]. Hence it provides an intuitive but powerful tool for process synthesis to science. Two potent analysis methods were especially developed for OUTDOOR. The first depicts a novel approach to multi-criteria superstructure optimization to increase capabilities in sustainable process design, while simplifying analyzing results. The second methodology presents a screening algorithm based on two-way sensitivity analysis. It reduces time and complexity of identification of optimal process configurations under uncertain data as often given with novel processes.

Owning to its open-source character, OUTDOOR can be easily adapted to further research in the field of conceptual process design, independent from the application. However, due to its modularity it could also serve as a starting point for the development of further features like additional analysis methods or advanced modeling approaches.

To meet the second goal, OUTDOOR was utilized to investigate two exemplary case studies in the field of petrochemical alternatives.

The first case study describes the multi-criteria design optimization of renewable methanol production. Unlike other studies, the presented superstructure includes and integrates both Power-to-X and Biogas-to-X process alternatives. Using the specially developed multi-criteria optimization method it demonstrates that a combination of BtX and PtX can boost the economics of the overall process. Nonetheless, a stand-alone Power-to-X process depicts a better trade-off if

production costs, greenhouse gas emissions and fresh water demand are considered simultaneously.

The second case study investigates the renewable production of jet fuel by a combined PtX and BtX refinery. While other studies investigate either biorefineries or Power-to-X processes, this case study integrates an algae-based biorefinery with PtX concepts like Fischer-Tropsch synthesis and methanol-to-jet. Using OUDOOR's powerful modeling capabilities a deep integration of the PtX and BtX branches is enabled. This integration includes coupled waste water treatment, energy production and heat integration but also the opportunity to use algae residue as feedstock for Fischer-Tropsch and methanol synthesis. Using the especially developed screening algorithm, the results indicate that a combination of PtX and BtX can boost the economics. Nonetheless, this effect is highly depending on the given boundary conditions. Additionally, an economic boost always comes at the cost of increased plant complexity and higher fresh water demand due to algae cultivation.

Both case studies proof that significant reductions of the petrochemical industry are possible by the given renewable alternatives. Renewable methanol can save up to 2.9 t_{CO_2}/ t_{MeOH} while renewable fuels can save up to 4.7 t_{CO_2}/ t_{Fuels}. This thesis also demonstrated that a combination of Power-to-X and Biomass-to-X processes can enhance economics. However, due to substantially larger fresh water consumption and land requirement of biomass-based processes a purely electricity-based production is often the better trade-off, especially for densely populated countries like Germany. For less populated regions like Morocco or Spain which also have increased solar potential, biomass cultivation could be an interesting option. Due to water scarcity, saline algae strains would be the favorable option in these regions. Especially for coastal areas with easy access to sea water this could be an interesting choice.

It is evident that to ensure sustainable solutions numerous aspects like raw material acquisition, product distribution and location-specific boundary conditions have to be considered for detailed engineering and process design. Such investigations should also consider the remaining products of the petrochemical industry like olefins and aromatics, as well as further options like crude or intermediates import especially for densely populated countries like Germany.

While all these alternatives are not cost competitive to conventional petrochemicals yet, they show great GHG reduction potentials. Therefore, an upcoming main goal should be to further increase the economics of such processes.

7.2 OUTLOOK

A recent review on process systems engineering published by Pistikopoulos et al. summarizes the need on further development especially in the areas of design of sustainable processes, multiscale modeling, integrated problem solution and unification of methods and software tools among others [30].

Gong and You invited the idea of sustainable design of energy systems by integrating superstructure optimization and life cycle optimization in 2019 [121]. They stated four major challenges which are automated superstructure generation, broader life cycle models as well as handling of uncertainty of nested superstructures [121]. The optimization framework presented in this thesis could work as a starting point to tackle these challenges. The simplified and generic modeling approach could lower the entrance barrier to completely automated superstructure construction, even including web-searching algorithms for data acquisition or connections to flowsheeting software in combination with large-scale open-source data bases. Actually first approaches in this direction already have been made at the university of Delft using OUTDOOR as starting point [122]. Next to production costs, two environmental metrics are already included. Combined with the developed multi-criteria optimization method OUTDOOR's sustainability assessment capabilities via life cycle optimization could be easily enhanced by adding more environmental objectives. Additionally, a first proposition to handling uncertainty and nested superstructures has been made in this thesis. The developed search algorithm deals with uncertain data inputs and was already tested on a highly integrated Power-to-X and biorefinery. Additional features could include a Monte-Carlo simulation. Monte-Carlo simulation describe multiple simulations with varying input parameters to investigate the effect on the results. Special feature of the Monte-Carlo simulation is, that multiple parameters are modified at once based on affiliated probability functions. However, for these methodology development steps, next to the conceptualization and programming, two major challenges arise. The first one addresses extreme computational effort with rising calculation numbers. The second one deals with the visualization of such massive amounts of results. Both challenges would have to be tackled in order to gain benefits from such an enhanced analysis method.

Multiscale modeling and integrated problem solutions can be viewed from a joined perspective. Future modeling and optimization capabilities should be able to answer tightly coupled questions. One approach was already presented by Galanopoulos et. al. who proposed a framework to couple process design and supply chain optimization while considering economics and environmental metrics. They used an iterative method of process simulation with Aspen Plus and supply chain optimization using AIMMS to design an optimal supply chain with detailed plant models [123]. On a different scale Skiborowski et al. provided a

review on conceptual process design methods on hybrid separation processes in process flowsheets, coupling unit-operation design with process synthesis [124]. Krone et al. proposed an optimization-based approach to include detailed thermodynamic models in superstructure optimization using the CAPE-OPEN model library in a recent work [46].

All of these challenges in process systems engineering will require software solutions that include models able to work at multiple scales, solvers that can solve large and complex problems in an appropriate amount of time as well as methods to handle large amounts of in- and output data. Writing compatible software with standards and protocols to ensure collaboration and maximize scientific output will be a major challenge in the future. Different approaches have been made in the recent past. General frameworks like oemof or the very new COMANDO provide general modeling capabilities which can be used for different applications in the domain of energy systems optimization [61], [125]. OUTDOOR joins this line of frameworks, however provides specialized capabilities in the domain of superstructure optimization. Nonetheless, it might develop into a general process system engineering toolbox including multiscale modeling e.g. adopting supply-chain models or more sophisticated unit-operation models. Such additions could be integrated in the general framework and would simplify data exchange on the different scales.

Next to the challenges discussed above, the main topics in process engineering will revolve around the general water-energy-food-environment-health nexus [30]. This increasing integration and the affiliated complexity will also be part of process design questions. Based on the case studies presented in this thesis upcoming topics could include other major petrochemicals like light olefins or the utilization of ligno-cellulosic biomass as raw material. Additionally, a link to agriculture, waste management or other base chemical industries will be created. This future research has to connect petrochemicals with ammonia and urea production, waste water treatment and algae cultivation or oxygen supply for cement factories among others to tackle the general threat of climate change and the transition of the energy system.

A. ADDITIONAL INFORMATION ON RENEWABLE METHANOL PRODUCTION CASE STUDY (CHAPTER 5)

TABLE A.1: LIST OF UNIT-OPERATIONS OF RENEWABLE METHANOL PRODUCTION SUPERSTRUCTURE AS WELL AS THEIR MODEL DATA SOURCE.

Abbreviation	Unit-operation	Data source
LT-DAC	Low temperature direct air capture	[86]
OXY	Oxyfuel fired cement factory	[87], [88]
CPU	Cooling and purification of oxyfuel cement factory flue gases	[87], [88]
AEL	Low pressure alkaline electrolyzer at 1 bar	[89], [90]
HP-AEL	High-pressure alkaline electrolyzer at 30 bar	[89], [90]
HP-PEMEL	High-pressure polymer electrolyte membrane electrolyzer at 30 bar	[89], [90]
SOEL	Solid oxide electrolyzer at 1 bar	[91]
ATR-SEL	Selexol-based CO_2 capture plant for ATR SynFeed	Simulation, [126]
TRIR-SEL	Selexol-based CO_2 capture plant for TRIR SynFeed	Simulation, [126]
H_2-PSA	Hydrogen pressure swing adsorption for H_2 separation from SMR SynFeed	Simulation, [93], [126]
BG-PSA	Biogas pressure swing adsorption for CO_2 separation	[24]
VP	Vacuum pump	[24]
H_2-LH-COMP	H_2 compressor from low (1 bar) to high (70 bar) pressure	Simulation, [82]
SMR-COMP	Compressor for raw SynFeed from SMR to 70 bar	Simulation, [126]
ATR-COMP	Compressor for raw SynFeed from ATR to 70 bar	Simulation, [126]
MeOH SYN	Methanol synthesis unit	[82]
MeOH FLASH	Purge gas flash	[82]
MeOH DC	Methanol distillation column for water separation	[82]
HEAT GEN	Heat furnace to produce superheated steam	[24]
EL GEN	Combined gas- and steam turbine to produce electricity	[24]
WWT	Waste water treatment plant	[94]
SMR	Steam methane reforming unit	Simulation, [126]
ATR	Autothermal reforming unit	Simulation, [126]
TRIR	Tri-reforming unit (for raw biogas)	Simulation, [126]

Abbreviation	Unit-operation	Data source
MEA-CC	Amine scrubbing-based carbon capture from flue gases	[82]
CO_2-COMP	CO_2 compressor to 70 bar	[82]
H_2-MH-COMP	H_2 compressor from medium (30 bar) to high (70 bar) pressure	Simulation, [82]
TRIR-COMP	Compressor for raw SynFeed from TRIR to 70 bar	Simulation, [126]
SYNFEED COMP	Compressor for SynFeed with molar H_2/CO_2 ratio of 3	Simulation, [126]
H2O-DIST	Purified water distributor	–
O2-DIST	Oxygen distributor	–
CH4-DIST	Bio-methane distributor	–
ATR-DIST	ATR-SynFeed distributor	–
TRIR-DIST	TRIR-SynFeed distributor	–
SMR-DIST	SMR-SynFeed distributor	–
H2-DIST	Hydrogen by-product distributor	–

TABLE A.2: KEY PERFORMANCE INDICATORS FOR VARIATION SCENARIO 1 OF RENEWABLE METHANOL PRODUCTION SUPERSTRUCTURE.

	NPC-Optimized	NPE-Optimized	NPFWD-Optimized	MCO-Optimized
NPC (€/t)	501	600	829	501
NPE (t_{CO_2}/ t)	–2.23	–2.26	–2.015	–2.2
NPFWD (t_{H_2O}/ t)	–3.39	–3.696	–4.717	–3.39

TABLE A.3: KEY PERFORMANCE INDICATORS FOR VARIATION SCENARIO 2 OF RENEWABLE METHANOL PRODUCTION SUPERSTRUCTURE.

	NPC-Optimized	NPE-Optimized	NPFWD-Optimized	MCO-Optimized
NPC (€/t)	5804	2245	2479	1348
NPE (t_{CO_2}/ t)	–0.4	–2.679	–2.479	–2.234
NPFWD (t_{H_2O}/ t)	2.581	–4.99	–5.55	–3.616

TABLE A.4: KEY PERFORMANCE INDICATORS FOR VARIATION SCENARIO 3 OF RENEWABLE METHANOL PRODUCTION SUPERSTRUCTURE.

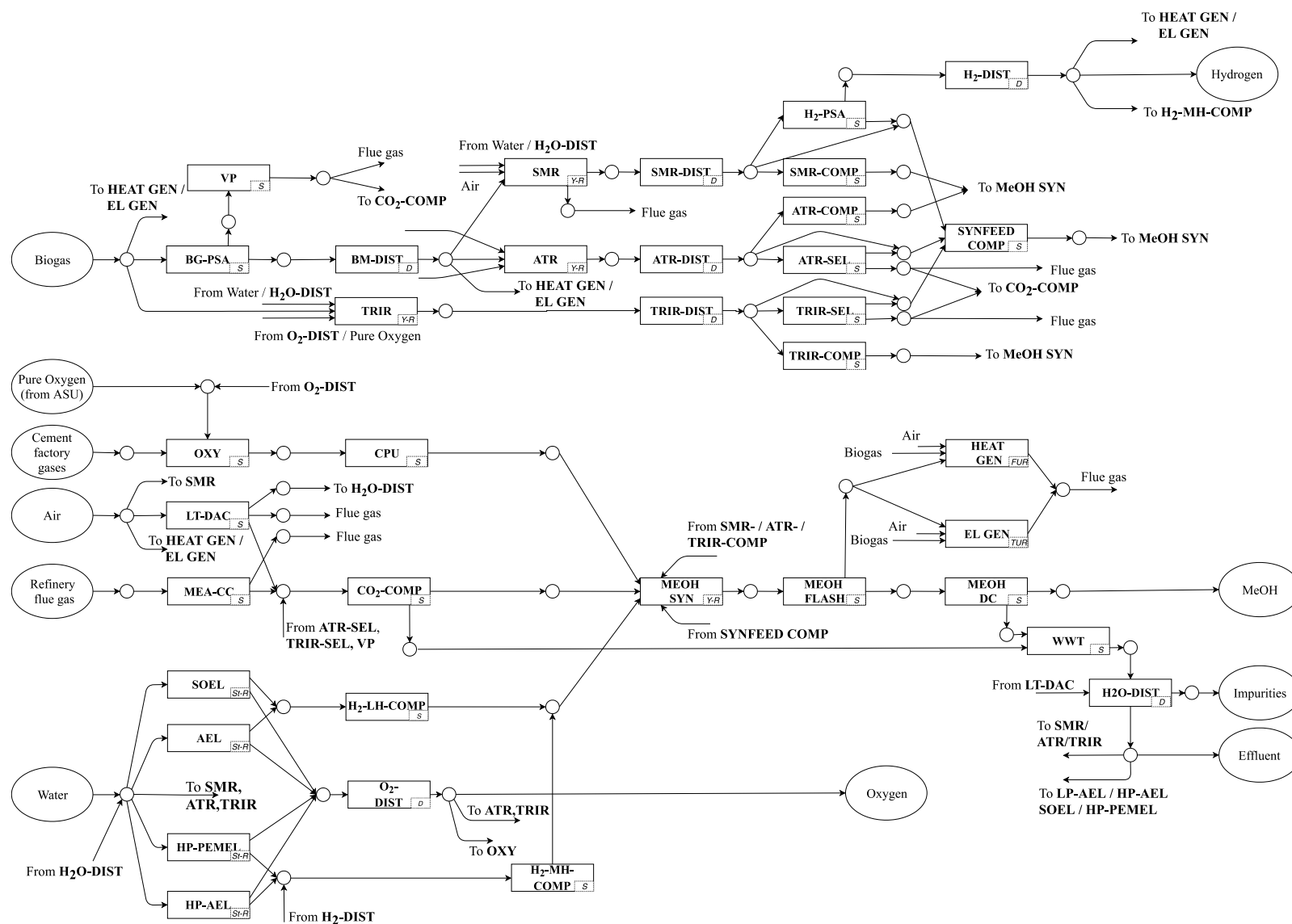|	NPC-Optimized	NPE-Optimized	NPFWD-Optimized	MCO-Optimized
NPC (€/t)	501	1446	1672	501
NPE (t_{CO_2}/ t)	–2.23	–2.679	–2.479	–2.234
NPFWD (t_{H_2O}/ t)	–3.39	–4.993	–5.55	–3.39

FIGURE A.1: SUPERSTRUCTURE REPRESENTATION OF RENEWABLE METHANOL PRODUCTION PLANT.

B. ADDITIONAL INFORMATION ON RENEWABLE REFINERY CASE STUDY (CHAPTER 6)

TABLE B.1: LIST OF UNIT-OPERATIONS OF RENEWABLE REFINERY SUPERSTRUCTURE AS WELL AS THEIR MODEL DATA SOURCE.

Abbreviation	Unit-operation	Data source
LT-DAC	Low temperature direct air capture	[86]
OXY	Oxyfuel fired cement factory	[87], [88]
CPU	Cooling and purification of oxyfuel cement factory flue gases	[87], [88]
AEL	Low pressure alkaline electrolyzer at 1 bar	[89], [90]
HP-AEL	High-pressure alkaline electrolyzer at 30 bar	[89], [90]
HP-PEMEL	High-pressure polymer electrolyte membrane electrolyzer at 30 bar	[89], [90]
SOEL	Solid oxide electrolyzer at 1 bar	[91]
ATR-SEL	Selexol-based CO_2 capture plant for ATR SynFeed	Simulation, [126]
TRIR-SEL	Selexol-based CO_2 capture plant for TRIR SynFeed	Simulation, [126]
H_2-PSA	Hydrogen pressure swing adsorption for H_2 separation from SMR SynFeed	Simulation, [93], [126]
BG-PSA	Biogas pressure swing adsorption for CO_2 separation	[24]
VP	Vacuum pump	[24]
H_2-LH-COMP	H_2 compressor from low (1 bar) to high (70 bar) pressure	Simulation, [82]
SMR-COMP	Compressor for raw SynFeed from SMR to 70 bar	Simulation, [126]
ATR-COMP	Compressor for raw SynFeed from ATR to 70 bar	Simulation, [126]
MeOH SYN	Methanol synthesis unit	[82]
MeOH FLASH	Purge gas flash	[82]
MeOH DC	Methanol distillation column for water separation	[82]
HEAT GEN	Heat furnace to produce superheated steam	[24]
EL GEN	Combined gas- and steam turbine to produce electricity	[24]
WWT	Waste water treatment plant	[94]
SMR	Steam methane reforming unit	Simulation, [126]
ATR	Autothermal reforming unit	Simulation, [126]
TRIR	Tri-reforming unit (for raw biogas)	Simulation, [126]
MEA-CC	Amine scrubbing-based carbon capture from flue gases	[82]
CO_2-COMP	CO_2 compressor to 70 bar	[82]

Abbreviation	Unit-operation	Data source
H_2-MH-COMP	H_2 compressor from medium (30 bar) to high (70 bar) pressure	Simulation, [82]
SYNFEED COMP	Compressor for SynFeed with molar H_2/CO_2 ratio of 3	Simulation, [126]
H2O-DIST	Purified water distributor	–
O2-DIST	Oxygen distributor	–
CH4-DIST	Bio-methane distributor	–
ATR-DIST	ATR-SynFeed distributor	–
TRIR-DIST	TRIR-SynFeed distributor	–
SMR-DIST	SMR-SynFeed distributor	–
H2-DIST	Hydrogen by-product distributor	–
H2-LM-COMP	H_2 compressor from low (1 bar) to medium (30 bar) pressure	Simulation, [82]
SONIC	Sonication algae pretreatment	[24]
HEX-EXT	Hexane-based lipids extraction	[24]
SUP-CO_2-EXT	Supercritical CO_2-based lipid extraction	[24]
BIO-U	Bio-oil upgrading	[115]
CENTR	Centrifugation	[24]
AAD	Anaerobic digestion	[24]
CENTR-DIST	Centrifugation water distributor	–
MTJ	Methanol-to-Jet	[18]
FT-M	Fischer-Tropsch synthesis mixer	[108]
RWGS	Reverse water gas shift	[108]
FT-R	Fischer-Tropsch reactor	[108]
FT-DC	Fischer-Tropsch distillation column	[108]
HYDRO	Fischer-Tropsch hydrocracker	[108]
FT-B	Fischer-Tropsch burner	[108]
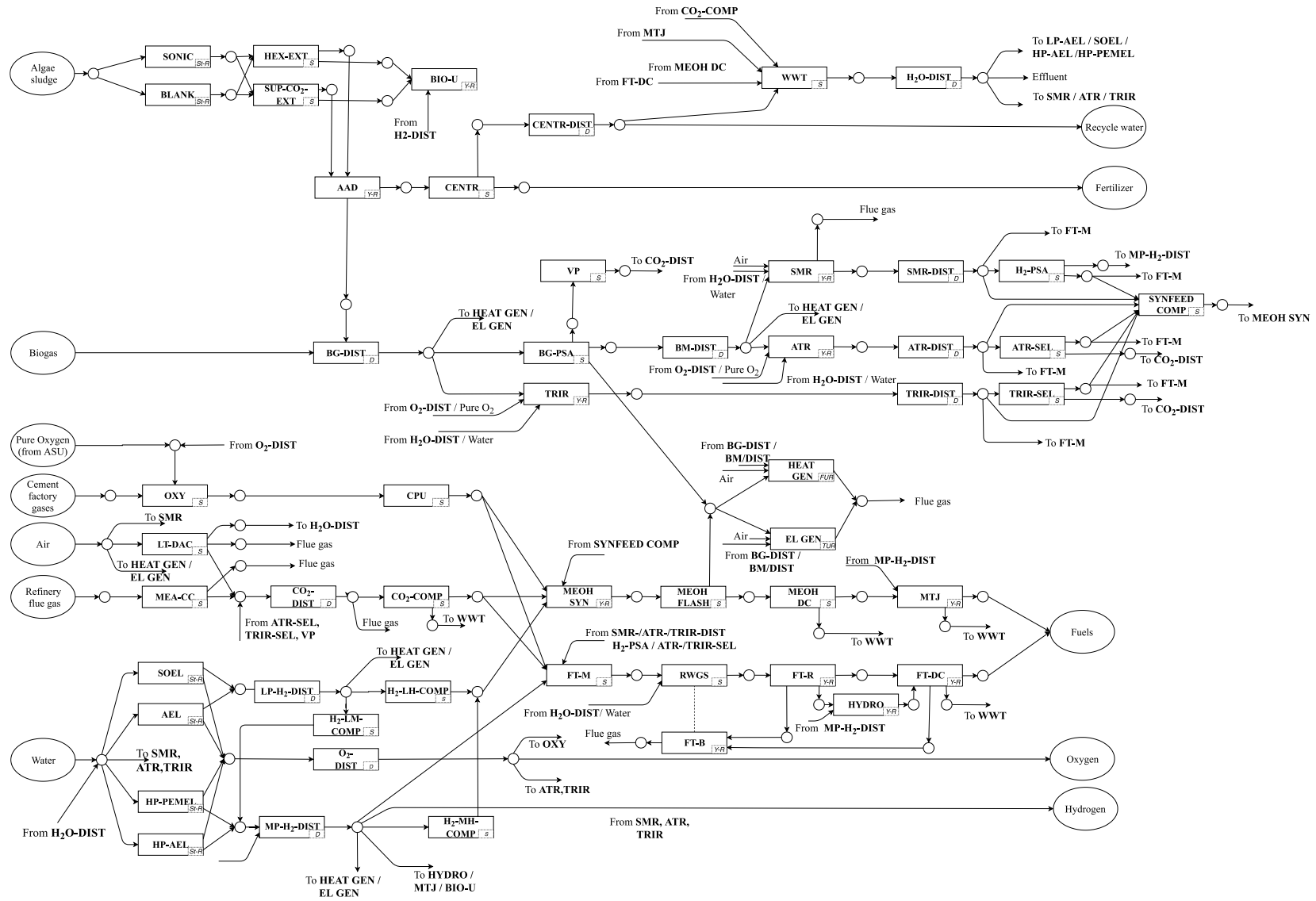
FIGURE B.1: SUPERSTRUCTURE REPRESENTATION OF RENEWABLE REFINERY FOR FUELS PRODUCTION.

C. ADDITIONAL INFORMATION ON BIOGAS REFORMING MODELS

The complete work as well as results of this appendix in combination with an additional techno-economic analysis have been published in:

Kenkel, P., Wassermann, T., & Zondervan, E. (2021). Biogas Reforming as a Precursor for Integrated Algae Biorefineries: Simulation and Techno-Economic Analysis. Processes, 9(8), 1348.

Models of biogas and bio-methane reforming as mentioned in Chapter 5.2.2 and 6.2.2 are based on detailed simulations performed using Aspen Plus V10. Bio-methane reforming is based on steam methane reforming (SMR) and autothermal reforming (ATR), biogas reforming is based on biogas tri-reforming (TRIR). Models were developed using Peng-Robinson equation of state based on reviewed literature [127], [128]. For every process concept three models, depicting different plant capacities, were set up. The given capacities based on the inlet gas molar flow, depicting either pure methane or biogas with a molar ratio of 0.65/0.35 methane/carbon dioxide:

- Large scale: 1000 kmol/h input, representing biogas production from a large biorefinery production 46 kt$_{\text{Jet Fuel}}$/a. [115]

- Medium scale: 500 kmol/h input.

- Small scale: 10 kmol/h input, representing a large biogas plant with approx. 2.5 MW$_{\text{el}}$ energy output.

The different process flowsheets all include an adiabatic pre-reformer, a main reformer as well as adiabatic two-stage high-temperature (HT-WGS) and low-temperature water gas shift reactor (LT-WGS). SMR utilizes an externally fired isothermal main reactor in combination with a detailed heat recovery and steam generation system to produce required electricity. ATR and TRIR utilize adiabatic main reactors with heat recovery to achieve an autothermal plant design. Reactor concepts are implemented as Gibbs (pre- and main reformer) or equilibrium reactor (HT- and LT-WGS) in Aspen Plus. Non-ideal conversion is considered using the temperature approach suggested by Hamelinck et al., as well as Katofsky, is used [83], [129].

The general plant design, as well as main design and operating parameters such as reactor temperature, pressure, pressure drops, steam to carbon were chosen based on given literature for the different plants [22], [23], [104], [127].

Figure C.1 shows the detailed flowsheet of the steam methane reforming process which is condensed into the SMR-unit in Figure 5.5. Table C.4 presents the associated stream results for the large-scale case. Figure C.2 and Figure C3 present the detailed flowsheets of the autothermal and biogas tri-reforming processes which are condensed into the ATR- and TRIR- unit in Figure 5.5. Table C.5 and Table C.6 present their associated stream results for the large-scale case.
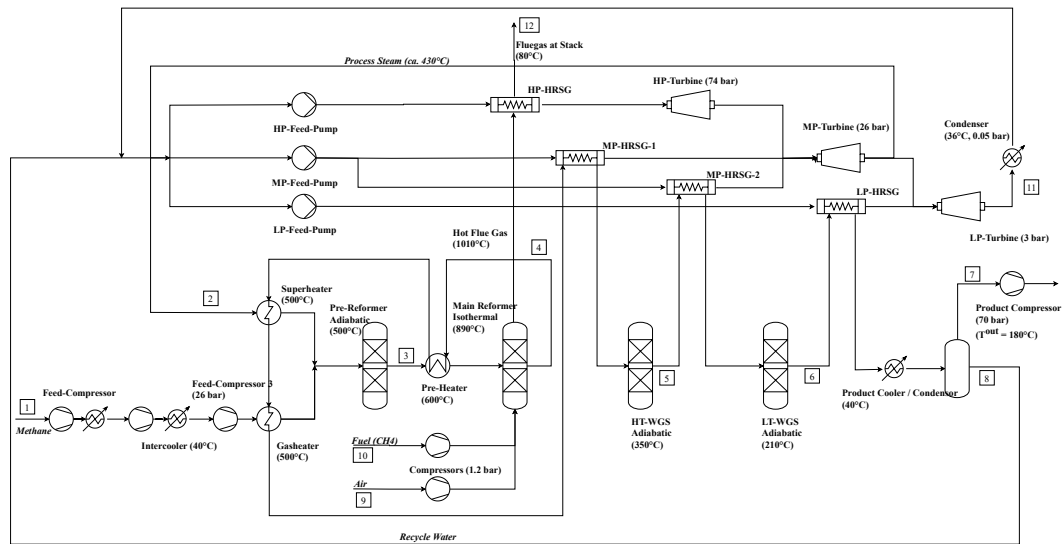

FIGURE C.1: PROCESS FLOW DIAGRAM OF ASPEN PLUS STEAM METHANE REFORMING PROCESS.
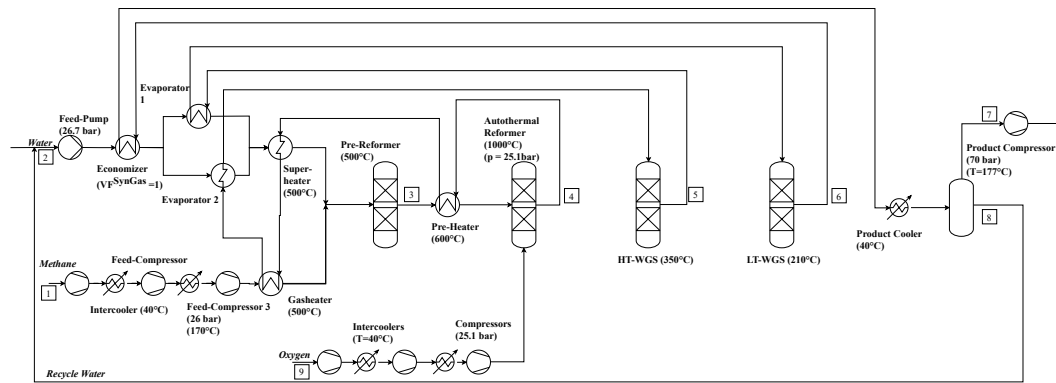
FIGURE C.2: PROCESS FLOW DIAGRAM OF ASPEN PLUS AUTOTHERMAL REFORMING PROCESS.
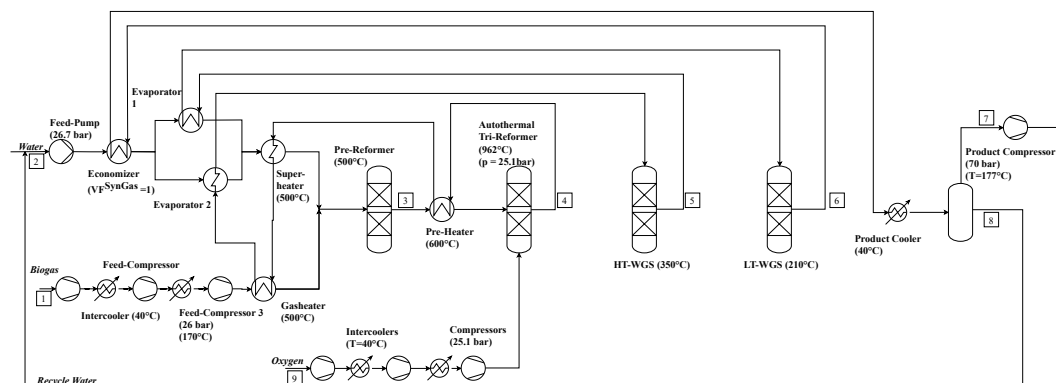
FIGURE C.3: PROCESS FLOW DIAGRAM OF ASPEN PLUS BIOGAS TRI-REFORMING PROCESS.

Steam to carbon as well as oxygen to carbon ratio for ATR and TRIR were chosen based on three design principles:

- The CO-content in the compressed product is limited to 1 mol. -%, since it serves as feed for direct hydrogenation methanol synthesis.

- The required heat is provided by heat integration of the partially oxidized feed, so that the ATR/TRIR process is fully autothermal.

- The amount of O_2 supplied is minimized, due to its energy-, emission- and cost-intensive provision.

For proper sizing and costing of heat exchangers, the thermal transmittance U for each exchanger was calculated based on the VDI-Wärmeatlas for all process flowsheets [130]. Main parameter assumptions for the different processes are presented in Table C.1.

TABLE C.1: KEY PARAMETERS AND REFERENCE FOR SMR, ATR AND TRIR PROCESS MODELS.

Parameter	SMR	ATR	TRIR	Note	Ref.
Main reformer feed pressure		25.1 bar		Based on outlet temperature of 180 °C max and pressure drop.	
Pre-reformer Temperature/ Approach		500 °C Delta T = −10 °C			[93], [130]
Pre-reformer pressure drop		−0.5 bar			[83], [129]
Main reformer Temperature/ Approach	890 °C ΔT = −10 °C	999 °C ΔT = −10 °C	962°C ΔT = −10 °C		[93], [129]
Main reformer pressure drop		−0.5 bar			[83]
Heat exchanger pressure drop		−0.2 bar			[129]
HRSG pressure drop	−0.5 bar liquid site −0.2 bar gas site	−			[129]
HT-WGS pressure drop		−0.5 bar			[83], [129]
HT-WGS Temperature/ Approach		350 °C ΔT = 10 °C			[83], [129], [131]
LT-WGS pressure drop		−0.5 bar			[83], [129]
LT-WGS Temperature/ Approach		210 °C ΔT = 20 °C		Temperature approach higher due to lower reaction rate at lower temperatures	[129], [131]
HP-TUR Inlet/Outlet pressure	74/26 bar		−	Outlet pressure chosen based on required feed pressure	Experience
MP-TUR Inlet/Outlet pressure	26/3 bar		−		Experience
LP-TUR Inlet/Outlet pressure	3/0.25 bar		−	Based on 0.05 bar outlet at condenser with 0.2 pressure drop	-
Efficiency Pumps/Compressors		80% isentropic 100% mechanical			Experience
Efficiency Turbine	89% isentropic 99% mechanical		−		[83]
U-Values for HE		Calculated based on linearized values			[130]
Molar Steam to CH$_4$	3.5 and 5	2.2:1	2.51:1	Based on literature and 95% CH$_4$ Conversion	[83]
Molar Oxygen to CH$_4$		0.574:1	0.6:1		

Based on the different flowsheet simulations linear dependent raw material demand, conversion and utility demand as well as non-linear dependent equipment costs for the plant were calculated. Equipment costs were derived from literature using economies of scale for the pre- and main reformer[83]. Costs for the remaining plant, including heat exchangers, pumps, compressors or turbines were derived from the Aspen Economic Analyzer. Table C.2 presents total equipment costs of the different plants as well as final compressor costs for compression to operating pressure of methanol synthesis (70 bar) in million euros. Table C.3 presents additional modeling results like water and oxygen demand as well as electricity and cooling demand.

TABLE C.2: PROCESS EQUIPMENT COSTS OF DIFFERENT REFORMING TECHNOLOGIES AS WELL AS COMPRESSORS IN M€.

	Small-scale	Medium-scale	Large-scale
SMR Plant	4.02	29.64	52.4
SMR Product compressor	1.21	1.74	2.17
ATR Plant	4.42	12.5	19.39
ATR Product compressor	1.08	1.59	1.99
TRIR Plant	4.06	10.15	15.34
TRIR Product compressor	1.01	1.46	1.77

TABLE C.3: ADDITIONAL TECHNO-ECONOMIC RESULTS OF PROCESS MODELS FOR SMR, ATR AND TRIR.

–	H_2O/CH_4 (t_{in}/t_{in})	O_2/CH_4 (t_{in}/t_{in})	Electricity BOP (MWh/$t_{SynFeed}$)	Cooling BOP (MWh/$t_{SynFeed}$)	Electricity Compressor (MWh/$t_{SynFeed}$)
SMR	1.34	1.83	-0.14	1.33	0.12
ATR	0.92	1.15	0.11	0.53	0.09
TRIR	0.84	1.21	0.10	0.45	0.07

TABLE C.4: STREAM DATA OF SMR PROCESS FOR LARGE CAPACITY.

Parameter	Unit	Stream Number											
		1	2	3	4	5	6	7	8	9	10	11	12
T	°C	25	457.4096	430.1723	890	404.9852	221.921	40	40	20	25	67.54796	80.07172
p	bar	1.01325	26	25.3	24.6	23.3	22.6	22.2	22.2	1.01325	1.01325	0.25	1
Mole Flow	kmol/h	1000	5000	6190.739	7900.167	7900.167	7900.167	4803.401	3096.766	7254.5	659.5	1420	7914
Mass Flow	kg/h	16,042.76	90,076.4	106,119.2	10,6119.2	106,119.2	106,119.2	50,325.22	55,793.94	208,569.9	10,580.2	25,581.7	219,150.1
H_2O	kg/h	0	90,076.4	86,654.15	64,789.12	57,560.62	56,053.17	267.8497	55,785.32	1306.918	0	25,581.7	25,069.06
CO_2	kg/h	0	0	4163.086	19,961.71	37620.31	41302.88	41,294.31	8.573509	0	0	0	29,024.45
CO	kg/h	0	0	21.70286	13907.42	2668.458	324.6558	324.6551	0.000629	0	0	0	0.011358
H_2	kg/h	0	0	767.4507	6660.113	7468.97	7637.651	7637.622	0.028881	0	0	0	0.001029
CH_4	kg/h	16042.76	0	14,512.77	800.8002	800.8002	800.8002	800.7841	0.016038	0	10,580.2	0	1.32E-27
O_2	kg/h	0	0	3.30E-26	2.57E-13	2.57E-13	2.57E-13	0	0	48,748.41	0	0	6542.009
N_2	kg/h	0	0	0	0	0	0	0	0	15,8514.6	0	0	158,514.6

TABLE C.5: STREAM DATA OF ATR PROCESS FOR LARGE CAPACITY.

Parameter	Unit	Stream Number								
		1	2	3	4	5	6	7	8	9
T	C	25	30	430.4176	999.0331	443.3008	243.5181	40	40	25
p	bar	1.01325	1.01325	25.3	24.6	23.3	22.6	22.2	22.2	1.01325
Mole Flow	kmol/hr	1000	2205	3313.463	5185.34	5185.34	5185.34	3796.082	1389.259	574.39
Mass Flow	kg/hr	16,042.76	39,723.69	55,766.45	74,146.24	74,146.24	74,146.24	49,115.53	25,030.72	18,379.79
H_2O	kg/hr	0	39,723.69	37,780	36,075.33	28,052.83	25,240.17	214.4203	25,025.75	0
CO_2	kg/hr	0	0	2361.578	15,893.04	35,491.32	42,362.41	42,357.45	495,2583	0
CO	kg/hr	0	0	15.99494	17,619.81	5146.322	773.1602	773.1594	0.000849	0
H_2	kg/hr	0	0	436.1441	4400.375	5298.079	5612.811	5612.799	0.012082	0
CH_4	kg/hr	16042.76	0	15,172.74	157.6972	157.6972	157.6972	157.6954	0.001787	0
O_2	kg/hr	0	0	1.09E-26	1.07E-11	1.07E-11	1.07E-11	0	0	18,379.79
N_2	kg/hr	0	0	0	0	0	0	0	0	0

TABLE C.6: STREAM DATA OF TRIR PROCESS FOR LARGE CAPACITY.

Parameter	Unit	Stream Number								
		1	2	3	4	5	6	7	8	9
T	C	25	30	451.3292	961.6535	448.3946	245.2516	40	40	25
p	bar	1.01325	1.01325	25.3	24.6	23.3	22.6	22.2	22.2	1.01325
Mole Flow	kmol/hr	1000	1625	2685.697	3911.885	3911.885	3911.885	2773.133	1138.752	393.5504
Mass Flow	kg/hr	25,831.22	29,274.83	55,106.05	67,699.19	67,699.19	67,699.19	47,181.06	20,518.14	12,593.14
H_2O	kg/hr	0	29,274.83	28,244.82	29,705.86	23,011.46	20,672.7	160.1096	20,512.59	0
CO_2	kg/hr	15,403.43	0	16,584.02	20,672.83	37,026.67	42,740.06	42,734.53	5.536185	0
CO	kg/hr	0	0	98.67892	14,669.34	4260.8	624.4631	624.4624	0.000769	0
H_2	kg/hr	0	0	237.6138	2545.975	3295.067	3556.771	3556.762	0.008646	0
CH_4	kg/hr	10,427.79	0	9940.921	105.1968	105.1968	105.1968	105.1954	0.001331	0
O_2	kg/hr	0	0	2.05E-25	3.83E-12	3.83E-12	3.83E-12	0	0	12,593.14
N_2	kg/hr	0	0	0	0	0	0	0	0	0

D. ADDITIONAL INFORMATION ON UPGRADING MODELS

The complete work as well as results of this appendix in combination with an additional techno-economic analysis have been published in:

Kenkel, P., Wassermann, T., & Zondervan, E. (2021). Biogas Reforming as a Precursor for Integrated Algae Biorefineries: Simulation and Techno-Economic Analysis. Processes, 9(8), 1348.

The models of bio-based SynFeed upgrading described in Chapter 5.2.2 and 6.2.2 are based on detailed simulations prepared in Aspen Plus V10.

Hydrogen separation from SMR-based SynFeed is performed by pressure swing adsorption (PSA). The derived flowsheet is presented in Figure D.1. It uses a black box (component separator) model of for the actual PSA-unit with a hydrogen recovery factor of 89 % based on Spallina et at. [93]. Afterwards a vacuum pump at 0.8 bar is implemented with subsequent multi-stage compression of the upgraded SynFeed to the initial pressure of approx. 23 bar. Costs for the PSA-unit are based on literature, costs for the heat exchangers as well as compressors are acquired from the Aspen Economic Analyzer [93]. The total capital investment for the three different capacities already defined in Appendix C are presented in Table D.5.
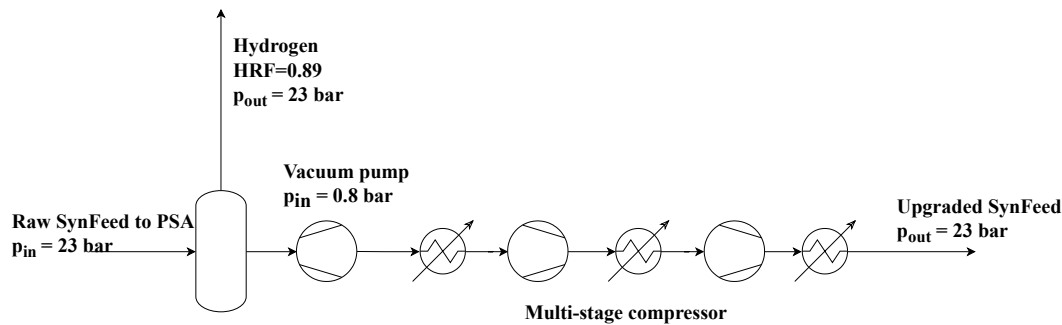
FIGURE D.1: PROCESS FLOW DIAGRAM OF ASPEN PLUS H_2-PSA MODEL.

Carbon capture is achieved with the industrial Selexol process. This process utilizes physical absorption based on the henry-law. The chosen solvent is a mixture of different polyethylene glycols with high affinity to CO_2 absorption at low temperatures around –1°C [132]. The flowsheet was developed based on given literature examples as depicted in Figure D.2 [133], [134]. It includes an absorber operating at the raw SynFeed outlet pressure. A sequence of pressure reduction units recovers the dissolved CO_2, where the first unit at 10.5 bar recycles the gas fraction to the absorber due to relatively large amounts of co-absorbed H_2. In order to close the mass balance make-up Selexol and water have to be supplied to the process. The actual amounts are, however, neglectable. The Aspen Plus model was

simulated using the PC-SAFT thermodynamic model in order to account for complex solvent–gas interaction [132]. Table D.1. and Table D.2 present stream data for the ATR-based inlet and TRIR-based inlet for large capacity, respectively. The upgraded SynFeed outlet composition is presented in Table D.3 while the composition of the nearly pure CO_2 is shown in Table D.4. Equipment costs of the complete plant are shown in M€ for the different capacities in Table D.5.
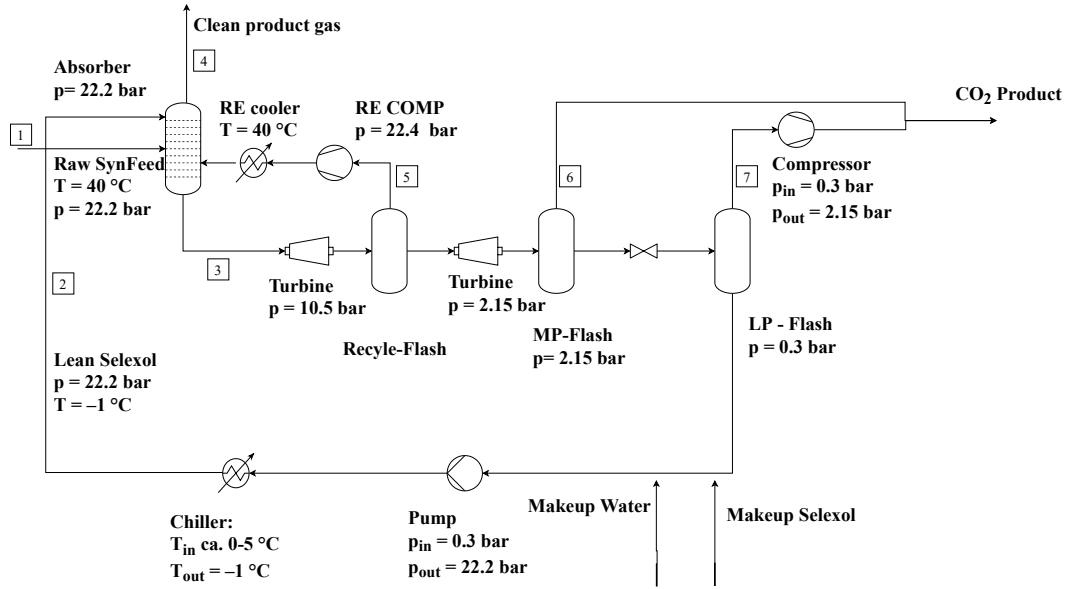
FIGURE D.2: PROCESS FLOW DIAGRAM OF ASPEN PLUS SELEXOL-BASED CARBON CAPTURE MODEL.

TABLE D.1: STREAM DATA FOR SELEXOL-BASED CARBON CAPTURE PROCESS WITH LARGE SCALE ATR-INLET FEED.

Parameter	Unit	Stream Number						
		1	2	3	4	5	6	7
T	C	40	−0.99981	−0.99981	2.043752	12.64989	6.492418	1.698376
p	bar	22.2	22.2	22.2	22.2	10.5	2.15	0.3
Mole Flow	kmol/h	3796.08	8113.983	8113.983	2903.783	49.84854	527.0901	377.9916
Mass Flow	kg/h	54,140.59	13,21759	13,21759	11,651.23	1329.498	24,943.54	17,799.57
DEPG	kg/h	0	12,38407	12,38407	0.000901	0.000154	0.002657	0.006017
CO	kg/h	852.1054	0.00156	0.00156	840.8976	11.22036	10.9416	0.266693
CO_2	kg/h	46,691.25	3218.225	3218.225	4440.694	1261.543	24,819.98	17,430.37
H_2	kg/h	6187.051	0.000724	0.000724	6163.267	51.55269	23.52053	0.265748
H_2O	kg/h	236.1789	80,134.28	80,134.28	39.96198	1.949985	81.90781	368.2506
CH_4	kg/h	174.0018	0.005658	0.005658	166.41	3.231662	7.181761	0.410241

TABLE D.2: STREAM DATA FOR SELEXOL-BASED CARBON CAPTURE PROCESS WITH LARGE SCALE TRIR-INLET FEED.

Parameter	Unit	Stream Number						
		1	2	3	4	5	6	7
T	C	40	−0.99975	15.95864	3.017213	15.09966	6.317703	1.427384
p	bar	22.2	22.2	22.2	22.2	10.5	2.15	0.3
Mole Flow	kmol/h	2773.133	6260.326	7209.441	1881.04	56.86575	605.3016	298.4395
Mass Flow	kg/h	52,008.21	1,022,311	1,067,134	9179.803	1992.169	28,999.04	14,060.38
DEPG	kg/h	0	958,154.1	958,154.1	0.000681	0.000268	0.002981	0.004562
CO	kg/h	688.3519	0.000658	17.76797	681.4286	10.84441	6.809869	0.11304
CO_2	kg/h	47,106.75	2513.095	47,109.29	4450.059	1940.007	28,884.21	13,771.98
H_2	kg/h	3920.659	0.00022	46.73519	3910.02	36.09693	10.5568	0.081235
H_2O	kg/h	176.4907	61,643.7	61,799.32	26.57529	2.389313	93.37981	288.0509
CH_4	kg/h	115.9581	0.002176	7.0713	111.7192	2.830401	4.080083	0.158639

TABLE D.3: VOLUMETRIC COMPOSITION OF UPGRADED SYNFEED OUTLET FROM CARBON CAPTURE PROCESS BASED ON INLET PROCESS.

	ATR	TRIR
CO (vol. −%)	0.94	1.17
CO_2 (vol. −%)	03.14	4.88
H_2 (vol. −%)	95.53	93.54
H_2O (vol. −%)	0.07	0.07
CH_4 (vol. −%)	0.32	0.34

TABLE D.4: MASS COMPOSITION OF CAPTURED CO_2 STREAM OUTLET FROM CARBON CAPTURE PROCESS BASED ON INLET PROCESS.

	ATR	TRIR
CO (wt. −%)	0.03	0.02
CO_2 (wt. −%)	98.84	99.05
H_2 (wt. −%)	0.06	0.03
H_2O (wt. −%)	1.05	0.89
CH_4 (wt. −%)	0.02	0.01

TABLE D.5: PROCESS EQUIPMENT COSTS FOR DIFFERENT UPGRADING TECHNOLOGIES FOR DIFFERENT CAPACITIES IN M€.

	Small-scale	Medium-scale	Large-scale
ATR	1.29	2.68	5.18
TRIR	1.26	2.25	3.81
H_2-PSE (including PSA, VP and Compression train)	1.92	7.09	18.05

LIST OF FIGURES

LIST OF TABLES

LIST OF SYMBOLS

Symbol	Description
Chemical formulation	
CH_4	Methane
CH_3OH	Methanol
CO	Carbon monoxide
CO_2	Carbon dioxide
DEPG	Dimethyl ethers of polyethylene gylcol
H_2	Hydrogen
H_2O	Water
N_2	Nitrogen
O_2	Oxygen
Abbreviations	
AEL	Alkaline electrolysis
AHP	Analytical Hierarchy Process
AIMMS	Advanced Interactive Multidimensional Modeling Systems
API	Application Programming Interface
ASU	Air separation unit
ATR	Autothermal reforming (of methane)
BOP	Balance of plant
BtX	Biomass-to-X
CAPEX	Capital expenditures
COP	Coefficient of performance
COMANDO	Component-Oriented Modeling and optimizAtion for Nonlinear Design and Operation of integrated energy systems
DM	Decision-maker
DME	Dimethyl ether
DWSIM	Daniel Wagner Simulator
ELECTRE	ÉLimination et Choix Traduisant la REalité
FAME	Fatty acid methyl ester
FLH	Full load hours
FTJ	Fischer-Tropsch to Jet
FTS	Fischer-Tropsch synthesis

Symbol	Description
FWD	Fresh water demand
GAMS	General Algebraic Modeling System
GDP	Generalized disjunctive programming
GHG	Greenhouse gases
HEFA	Hydroprocessed esters and fatty acids
HEN	Heat exchanger networ
HEX	Heat exchanger
HP-TUR	High pressure steam turbine
HRSG	Heat recovery and steam generation
HT-FTS	High temperature Fischer-Tropsch synthesis
HT-WGS	High temperature water gas shift reaction/reactor
IDE	Integrated Development Environment
IDEAS	–
LCA	Life cycle assessment
LCC	Life cycle costing
LCSA	Life cycle sustainability analysis
LP-TUR	Low pressure steam turbine
LPG	Liquified petroleum gas
LT-FTS	Low temperature Fischer-Trospch synthesis
LT-WGS	Low temperature water gas shift reaction/reactor
MADM	Multi- attribute decision making
MATLAB	MATrix LABoraty
MAUT	Multi attribute utility theory
MCDA	Multi-criteria decision-making
MCO	Multi-criteria optimization
MENA	Middle East & North Africa
MeOH	Methanol
MEREC	Method based on the Removal Effects of Criteria
MI(N)LP	Mixed-Integer (Non) linear programming
MIPSYN	–
MODM	Multi-objective decision-making
MP-TUR	Medium pressure stea turbine
MTJ	Methanol-to-Jet
NPC	Net production costs
NPE	Net production (greenhouse gas) emissions
NPFWD	Net production fresh water demand
OPEX	Operational expenditures
OUTDOOR	Open superstructure modeling and optimization framework

Symbol	Description
PE	Polyethylene
PEMEL	Polymer electrolyte membrane electrolysis
PET	Polyethlyene terephthalate
PLA	Polylactic acid
POX	Partial oxidation
PP	Polypropylene
PROCAFD	–
PROMETHEE	Preference Ranking Organization Method for Enrichment Evaluations
PSE	Process systems engineering
PtX	Power-to-X
Pyomo	Python Optimization Modeling Objects
Pyosyn	–
sLCA	Social life cycle assessment
SMART	Simple Multi-attribute Ranking Technique
SMR	Steam methane reforming
SOEL	Solid oxide electrolysis
SynFeed	H_2/CO_2 mixture
Synopsis	–
TNT	Trinitrotoluene
TOPSIS	Technique for Order Preference by Similarity to Ideal Solution
TRIR	Tri-reforming (of biogas)
WSM	Weighted sum method

Symbol	Description	Unit
Optimization model – Simple Sets		
U	All processes / Unit-operations	–
$U_{STOICH} \subseteq U$	Stoichiometric reactor unit-operations	–
$U_{YIELD} \subseteq U$	Yield reactor unit-operations	–
$U_C \subseteq U$	Unit-operations that include capital costs	–
$U_D \subseteq U$	Distributor unit-operations	–
$U_{TUR} \subseteq U_{STOICH}$	Electricity generator units (e.g. steam turbine)	–
$U_{FUR} \subseteq U_{STOICH}$	Steam generator units (e.g. combustion furnace)	–
$U_{PP} \subseteq U$	Product pool units	–
$U_S \subseteq U$	Raw material sources	–
UT	Utilities	–
$HUT \subseteq UT$	Heating and cooling utilities	

Symbol	Description	Unit
I	Chemical components	–
P	Fixed interval grid points for piece-wise linearization	–
$PI \subseteq P$	Fixed intervals for piece-wise linearization	–
$M \subseteq I$	Reactants	–
R	Reactions	–
HI	Heat intervals	–
$HI^M \subseteq HI$	Highest heat interval	–
$HI^{HP,IN}$ $HI^{HP,OUT} \subseteq HI$	Heat interval for heat pump inlet and outlet temperature	–
$G_{G1}\ G_{G2}$	Unit-operations of group 1 (connected processes) and 2 (conditional processes) for logic constraints	–

Optimization model – Complex sets

$U_{SP} \subseteq U_S \cdot U$	Combinatorial set of connected raw material source and target unit operation (u_s, u)	–
$UI_{INERT} \subseteq U \cdot I$	Combinatorial set of inert chemical components i in yield reactor unit-operation u (u, i)	–
UK_D $\subseteq (U \cdot U), UK$	Combinatorial set of k-th amount distribution from unit-operation u to u' (u, u', u, k)	–
$U_{DIST} \subseteq U_D \cdot U$	Combinatorial set of allowed distributor–target unit-operations combinations (u, u')	–
$UK \subseteq U \cdot K$	Base set of available k shares for distributor u (u, k)	–

Optimization model – Parameters

Roman

b^{HEN}	Minimum annual heat exchanger capital costs	M€
cap^{PROD}	Desired yearly capacity of main product	t/a
c_u^{RE}	Percentage value of periodic capital costs in unit-operation $u \in U_C$	–
cop^{HP}	Coefficient of performance of heat pump	–
con_u	Required concentration factor in unit-operation $u \in U$	t/t
crf_u^{UNITS}	Annualization factor for unit-operation $u \in U_C$	1/a
crf^{HP}	Annualization factor for heat pump	1/a
$d_{u,k}^{DIST}$	Distribution share of k'th part in unit-operation $u \in U_{DIST}$	–
ec^{HP}	Linear equipment costs of heat pump	€/kW
f_u^{DC}	Direct cost factor for unit-operation $u \in U_C$	–
f_u^{IDC}	Indirect cost factor for unit-operation $u \in U_C$	–
$f_u^{O\&M}$	Operating and maintenance cost factor for unit operation $u \in U_C$	1/a
flh_u	Yearly full load hours of unit-operation $u \in U$	h/a
fwd^{HEAT}	Fresh water demand of heat / steam	t_{H_2O}/MWh
$fwd_{u_{pp}}^{POOL}$	Avoided burden fresh water demand of products $u \in U_{PP}$	t_{H_2O}/t
$fwd_{u_s}^{SOURCE}$	Fresh water demand of raw materials $u \in U_S$	t_{H_2O}/t
fwd_{ut}^{UT}	Fresh water demand of utilities $u \in UT \notin HUT$	t_{H_2O}/MWh

Symbol	Description	Unit
$f(x)_{k,u}$	Pre-calculated Equipment costs of unit-operation $u \in U_C$ in linear interval k	M€
gwp_i	Global warming potential of component $i \in I$	$t_{CO_2-eq.}/t$
gwp^{HEAT}	Global warming potential of external steam	$t_{CO_2-eq.}/MWh$
gwp_u^{POOL}	Avoided burden global warming potential of products in product pool $u \in U_{PP}$	$t_{CO_2-eq.}/t$
gwp_u^{SOURCE}	Global warming potential of raw material sources $u \in U_S$	$t_{CO_2-eq.}/t$
gwp_{ut}^{UT}	Global warming potential of external utilities $ut \in UT \notin HUT$	$t_{CO_2-eq.}/MWh$
hr	General full load operating hours per year	h/a
lhv_i	Lower heating value of component $i \in I$	MWh/t
mw_u	Molecular weight of chemical component i	t/kmole
m^{HEN}	Slope for cost calculation of virtual heat exchanger	M€/MW
n_u^{RE}	Number of periodic turnovers $u \in U_C$	–
uc	Unit converting energy	MWh/MJ
ul_u^1 / ul_u^2	Upper limits for added flows 1 and 2 in unit-operation $u \in U_S$	t/h
$x_{k,u}$	Pre-calculated reference flows for non-linear EC calculation $u \in U_C$	Case specific

Greek

Symbol	Description	Unit
α_u	Upper bound parameter for Big-M constraint $u \in U$	t/h
α^{HEX}	Upper bound paramter or Big-M constraint in HEX calculation	MW
$\beta_{u,ut,hi}^H$	Energy demand ration of unit-operation u in heat interval hi and heat ut $u \in U, ut \in HUT, hi \in HI$	MW
$\gamma_{i,r,u}$	Stoichiometric reaction coefficient of component i, reaction r, unit u $u \in U_{STOICH}, i \in I, r \in R$	t
δ^{COOL}	Cooling water price	€/MWh
δ^{EL}	Electricity price	€/MWh
δ_{hi}^{HEAT}	Steam price for heat interval $hi \in HI$	€/MWh
δ_u^{PP}	Product price of product pool $u \in U_{PP}$	€/t
$\delta_{u_s}^{RM}$	Raw material costs of component $u \in U_S$	€/t
$\zeta_{u,i}$	Yield factor of unit-operation $u \in U_{YIELD}$ and component, $i \in I \notin UI_{INERT}$	–
$\eta_u^{EL} / \eta_u^{HEAT}$	Efficiency of electricity $u \in U_{TUR}$ / heat generation in generator $u \in U_{FUR}$	–
$\theta_{m,r,u}$	Stoichiometric conversion factor of reactant m, reaction r, unit $u \in U_{STOICH}, m \in M, r \in R$	–
$\kappa_{u,i}^{1,CAPEX}$	Binary parameter for component $i \in I$ in equipment cost calc. of unit $u \in U_C$	–
$\kappa_{u,i}^{1,RHS} / \kappa_{u,i}^{1,LHS}$	Binary parameter for component i in concentration calc. of unit $u \in U, i \in I$	–
$\kappa_{u,i}^{2,RHS} / \kappa_{u,i}^{2,LHS}$	Integer parameter that decides on concentration calculation mode $u \in U, i \in I$	
$\kappa_{ut\,u,i}^{1,UT}$	Binary parameter for component $i \in I$ in heat calc. of unit $u \in U, ut \in UT$	–
$\mu_{u,u',i}$	Split factor of unit-operation $u \in U$, to unit-operation $u' \in U$, component $i \in I$, $(u,u') \notin U_{DIST}$	–

Symbol	Description	Unit
$\varphi_{u_s,i}$	Concentration of component $i \in I$ in raw material source $u \in U_S$	–
$\tau_{ut,u}^{COOL}$	Specific cooling demand $ut \in HUT, u \in U$	MWh/[unit specific]
$\tau_{ut,u}^{HEAT}$	Specific heat demand $ut \in HUT, u \in U$	MWh/[unit specific]
$\tau_{ut,u}^{UT}$	Specific utility demand of unit-operation $ut \in UT \notin HUT, u \in U$	MWh/[unit specific]

Optimization model – Variables

ACC_u	Annualized capital costs of unit-operation u	M€/a
ACC_{hi}^{HEN}	Annualized capital costs of virtual heat exchanger on heat interval hi	M€/a
ACC^{HP}	Annualized costs of heat pump	M€/a
ACC_u^{RE}	Periodical recurring costs of unit-operation u	M€/a
$CAPEX$	Total annualized capital costs	M€/a
$C^{COOLING}$	Costs for total cooling demand	M€/a
C^{HEAT}	Costs for total external heating demand	M€/a
C_{ut}^{UT}	Costs for utility demand other than heat and cooling	M€/a
$C^{UT,TOT}$	Total costs for external utilities	M€/a
$C^{O\&M}$	Operating and Maintenance costs	M€/a
C_u^{RM}	Total Costs for raw materials	M€/a
C^{UT}	Costs for utilities	
EC_u	Purchase equipment costs of unit-operation u	M€
$E_{u,ut}^{UT}$	Utility demand of unit-operation u and utility ut	MW
$E^{EL,HP}$	Electricity demand of heat pump	MW
$E_u^{EL,PROD}$	Electricity produced in unit-operation u	MW
E_{ut}^{TOT}	Total utility demand of the plant	MW
$F_{u',u,i}$	Flow from unit operation u' to u of component i	t/h
FCI_u	Fixed capital investment of unit operation u	M€
$F_{u_s,u}^{ADD}$	Flow from raw material source to target process	t/h
$F_{u,i}^{ADD,TOT}$	Total externally added component i to unit-operation u	t/h
$F_{(uu'),(u,k),i}^{DIST}$	Slack variable for *k*-th flow of *I* from *u* to *u'*	t/h
$F_{u,i}^{IN}$	Inlet flow of unit-operation u, component i	t/h
$F_{u,i}^{OUT}$	Outlet flow of unit-operation u, component i	t/h
$F_{u_s}^{SOURCE}$	Total demand of raw material source	t/h
$F_{u,i}^{WASTE}$	Waste flow of unit-operation u, component i	t/h
$F_i^{WASTE,TOT}$	Total waste flow of component i	t/h
$GWP^{CAPTURE}$	CO₂ emissions captured by capture technologies	$t_{CO_2-eq.}$/a
GWP^{HEAT}	Global warming potential for heating	$t_{CO_2-eq.}$/a
GWP_{ut}^{UT}	Global warming potential of utilities other than heating	$t_{CO_2-eq.}$/a

Symbol	Description	Unit
$GWP^{UT,TOT}$	CO_2 emissions induced from utilities	$t_{CO_2-eq.}/a$
$GWP^{EMITTED}$	CO_2 emissions induced by unit operations	$t_{CO_2-eq.}/a$
$GWP^{CREDITS}$	CO_2 emissions induced by external heat supply	$t_{CO_2-eq.}/a$
M_u^{CAPEX}	Reference flow for CAPEX calculation in unit-operation u	Case specific
$M_u^{REF,UT}$	Reference flow for utility demand calculation of unit-operation u	Case specific
$NPFWD$	Net present fresh water demand	t_{H_2O}/a
FWD^{RM}	Fresh water demand from raw materials	t_{H_2O}/a
$FWD^{UT,TOT}$	Fresh water demand from utilities	t_{H_2O}/a
FWD^{HEAT}	Fresh water demand from heating	t_{H_2O}/a
FWD_{ut}^{UT}	Fresh water demand for utilities other than heating	t_{H_2O}/a
$FWD^{CREDITS}$	Fresh water credits for avoided burdens	t_{H_2O}/a
$OPEX$	Total annual operational costs	€/a
$PROFITS$	Total annual profits	€/a
$Q_{u,hi}^{C}$	Cooling demand of unit-operation u on heat interval hi	MW
Q^{COOL}	Total external cooling demand	MW
Q_{hi}^{DEFI}	Heat deficit on heat interval hi	MW
Q_{hi}^{EX}	Exchanged heat on heat interval hi	MW
$Q_{u,hi}^{H}$	Heat demand of unit-operation u on heat interval hi	MW
Q^{HP}	Waste heat absorbed by heat pump	MW
$Q^{HP,USE}$	Used heat from heat pump	MW
Q_u^{PROD}	Produced super-heated steam by unit-operation u	MW
$Q^{PROD,SELL}$	Produced super-heated steam that is sold to market	MW
$Q^{PROD,USE}$	Produced super-heated steam that is used internally for heat supply	MW
Q_{hi}^{RESI}	Residual heat on heat interval hi	MW
$S_{u,k}^{CAPEX}$	S – Variable for SOS2 Constraint	–
Y_u	Binary decision variable of unit-operation u	
$Y_{(u,u'),(u,k)}^{DIST}$	Binary decision variable for k -th flow from u to u'	–
Y_{hi}^{HEX}	Binary decision variable for heat exchanger on heat interval hi	–
$Z_{u,k}^{CAPEX}$	Z – Variable for SOS2 Constraint	–
$\lambda_{k,u}$	Lambda-Variable for piece-wise linearization	–

Further symbols

$a_{i,j}$	Entry of comparison matrix of row i and column j	–
$CECPI$	Chemical engineering plant index of the investigated year	–
$CECPI_u^{REF}$	Reference CECPI of a known unit-operation u	–
C_{MTJ}	Costs of methanol-to-jet process	$€/t_{Jet}$
C_u^{REF}	Known reference costs of unit-operation u	M€

Symbol	Description	Unit
C_t	Relative closeness factor of technology t	–
D_t^+ / D_t^-	Manhatten distance of technology t to best and worst solution	–
el	Exemplary variable for representation of OUTDOORs translation functions	–
f_u	Exponent for non-linear equipment cost calculation in unit-operation u	–
IN	Exemplary variable for representation of OUTDOORs translation functions	–
ir	Interest rate	–
lt_u	Lifetime in years of unit-operation $u \in U_C$	h/a
$lt_u^{RE,y}$ / $lt_u^{RE,h}$	Period of time (in years or hours) for periodic costs in unit-operation $u \in U_C$	a / h
M_u^{REF}	Reference flow of a known unit-operation u equipment cost calculation	Case specific
OUT	Exemplary variable for representation of OUTDOORs translation functions	–
sp	Exemplary variable for representation of OUTDOORs translation functions	–
T_{hi}	Grid temperature of heat interval hi	°C
ΔT_u	Difference of inlet and outlet temperature in unit-operation u	K
U	Thermal transmittance value	W/m²K
V_i^+ / V_i^-	Best and worst normalized, weighted value score of criterion i	–
$V_{t,i}$	Normalized and weighted value score of technology t and criterion i	–
$v_{t,i}$	Normalized value score of technology t and criterion i	–
$V_{t,i}^O$	Reformulated objective variable for technology /process pathway t and criterion i, including normalization and weighting	–
w_i	Weighting factor of criterion i	–
w_i^{norm}	Normalized weighting factor of criterion i	–
$x_{t,i}$	Calculated value of technology t and criterion i	–
x_i^{MAX}	Maximum value of criterion i, from given solutions	–
x_i^{MIN}	Minimal value of criterion i, from given solutions	–

REFERENCES

[1]   "Bundesregierung   CO2   Ziel."   [Online].   Available:
        https://www.bundesregierung.de/breg-de/themen/energiewende/co2-
        kohlenstoffdioxid-oder-kohlendioxid-emission-614692. [Accessed: 12-May-
        2021].

[2]   "Umweltbundesamt   Trendtabelle   Sektoren."   [Online].   Available:
        https://www.umweltbundesamt.de/dokument/trendtabelle-sektoren-
        vorlaeufige-thg-daten-2019. [Accessed: 12-May-2021].

[3]   Umweltbundesamt, "Berichterstattung unter der Klimarahmenkonvention
        der Vereinten Nationen und dem Kyoto-Protokoll 2020 Nationaler," *Clim.
        Chang. | 22/2020*, vol. 22, no. 2020, p. 1004, 2019.

[4]   J. G. Speight, *Handbook of Industrial Hydrocarbon Processes*. 2019.

[5]   P. R. R. Chang Samuel Hsu, *Handbook of Petroleum Technology*. 2017.

[6]   W. Langhoff, "MWV - Jahresbericht 2020," 2020.

[7]   D. S. . Jones and P. R. Pujado, *Handbook of Petroleum Processing*. 2006.

[8]   K. Wagemann and F. Ausfelder, "E-Fuels - Mehr als eine Option,"
        DECHEMA e.V. - Whitepaper, 2017.

[9]   R. A. Lee and J. M. Lavoie, "From first- to third-generation biofuels:
        Challenges of producing a commodity from a biomass of increasing
        complexity," *Anim. Front.*, vol. 3, no. 2, pp. 6–11, 2013.

[10]   A. Buttler and H. Spliethoff, "Current status of water electrolysis for energy
        storage, grid balancing and sector coupling via power-to-gas and power-to-
        liquids: A review," *Renew. Sustain. Energy Rev.*, vol. 82, no. February, pp.
        2440–2454, 2018.

[11]   M. Sterner and I. Stadler, *Energiespeicher-Bedarf, Technologien, Integration*.
        2014.

[12]   ENCON.Europe GmbH, "Potentialatlas für Wasserstoff - Analyse des
        Marktpotentials für Wasserstoff, der mit erneuerbaren Strom hergestellt
        wird, im Raffineriesektor und im zukünftigen Mobilitätssektor," p. 64, 2018.

[13]   P. Bains, P. Psarras, and J. Wilcox, "CO2 capture from the industry sector,"
        Prog. Energy Combust. Sci., vol. 63, pp. 146–172, 2017.

[14]   O. Abass A, "CO2 capture and separation technologies for end-of-pipe
        applications - A review," *Energy*, 2010.

[15]   M. Bertau, H. Offermanns, L. Plass, F. Schmidt, and H. J. Wernicke,
        *Methanol: The basic chemical and energy feedstock of the future: Asinger's vision
        today*. 2014.

[16] F. J. Keil, "Methanol-to-hydrocarbons: Process technology," *Microporous Mesoporous Mater.*, vol. 29, no. 1–2, pp. 49–66, 1999.

[17] M. R. Gogate, "Methanol-to-olefins process technology: current status and future prospects," *Pet. Sci. Technol.*, vol. 37, no. 5, pp. 559–565, 2019.

[18] W. Von Liebner and M. Wagner, "MtSynfuels®, die effiziente und wirtschaftliche Alternative zu Fischer-Tropsch-Treibstoffen," *Erdoel Erdgas Kohle*, vol. 120, no. 10, pp. 323–326, 2004.

[19] S. S. Ail and S. Dasappa, "Biomass to liquid transportation fuel via Fischer Tropsch synthesis - Technology review and current scenario," *Renew. Sustain. Energy Rev.*, vol. 58, pp. 267–286, 2016.

[20] I. Lewandoswki, *Bioeconomy: Shaping the Transition to a Sustainable, Biobased Economy*. Springer, 2018.

[21] B. Kamm, P. R. Gruber, and M. Kamm, *Handbook of Fuels Beyond Oil and Gas : The Methanol Economy Bailey ' s Industrial Oil and Fat Products Oil Refineries in the 21st Century*, vol. 1. 2006.

[22] R. Y. Chein and W. H. Hsu, "Analysis of syngas production from biogas via the tri-reforming process," *Energies*, vol. 11, no. 5, 2018.

[23] X. Zhao, B. Joseph, J. Kuhn, and S. Ozcan, "Biogas Reforming to Syngas: A Review," *iScience*, vol. 23, no. 5, p. 101082, 2020.

[24] J. Gong and F. You, "Value-added chemicals from microalgae: Greener, more economical, or both?," *ACS Sustain. Chem. Eng.*, vol. 3, no. 1, pp. 82–96, Jan. 2015.

[25] K. W. Chew *et al.*, "Microalgae biorefinery: High value products perspectives," *Bioresour. Technol.*, vol. 229, pp. 53–62, 2017.

[26] Y. S. Jang *et al.*, "Bio-based production of C2-C6 platform chemicals," *Biotechnol. Bioeng.*, vol. 109, no. 10, pp. 2437–2459, 2012.

[27] World commission on Environment and Developement, "Our common future," Oxford, 1987.

[28] J. Ren, *Energy Systems Evaluation (Volume 2)*, vol. 1, no. Volume 1. 2021.

[29] R. Horne, T. Grant, and K. Verghese, "Life cycle assessment: principles, practice, and prospects," 2009.

[30] E. N. Pistikopoulos *et al.*, "Process systems engineering – The generation next?," *Comput. Chem. Eng.*, vol. 147, p. 107252, 2021.

[31] R. W. H. Sargent, "Advances in modelling and analysis of chemical process systemes," *Comput. Chem. Eng.*, vol. 7, no. 4, pp. 219–237, 1983.

[32] I. E. Grossmann and A. W. Westerberg, "Research challenges in Process Systems Engineering," *AIChE J.*, vol. 46, no. 9, pp. 1700–1703, 2000.

[33] L. Mencarelli, Q. Chen, A. Pagot, and I.- Grossmann, "A review on superstructure optimization approaches in process system engineering," *Comput. Chem. Eng.*, p. 106808, 2020.

[34] J. Burre, D. Bongartz, and A. Mitsos, "Comparison of MINLP formulations

for global superstructure optimization," *Optim. Eng.*, no. 0123456789, 2022.

[35]   T. Umeda, A. Hirai, and A. Ichikawa, "Synthesis of optimal processing system by an integrated appraoch," *Chem. Eng. Sci.*, vol. 27, no. 4, pp. 795--807, 1972.

[36]   E. Zondervan, M. Nawaz, A. B. de Haan, J. M. Woodley, and R. Gani, "Optimal design of a multi-product biorefinery system," *Comput. Chem. Eng.*, vol. 35, no. 9, pp. 1752–1766, 2011.

[37]   H. Yeomans and I. E. Grossmann, "A systematic modeling framework of superstructure optimization in process synthesis," *Comput. Chem. Eng.*, vol. 23, no. 6, pp. 709–731, Jun. 1999.

[38]   M. O. Bertran, R. Frauzem, A. S. Sanchez-Arcilla, L. Zhang, J. M. Woodley, and R. Gani, "A generic methodology for processing route synthesis and design based on superstructure optimization," *Comput. Chem. Eng.*, vol. 106, pp. 892–910, 2017.

[39]   A. Quaglia, C. L. Gargalo, S. Chairakwongsa, G. Sin, and R. Gani, "Systematic network synthesis and design : Problem formulation , superstructure generation , data management and solution," *Comput. Chem. Eng.*, vol. 72, pp. 68–86, 2015.

[40]   I. E. Grossmann and R. W. H. Sargent, "Optimium design of heat exchanger networks," *Comput. Chem. Eng.*, vol. 2, no. 1, pp. 1--7, 1978.

[41]   G. R. Kocis and I. E. Grossmann, "A modelling and decomposition strategy for the minlp optimization of process flowsheets," *Comput. Chem. Eng.*, vol. 13, no. 7, pp. 797--819, 1989.

[42]   A. R. Ciric and C. A. Floudas, "Heat exchanger network synthesis without decomposition," *Comput. Chem. Eng.*, vol. 15, no. 6, pp. 385–396, Jun. 1991.

[43]   T. F. Yee and I. E. Grossmann, "Simultaneous optimization models for heat integration-II. Heat exchanger network synthesis," *Comput. Chem. Eng.*, vol. 14, no. 10, pp. 1165–1184, Oct. 1990.

[44]   C. Galanopoulos, P. Kenkel, and E. Zondervan, "Superstructure optimization of an integrated algae biorefinery," *Comput. Chem. Eng.*, vol. 130, p. 106530, 2019.

[45]   J. M. Restrepo-Flórez and C. T. Maravelias, "Advanced fuels from ethanol- a superstructure optimization approach," *Energy Environ. Sci.*, vol. 14, no. 1, pp. 493–506, 2021.

[46]   D. Krone, E. Esche, N. Asprion, M. Skiborowski, and J. U. Repke, *Conceptual Design Based on Superstructure Optimization in GAMS with Accurate Thermodynamic Models*, vol. 48, no. Dll. Elsevier Masson SAS, 2020.

[47]   W. R. Huster, A. M. Schweidtmann, J. T. Lüthje, and A. Mitsos, "Deterministic global superstructure-based optimization of an organic Rankine cycle," *Comput. Chem. Eng.*, vol. 141, p. 106996, 2020.

[48]   H. W. Lee *et al.*, "Toward the practical application of direct CO_2 hydrogenation technology for methanol production," *Int. J. Energy Res.*, vol.

44, no. 11, pp. 8781–8798, 2020.

[49] A. Maggi, M. Wenzel, and K. Sundmacher, "Mixed-Integer Linear Programming (MILP) Approach for the Synthesis of Efficient Power-to-Syngas Processes," *Front. Energy Res.*, vol. 8, no. September, 2020.

[50] O. Onel, A. M. Niziolek, J. A. Elia, R. C. Baliban, and C. A. Floudas, "Biomass and natural gas to liquid transportation fuels and olefins (BGTL+C2-C4): Process synthesis and global optimization," *Ind. Eng. Chem. Res.*, vol. 54, no. 1, pp. 359–385, 2015.

[51] A. M. Niziolek, O. Onel, J. A. Elia, R. C. Baliban, and C. A. Floudas, "Coproduction of liquid transportation fuels and C6_C8 aromatics from biomass and natural gas," *AIChE J.*, 2015.

[52] R. C. Baliban, J. A. Elia, V. Weekman, and C. A. Floudas, "Process synthesis of hybrid coal, biomass, and natural gas to liquids via Fischer-Tropsch synthesis, ZSM-5 catalytic conversion, methanol synthesis, methanol-to-gasoline, and methanol-to-olefins/distillate technologies," *Comput. Chem. Eng.*, 2012.

[53] L. Kong, S. M. Sen, C. A. Henao, J. A. Dumesic, and C. T. Maravelias, "A superstructure-based framework for simultaneous process synthesis, heat integration, and utility plant design," *Comput. Chem. Eng.*, vol. 91, pp. 68–84, 2016.

[54] T. F. Yee, I. E. Grossmann, and Z. Kravanja, "Simultaneous optimization models for heat integration-I. Area and energy targeting and modeling of multi-stream exchangers," *Comput. Chem. Eng.*, vol. 14, no. 10, pp. 1151–1164, Oct. 1990.

[55] A. K. Tula, D. K. Babi, J. Bottlaender, M. R. Eden, and R. Gani, "A computer-aided software-tool for sustainable process synthesis-intensification," *Comput. Chem. Eng.*, vol. 105, pp. 74–95, 2017.

[56] Z. Kravanja and I. E. Grossmann, "Prosyn-an MINLP process synthesizer," *Comput. Chem. Eng.*, vol. 14, no. 12, pp. 1363–1378, Dec. 1990.

[57] Y. Tian, M. Sam Mannan, Z. Kravanja, and E. N. Pistikopoulos, "Towards the synthesis of modular process intensification systems with safety and operability considerations - application to heat exchanger network," in *Computer Aided Chemical Engineering*, vol. 43, Elsevier B.V., 2018, pp. 705–710.

[58] Q. Chen *et al.*, "Pyosyn: A Collaborative Ecosystem for Process Design Advancement," *AIChE Annu. Meet.*, vol. AIChE, 2019.

[59] F. Friedler, K. . Aviso, B. Bertok, D. C. Foo, and T. R.R., "Prospects and challenges for chemical process synthesis with P-graph," *Curr. Opin. Chem. Eng.*, vol. 26, pp. 58–64, 2019.

[60] Q. Chen, Y. Liu, G. Seastream, J. D. Siirola, and I. E. Grossmann, "Pyosyn: A new framework for conceptual design modeling and optimization," *Comput. Chem. Eng.*, vol. 153, 2021.

[61] M. Langiu *et al.*, "COMANDO: A Next-Generation Open-Source

Framework for Energy Systems Optimization," *Comput. Chem. Eng.*, vol. 152, pp. 1–24, 2021.

[62]   J. Steimel and S. Engell, "Conceptual design and optimization of chemical processes under uncertainty by two-stage programming," *Comput. Chem. Eng.*, vol. 81, pp. 200–217, 2015.

[63]   J. Steimel, M. Harrmann, G. Schembecker, and S. Engell, "A framework for the modeling and optimization of process superstructures under uncertainty," *Chem. Eng. Sci.*, vol. 115, pp. 225–237, 2014.

[64]   N. V. Sahinidis, "Optimization under uncertainty: State-of-the-art and opportunities," *Comput. Chem. Eng.*, vol. 28, no. 6–7, pp. 971–983, 2004.

[65]   G. Mavrotas, K. Florios, and D. Vlachou, "Energy planning of a hospital using Mathematical Programming and Monte Carlo simulation for dealing with uncertainty in the economic parameters," *Energy Convers. Manag.*, vol. 51, no. 4, pp. 722–731, 2010.

[66]   A. Ishizaka and P. Nemery, *Multi-criteria decision analysis: methods and software*. 2013.

[67]   S. Greco, J. Figueira, and M. Ehrgott, *Multiple criteria decision analysis*. 2016.

[68]   O. Erdinc and M. Uzunoglu, "Optimum design of hybrid renewable energy systems: Overview of different approaches," *Renew. Sustain. Energy Rev.*, vol. 16, no. 3, pp. 1412–1425, 2012.

[69]   E. Løken, "Use of multicriteria decision analysis methods for energy planning problems," *Renew. Sustain. Energy Rev.*, vol. 11, no. 7, pp. 1584–1595, 2007.

[70]   Q. Kong and N. Shah, "Development of an Optimization-Based Framework for Simultaneous Process Synthesis and Heat Integration," *Ind. Eng. Chem. Res.*, vol. 56, no. 17, pp. 5000–5013, May 2017.

[71]   J. Bisschop, "AIMMS Modeling Guide - Integer Programming Tricks," 2016.

[72]   R. Morrison, "SOS2 constraints in GLPK," *http://winglpk.sourceforge.net/media/glpk-sos2_02.pdf*, 2008. .

[73]   M. S. Peters, K. D. Timmerhaus, and R. E. West, *Plant Design and Economics for Chemical Engineers*, Fifth Edit. New York: McGraw-Hill, 2003.

[74]   P. Kenkel, T. Wassermann, C. Rose, and E. Zondervan, "A generic superstructure modeling and optimization framework on the example of bi-criteria Power-to-Methanol process design," *Comput. Chem. Eng.*, vol. 150, p. 107327, 2021.

[75]   J. J. Wang, Y. Y. Jing, C. F. Zhang, and J. H. Zhao, "Review on multi-criteria decision analysis aid in sustainable energy decision-making," *Renew. Sustain. Energy Rev.*, vol. 13, no. 9, pp. 2263–2278, 2009.

[76]   M. Keshavarz-Ghorabaee, M. Amiri, E. K. Zavadskas, Z. Turskis, and J. Antucheviciene, "Determination of objective weights using a new method based on the removal effects of criteria (Merec)," *Symmetry (Basel).*, vol. 13, no. 4, pp. 1–20, 2021.

[77] T. L. Saaty, "The analytic hierarchy process: planning, priority setting, resource allocation.," *McGraw-Hill*, 1980.

[78] A. Breiing and R. Knosala, *Bewerten technischer Systeme: Theoretische und methodische Grundlagen bewertungstechnischer Entscheidungshilfen*. Springer Berlin Heidelberg, 1997.

[79] T. L. Saaty, "A scaling method for priorities in hierarchical structures," *J. Math. Psychol.*, vol. 15, no. 3, pp. 234–281, 1977.

[80] N. Vafaei, R. A. Ribeiro, and L. M. Camarinha-Matos, "Normalization techniques for multi-criteria decision making: Analytical hierarchy process case study," *IFIP Adv. Inf. Commun. Technol.*, vol. 470, pp. 261–268, 2016.

[81] T. M. Lakshmi and V. P. Venkatesan, "A Comparison of various normalization in techniques for order performance by similarity to ideal solution (TOPSIS)," *Int. J. Comput. Algorithm*, vol. 3, pp. 882–888, 2014.

[82] T. Wassermann, C. Schnuelle, P. Kenkel, and E. Zondervan, "Power-to-Methanol at Refineries as a Precursor to Green Jet Fuel Production: a Simulation and Assessment Study," in *Computer Aided Chemical Engineering*, vol. 48, Elsevier B.V., 2020, pp. 1453–1458.

[83] C. N. Hamelinck and A. P. C. Faaij, "Future prospects for production of methanol and hydrogen from biomass," *J. Power Sources*, vol. 111, no. 1, pp. 1–22, 2002.

[84] M. Rivarolo, D. Bellotti, L. Magistri, and A. F. Massardo, "Feasibility study of methanol production from different renewable sources and thermo-economic analysis," *Int. J. Hydrogen Energy*, vol. 41, no. 4, pp. 2105–2116, 2016.

[85] G. A. Olah, A. Goeppert, and G. K. S. Prakash, *Beyond Oil and Gas: The Methanol Economy: Second Edition*. Weinheim, Germany: Wiley-VCH Verlag GmbH & Co. KGaA, 2009.

[86] M. Fasihi, O. Efimova, and C. Breyer, "Techno-economic assessment of CO2 direct air capture plants," *J. Clean. Prod.*, 2019.

[87] M. Voldsund *et al.*, "Comparison of technologies for CO 2 capture from cement production—Part 1: Technical evaluation," *Energies*, vol. 12, no. 3, 2019.

[88] S. O. Gardarsdottir *et al.*, "Comparison of technologies for CO 2 capture from cement production—Part 2: Cost analysis," *Energies*, vol. 12, no. 3, 2019.

[89] J. Proost, "State-of-the art CAPEX data for water electrolysers, and their impact on renewable hydrogen price settings," *Int. J. Hydrogen Energy*, vol. 44, no. 9, pp. 4406–4413, Feb. 2019.

[90] T. Smolinka *et al.*, "Industrialisierung der Wasserelektrolyse in Deutschland: Chancen und Herausforderungen für nachhaltigen Wasserstoff für Verkehr," *Strom und Wärme, Natl. Organ. Wasserstoff-und Brennstoffzellentechnologie (NOW GmbH)*, 2018.

[91] L. Wang *et al.*, "Power-to-fuels via solid-oxide electrolyzer: Operating window and techno-economics," *Renew. Sustain. Energy Rev.*, vol. 110, pp. 174–187, Aug. 2019.

[92] Umweltbundesamt, "Optionen für Biogas-Bestandanlagen bis 2030 aus ökonomischer und energiewirtschaftlicher Sicht," 2020.

[93] V. Spallina, D. Pandolfo, A. Battistella, M. C. Romano, M. Van Sint Annaland, and F. Gallucci, "Techno-economic assessment of membrane assisted fluidized bed reactors for pure H2 production with CO2 capture," *Energy Convers. Manag.*, vol. 120, pp. 257–273, 2016.

[94] F. G. Albrecht, D. H. König, N. Baucks, and R. Dietrich, "A standardized methodology for the techno-economic evaluation of alternative fuels – A case study," *Fuel*, vol. 194, pp. 511–526, 2017.

[95] T. Wassermann, H. Mühlenbrock, P. Kenkel, J. Thöming, and E. Zondervan, "Optimization of hydrogen supply from renewable electricity including cavern storage," *Phys. Sci. Rev.*, p. Submitted, 2022.

[96] G. Wernet, C. Bauer, B. Steubing, J. Reinhard, E. Moreno-ruiz, and B. Weidema, "The ecoinvent database version 3 (part I): overview and methodology," *Int. J. Life Cycle Assess.*, vol. 3, pp. 1218–1230, 2016.

[97] Fraunhofer ISE, "Stromgestehungskosten Erneuerbare Energien," 2021.

[98] "Methanex," *"Durchschnittlicher Preis für Methanol auf dem europäischen Markt in den Jahren von 2012 bis 2019 (in Euro je Tonne)." Chart. 19. November, 2019. Statista. Zugegriffen am 26. November 2019: https://de.statista.com/statistik/daten/studie/*, 2019. .

[99] R. Turton, R. C. Bailie, and W. B. Whiting, *Analysis, synthesis, and design of chemical processes*, vol. 36, no. 02. 1998.

[100] F. Schimek *et al.*, "Gutachten H2-Erzeugung und Märkte Schleswig-Holstein," 2021.

[101] M. A. Adnan and M. G. Kibria, "Comparative techno-economic and life-cycle assessment of power-to-methanol synthesis pathways," *Appl. Energy*, vol. 278, no. September, p. 115614, 2020.

[102] Verband der Chemischen Industrie e.V., "Chemiewirtschaft In Zahlen 2020," *Verband der Chem. Ind. e.V.*, no. 62, pp. 1–177, 2020.

[103] "Thyssenkrupp Methanolanlagen." [Online]. Available: https://www.thyssenkrupp-industrial-solutions.com/de/produkte-und-services/chemische-anlagen-und-prozesse/methanol-plants/. [Accessed: 06-May-2022].

[104] D. P. Minh *et al.*, *Hydrogen production from biogas reforming: An overview of steam reforming, dry reforming, dual reforming, and tri-reforming of methane.* Elsevier Ltd., 2018.

[105] Umweltbundesamt, "PRTR-Gesamtdatenbestand. Pollutant Release and Transfer Register," 2020. [Online]. Available: https://www.thru.de/thrude/downloads/. [Accessed: 06-May-2022].

[106] S. Block and P. Viebahn, "Direct Air Capture (DAC) in Germany: resource implications of a possible rollout in 2045," *Ann. des Mines - Responsab. Environ.*, vol. 105, no. 1, pp. 78–82, 2022.

[107] Prognos, Öko-Institut, and Wuppertal-Institut, "Klimaneutrales Deutschland. Studie im Auftrag von Agora Energiewende, Agora Verkehrswende und Stiftung Klimaneutralität," 2020.

[108] D. H. König, "Techno-ökonomische Prozessbewertung der Herstellung synthetischen Flugturbinentreibstoffes aus CO2 und H2," 2016.

[109] R. Davis, J. Markham, C. Kinchin, N. Grundl, E. Tan, and D. Humbird, "Process Design and Economics for the Production of Algal Biomass: Algal Biomass Production in Open Pond Systems and Processing Through Dewatering for Downstream Conversion," *Natl. Renew. Energy Lab.*, no. February, p. 128, 2016.

[110] J. Lorenzen *et al.*, "Extraction of microalgae derived lipids with supercritical carbon dioxide in an industrial relevant pilot plant," *Bioprocess Biosyst. Eng.*, vol. 40, no. 6, pp. 911–918, 2017.

[111] A. C. Apel *et al.*, "Open thin-layer cascade reactors for saline microalgae production evaluated in a physically simulated Mediterranean summer climate," *Algal Res.*, vol. 25, no. May, pp. 381–390, 2017.

[112] F. A. Fernández, J. M. F. Sevilla, and E. M. Grima, "Cost analysis of microalgae production," in *Biofuels from algae*, Elsevier, 2019, pp. 551–566.

[113] S. Nagarajan, S. K. Chuo, S. Cao, C. Wu, and Z. Zhou, "An updated comprehensive techno-economic analysis of algae biodiesel," *Bioresour. Technol.*, vol. 145, pp. 150--156, 2013.

[114] J. R. Benemann and W. J. Oswald, "Systems and economic analysis of microalgae ponds for conversion of CO2 to biomass. Final report," 1996.

[115] D. Klein-Marcuschamer *et al.*, "Technoeconomic analysis of renewable aviation fuel from microalgae, Pongamia pinnata, and sugarcane," *Biofuels, Bioprod. Biorefining*, vol. 7, no. 4, pp. 416–428, Jul. 2013.

[116] F. Capra, F. Magli, and M. Gatti, "Biomethane liquefaction: A systematic comparative analysis of refrigeration technologies," *Appl. Therm. Eng.*, vol. 158, no. January, p. 113815, 2019.

[117] M. M. F. Hasan, R. C. Baliban, J. A. Elia, and C. A. Floudas, "Modeling, Simulation, and Optimization of Postcombustion CO 2 Capture for Variable Feed Concentration and Flow Rate. 2. Pressure Swing Adsorption and Vacuum Swing Adsorption Processes," *Ind. Eng. Chem. Res.*, vol. 51, no. 48, pp. 15665–15682, Dec. 2012.

[118] "IATA Jet fuel price monitor," 2021. [Online]. Available: https://www.iata.org/en/publications/economics/fuel-monitor/.

[119] Wirtschaftsverband Fuels und Energie e.V., "Verbraucherpreise." [Online]. Available: https://en2x.de/service/statistiken/verbraucherpreise/. [Accessed: 05-May-2022].

[120] T. Wassermann, H. Muehlenbrock, P. Kenkel, and E. Zondervan, "Supply chain optimization for electricity-based jet fuel: The case study Germany," *Appl. Energy*, vol. 307, no. August 2021, p. 117683, 2022.

[121] J. Gong and F. You, *Sustainable Design of Energy Systems by Integrating Life Cycle Optimization With Superstructure Optimization*, vol. 47. Elsevier Masson SAS, 2019.

[122] N. Oye, "Personal communication." .

[123] C. Galanopoulos, A. Giuliano, D. Barletta, and E. Zondervan, "An integrated methodology for the economic and environmental assessment of a biorefinery supply chain," *Chem. Eng. Res. Des.*, vol. 160, no. May, pp. 199–215, 2020.

[124] M. Skiborowski, A. Harwardt, and W. Marquardt, "Conceptual design of distillation-based hybrid separation processes," *Annu. Rev. Chem. Biomol. Eng.*, vol. 4, pp. 45–68, 2013.

[125] S. Hilpert, C. Kaldemeyer, U. Krien, S. Günther, C. Wingenbach, and G. Plessmann, "The Open Energy Modelling Framework (oemof) - A new approach to facilitate open science in energy system modelling," *Energy Strateg. Rev.*, vol. 22, no. 0, pp. 16–25, 2018.

[126] P. Kenkel, T. Wassermann, and E. Zondervan, "Biogas Reforming as a Precursor for Integrated Algae Biorefineries : Simulation and Techno-Economic Analysis," *Processes*, vol. 9, 2021.

[127] G. Di Marcoberardino, D. Vitali, F. Spinelli, M. Binotti, and G. Manzolini, "Green hydrogen production from raw biogas: A techno-economic investigation of conventional processes using pressure swing adsorption unit," *Processes*, vol. 6, no. 3, 2018.

[128] F. De Rosa, B. M. Smyth, G. McCullough, and A. Goguet, "Using multi-criteria and thermodynamic analysis to optimize process parameters for mixed reforming of biogas," *Int. J. Hydrogen Energy*, vol. 43, no. 41, pp. 18801–18813, 2018.

[129] R. E. Katofsky, "The production of fluid fuels from biomass." 1993.

[130] VDI Gesellschaft, *VDI-Wärmeatlas*, 2005th ed. Springer Berlin Heidelberg (Wiesbaden), 2005.

[131] T. L. Levalley, A. R. Richard, and M. Fan, "The progress in water gas shift and steam reforming hydrogen production technologies - A review," *Int. J. Hydrogen Energy*, vol. 39, no. 30, pp. 16983–17000, 2014.

[132] J. Dyment and S. Watanasiri, "Acid Gas Cleaning using Amine Solvents : Validation with Experimental and Plant Data," *Aspen Technol. Inc*, pp. 2–10, 2015.

[133] T. Danlami, "Economic Evaluation of Selexol – Based CO_2 Capture Process for a Cement Plant Using Post – Combustion Technology," *Int J Sci Res Sci Technol*, vol. 1, no. 5, pp. 194–203, 2015.

[134] N. Ramzan, U. Shakeel, A. Gungor, and M. Zaman, "Techno-Economic

Analysis of Selexol and Sulfinol Processes for Pre-Combustion CO2 Capture," in *4th International Conference on Power Generation Systems and Renewable Energy Technologies, PGSRET 2018*, 2019.

LIST OF STUDENT WORKS INCLUDED IN THIS THESIS

Celina Rose, Master thesis 2021, University of Bremen, *Superstructure optimization of coupled power-to-x and biorefineries for the investigation of synergy effects.*